NASA Contractor Report 179622
PWA 5574-206

Materials for Advanced Turbine Engines (MATE)

Project 4—Erosion Resistant Compressor Airfoil Coating

J.M. Rashid, M. Freling,
and L.A. Friedrich
United Technologies Corporation
Pratt & Whitney
East Hartford, Connecticut

May 1987

Prepared for
Lewis Research Center
Under Contract NAS3-20072

National Aeronautics and
Space Administration

FOREWORD

This work was performed under the National Aeronautics and Space Administration Materials for Advanced Turbine Engines (MATE) contract NAS3-20072, Project 4 - Erosion Resistant Compressor Airfoil Coatings. The NASA MATE Program Managers were Charles P. Blankenship and Salvatore J. Grisaffe; the Project 4 Managers were P. E. Hodge and Susan M. Benford. This work was performed in the Pratt & Whitney Engineering Division Materials Engineering and Research Laboratory under the direction of Allan H. Hauser. Pratt & Whitney MATE Program Managers were William A. Owczarski and Sid S. Blecherman; Project 4 Manager was Leonard A. Friedrich. The effort on all tasks was performed under the direction of James M. Rashid and Melvin Freling with technical support provided by David L. Lambert, William A. Lee and Frederick Wiese. The Task IV analytical analyses was performed under the direction of Hans Stargardter. Task VI fatigue data analyses was performed by Michael D. Pollard and Reginald H. Spalding. Assistance for preparation of this final report was provided by Abamilik Catao.

TABLE OF CONTENTS

SUMMARY

The objective of this program was to identify and demonstrate the ability of coatings to provide at least a 2X improvement in particulate erosion resistance for steel (AMS 5616), nickel (Incoloy 901) and titanium (AMS 4928) alloy compressor airfoils. The coatings consisted of plasma sprayed cobalt tungsten carbide and nickel (tungsten, titanium) carbide on all three alloys. Diffusion applied chromium plus boron coating was evaluated on Incoloy 901. All coatings were applied to a thickness of 25 to 63 microns (1 to 2.5 mils).

Initial program tasks were directed towards the evalution of processing parameters. For plasma spray processing, the parameters consisted of spray equipment, powder size, powder composition, surface preparation, susbstrate coating temperature and post coating heat treatment. Diffusion coating parameters evaluated were pack composition, processing temperature and time, surface preparation, masking techniques and post coating heat treatment. The coatings were metallographically examined for coating uniformity, density, homogeneity, oxide content and condition of the substrate interface. This examination was used as a preliminary screening technique to identify the coating systems having the most potential for providing airfoil erosion resistance.

The initial coatings selected for laboratory erosion and specimen high cycle fatigue (HCF) tests were predominantly plasma spray materials. Erosion tests were performed on panels at 20°, 45°, and 90° abrasive impingement angles using an S.S. White Abrasive Unit. Aluminum oxide, 27μ normal size, accelerated to speeds greater than 0.3 Km/sec (1000 ft/sec) was used as the erodent material. It was ascertained that plasma spray coatings characterized by high concentrations of discrete carbides were the most erosion resistant plasma sprayed materials. The highest level of erosion resistance for all coatings was obtained at shallow impingement angles. Panel specimen HCF tests showed that the coatings had 1) a maximum 30% HCF debit on AMS 5616 2) no effect on Incoloy 901 and 3) an approximate 60% debit on AMS 4928.

An analytical evaluation was performed on JT8D and JT9D high compressor airfoils to determine which airfoil regions could be coated without compromising component fatigue strength. Based upon this analysis and coating application techniques, it was decided to coat the outer 50% of the airfoil on two stages each of AMS 5616, Incoloy 901 and AMS 4928 compressor blades.

Based on laboratory results and analytical analyses, coating systems were selected for additional evaluation on engine components. This test phase consisted of developing coating application techniques, establishing surface smoothness criteria, performing burner rig erosion tests and HCF tests. The erosion tests were performed at conditions which simulated a particular engine rotor condition. From these tests, coatings were identified for all airfoil alloys which met the target of a 2X improvement in erosion resistance. Airfoil HCF tests were used to confirm the results of specimen tests. Based upon the tests performed, the following coatings were recommended for subsequent engine testing; Gator-Gard ® plasma spray 88WC-12Co on titanium alloy airfoils, plasma spray 83WC-17Co on steel and nickel alloy airfoils, and Cr+B diffusion coating on nickel alloy airfoils.

INTRODUCTION

Ingestion of debris has been determined to be the major cause of gas turbine compressor airfoil erosion. In the high compressor this erosion has resulted in a change in airfoil shape which reduced engine performance. Under NASA contract, NAS3-20632, Engine Component Improvement Program - JT9D Engine Diagnostics, performance was quantified for the JT9D commercial aircraft engine fleet and indicated that erosion and associated performance deterioration of the compressor was related to engine cycles rather than engine operating hours. Erosion was observed to increase in severity for short routes where flight cycles rather than flight hours were the controlling factor. As a result of this fleet wide problem, operating costs/hour of flight time have increased for airline operators.

Initial laboratory and rig testing at the Materials Engineering and Research Laboratory of Pratt & Whitney had previously indicated that the use of plasma applied coatings on airfoils could provide a reduction in erosion from two to four times as compared to current bill-of-material uncoated airfoils. Tungsten carbide-cobalt coatings, applied by plasma spray techniques to a thickness of 25.4 microns (1 mil), demonstrated their effectiveness in reducing erosion on both titanium and steel compressor airfoils. Additional laboratory testing with electro-deposited titanium diboride indicated a 10X improvement in erosion resistance on steel; however, coated steel compressor blades in a JT8D engine service evaluation program revealed that this coating suffered from leading edge chipping which limited its usefulness. The leading edge chipping was also observed in laboratory tests. Rig testing of plasma spray coated compressor blades indicated that these coating systems did not undergo the leading edge damage that has prevented the use of titanium diboride coatings. In addition to plasma coatings, the use of diffusion coatings on nickel alloy compressor blades becomes very attractive since there is a strong technology base in diffusion coating technology for nickel base turbine airfoils. Previous limited testing had indicated diffusion coatings were capable of providing erosion resistance. Thus, plasma and diffusion coatings were the primary apporaches considered to alleviate erosion induced compressor performance deterioration while capitalizing on a large industry base to provide low cost coatings.

Under this program, laboratory evaluation, rig and engine erosion test effects were conducted on several plasma and diffusion coating systems applied to three compressor airfoil alloy systems. The laboratory program included controlled erosion tests, microstructural and chemical analyses of the coatings. A fatigue test program was included to insure adequate fatigue strength for the coated airfoils. Surface finishing techniques were evaluated to define techniques which would provided smooth, aerodynamically efficient coating surfaces. Finally, an engine test demonstration of coated steel, nickel and titanium alloy airfoils was performed to confirm coating benefits in the complex stress environment of a high by-pass ratio gas turbine engine.

TECHNICAL APPROACH

Laboratory and rig testing has shown that coated airfoils have the potential of providing two to four times improvement in erosion resistance as compared to bill-of-material uncoated airfoils. Plasma applied coatings have been evaluated quite extensively and limited experience has been obtained with diffusion coatings, particularly on steel and nickel alloys. To properly evaluate the material, processing, design and operating characteristics of erosion resistant coatings, a seven task approach was used for the selection, process definition, laboratory evaluation, design evaluation, coating optimization and fabrication, and engine test of candidate coatings.

The goal of this approach was to demonstrate coatings capable of improving the erosion resistance of steel (AMS 5616), nickel (Incoloy 901) and titanium (AMS 4928) alloy compressor airfoils by at least a factor of two. To meet the objectives of the program, the following tasks were performed.

- Task I - Coating Systems Selection - Available erosion resistant coating systems were reviewed to select plasma and diffusion coatings for use on steel (AMS 5616), nickel (Incoloy 901) and titanium (AMS 4928) alloys.

- Task II - Coating Comparison and Process Parameter Definition - Plasma (composition and/or process variables) and diffusion coating parameters were investigated to define the limits for applying the coatings selected in Task I to laboratory specimens. These parameters were evaluated by microstructural and visual characterizations.

- Task III - Laboratory Evaluation of Coatings - Plasma and diffusion coatings applied to steel, nickel and titanium alloys were more closely evaluated for erosion resistance, microstructure and composition. Coating/alloy combinations, along with uncoated baseline specimens were high cycle fatigue tested.

- Task IV - Design Analysis and Component/Coating Systems Selection - Steel, nickel and titanium alloy compressor blade designs were selected to demonstrate the effectiveness of the erosion resistant coatings. The effect of the coating on the fatigue strength of the blade was considered. Detailed analyses were conducted to locate the coating in the area of maximum erosion and to avoid coating sections of airfoils sensitive to fatigue.

- Task V - Airfoil Coating Optimization - Coating process parameters, masking and post-coating heat treatment, were optimized for application of the recommended coatings. Post-coat finishing techniques were developed to produce a 20-30AA airfoil surface finish.

- Task VI - Component Fabrication and Test - Based on the processes developed in Task V, compressor airfoils of each alloy were coated for component testing. Rig erosion and high cycle fatigue tests were performed and, based on the results, one coating per alloy was selected for further evaluation.

- Task VII - Engine Testing - JT8D and JT9D ground based engine tests were performed to evaluate coated steel and titanium alloy airfoils and evaluate coated nickel and titanium alloy airfoils, respectively. Both engines were subjected to a cyclic endurance test with a target duration of 150 hours.

TECHNICAL PROGRAM

TASK I - COATING SYSTEM SELECTION

Candidate coatings for steel, nickel and titanium base compressor airfoil alloys were selected based on the following factors: earlier experience in the industry, demonstrated and/or potential erosion resistance and producibility. Plasma and diffusion applied coatings were prime candidates since a large multiple source production base was available for each of these coating systems. The coating systems were then assessed according to the following factors:

- o Material erosion resistance
- o Compatibility with compressor airfoil material
- o Ease of coating application
- o Cost
- o Potential of achieving a 2X improvement in airfoil life compared to the uncoated condition
- o Cost/benefits as related to engine application.

The following coatings were selected for evaluation in Task II:

(a) Plasma applied coatings for steel, nickel and titanium alloys
  (1) cobalt tungsten carbide
  (2) nickel (tungsten, titanium) carbide

(b) Diffusion coatings for steel and nickel alloys

  (1) chromium-boron
  (2) titanium-boron

(c) Diffusion coatings for titanium alloys

  (1) chemical vapor deposited titanium diboride (TiB_2)
  (2) nitride

TASK II - COATING COMPOSITION AND PLASMA PARAMETER DEFINITION

Coating processing parameters were varied for both plasma spray and diffusion applied coatings so that a thorough comparison could be made between processing variables, coating microstructure morphology and erosion performance on AMS 5616, Incoloy 901 and AMS 4928 substrates. Flow charts depicting plasma spray (Figures 1 and 2) and diffusion coating (Figure 3) process variants for Task II are described in more detail below.

(A) PLASMA SPRAY COATING DEFINITION ON ALL ALLOYS

(1) Coating Equipment

Four sources were utilized to evaluate the effect of coating equipment on coating microstructure: Pratt & Whitney, The Linde Division of Union Carbide Corp., Metco Inc, and United Technologies Metal Products, Inc (presently owned and operated by Sermetech Inc.).

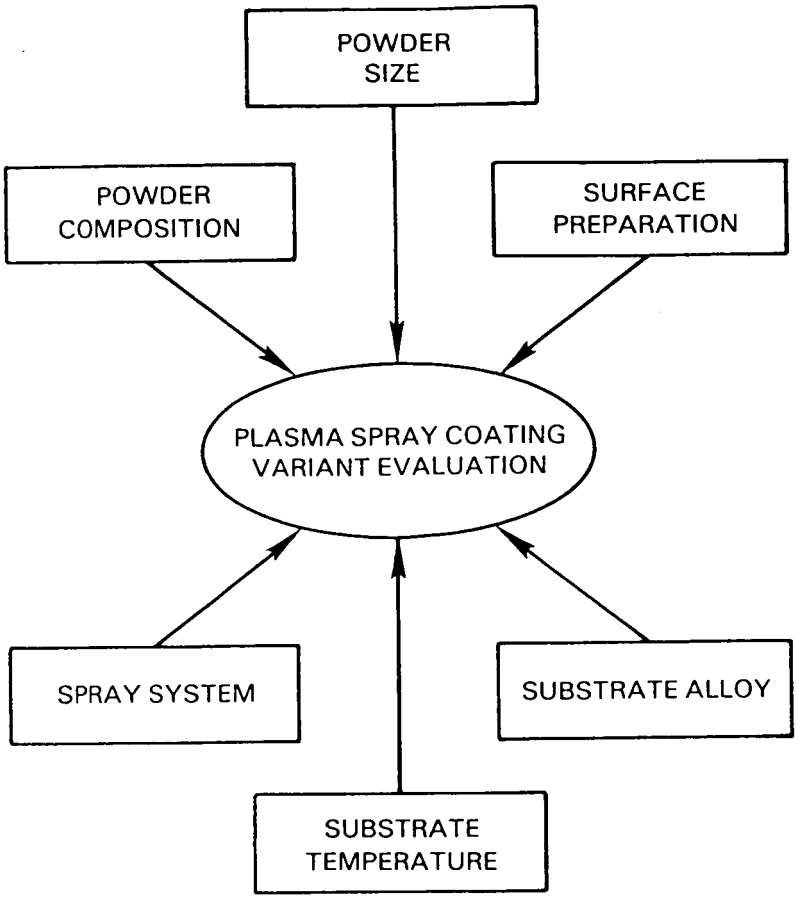

Figure 1 Plasma Spray Coating Process Screening

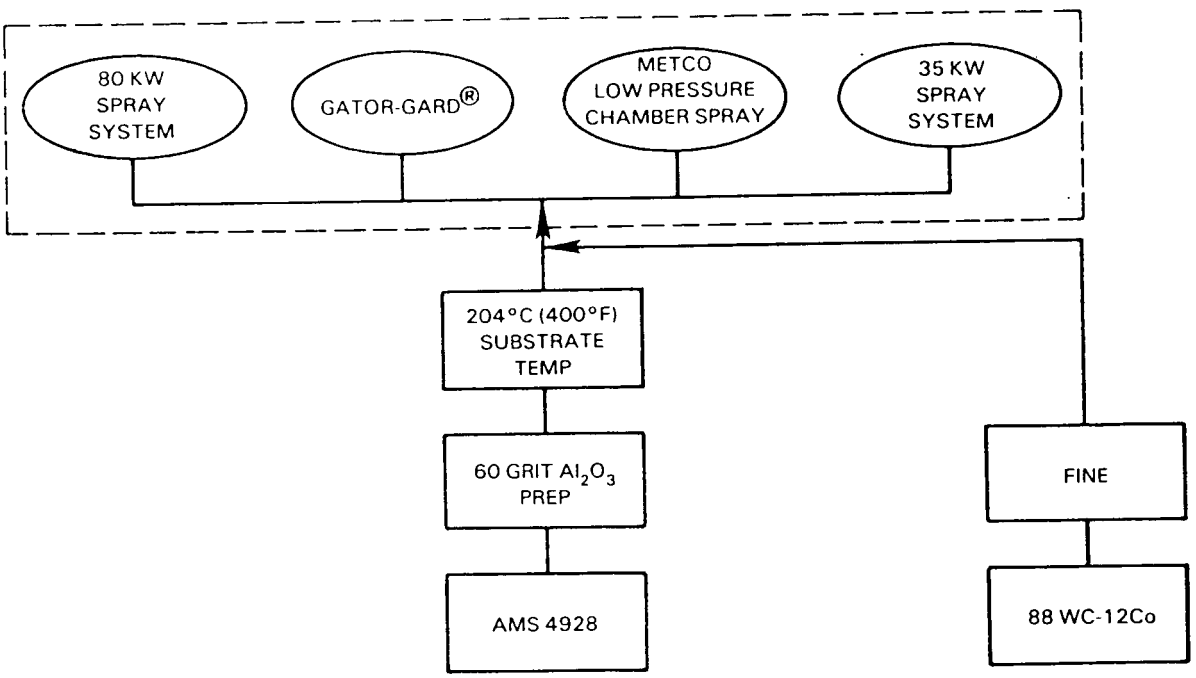

Figure 1a Evaluation of Plasma Spray Gun Variant

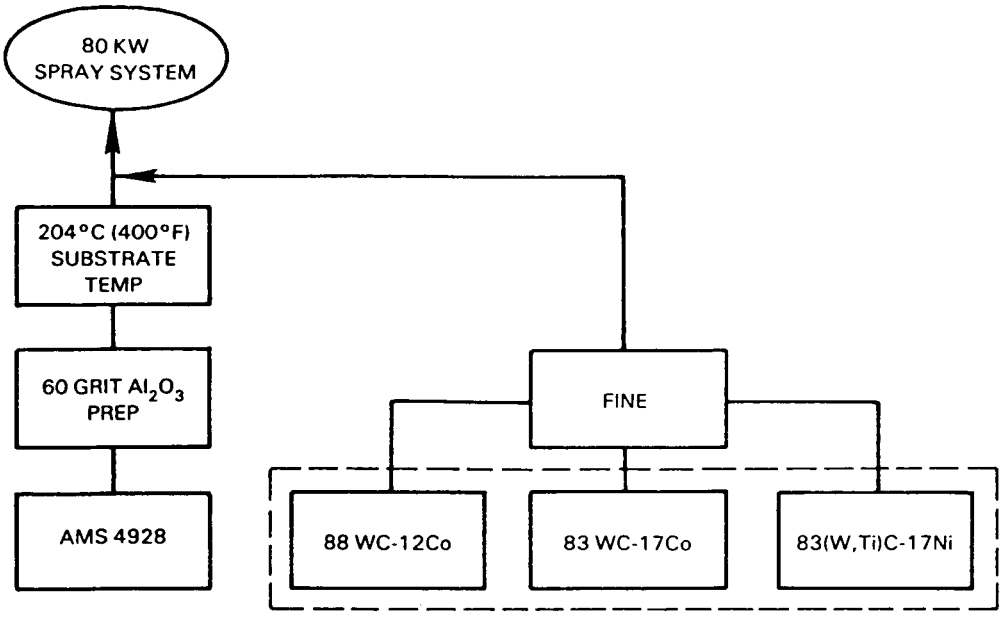

Figure 1b Evaluation of Spray Powder Composition Variant

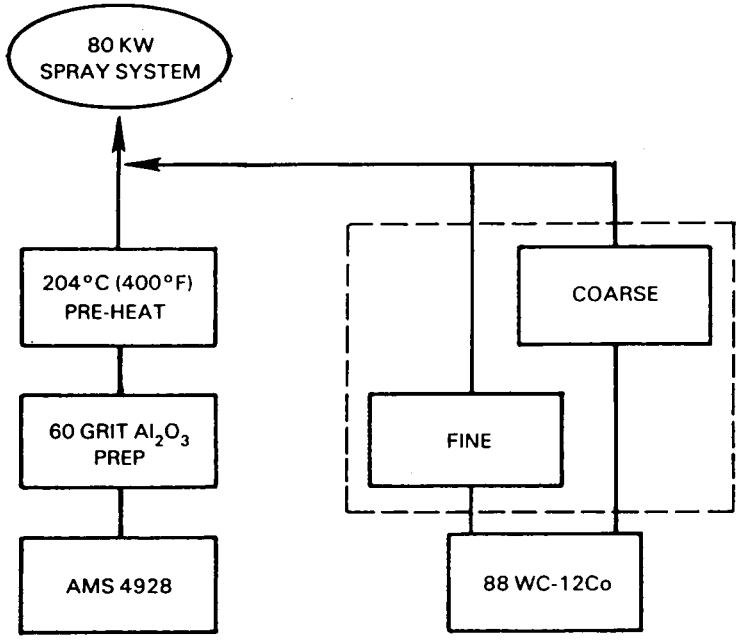

Figure 1c Evaluation of Powder Size Variant

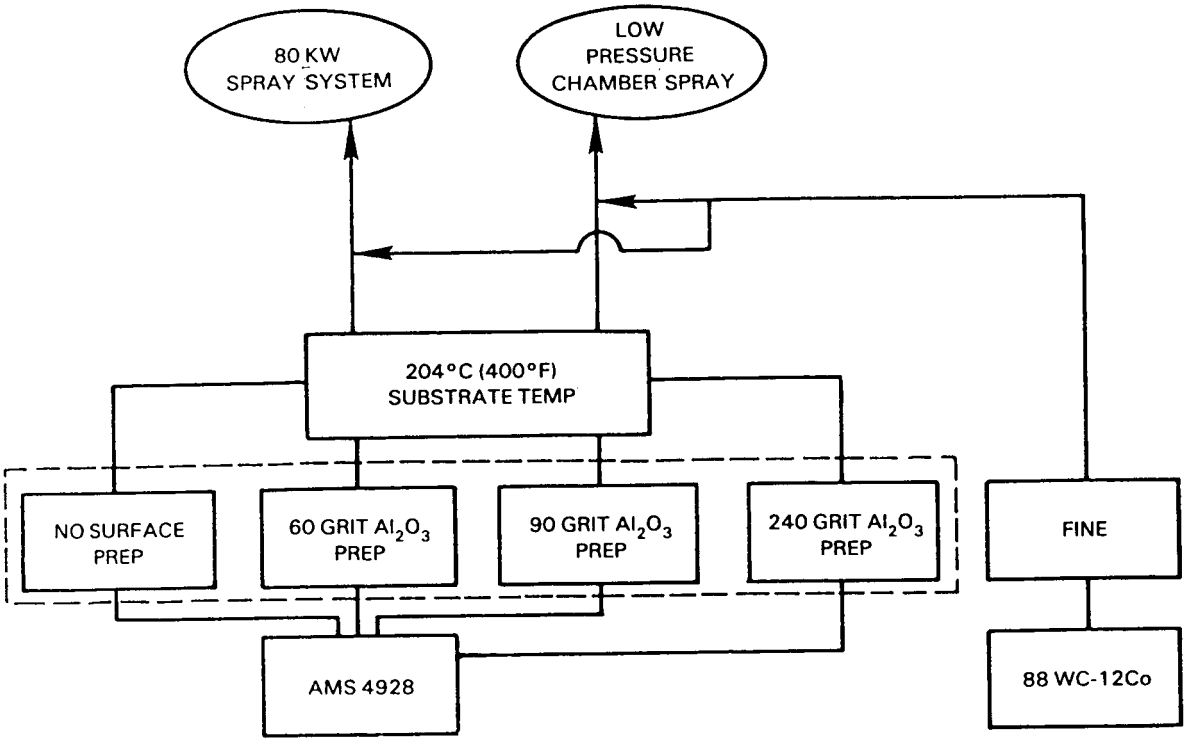

Figure 1d Evaluation of Surface Preparation Variant

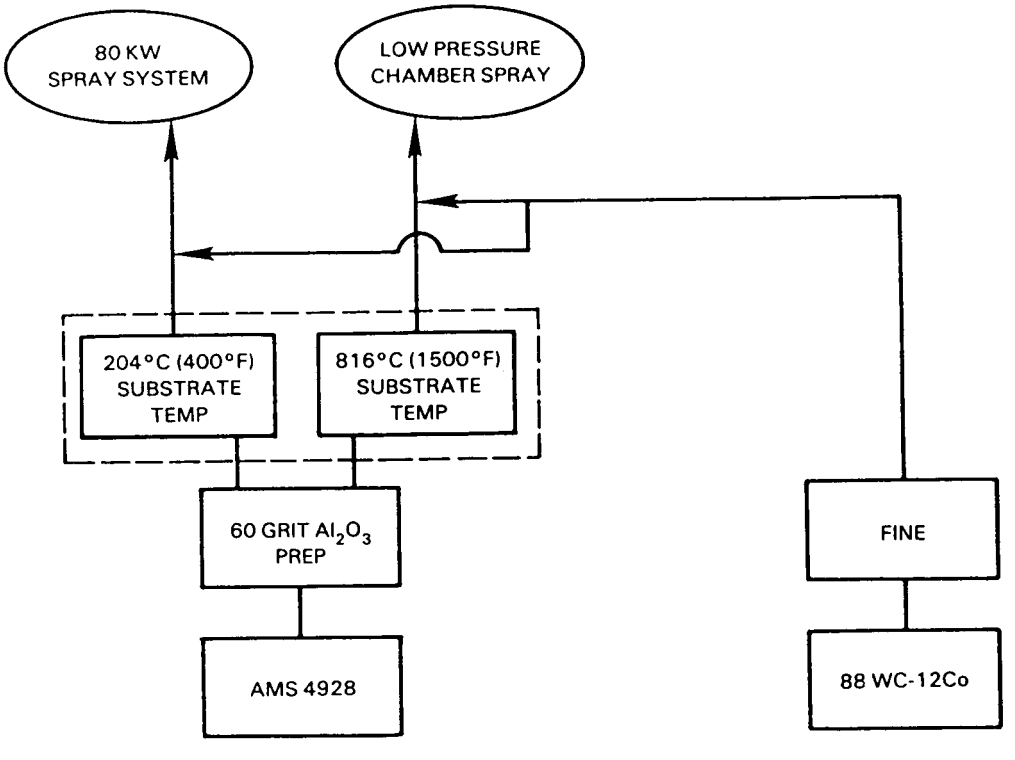

Figure 1e Evaluation of Substrate Temperature Variant

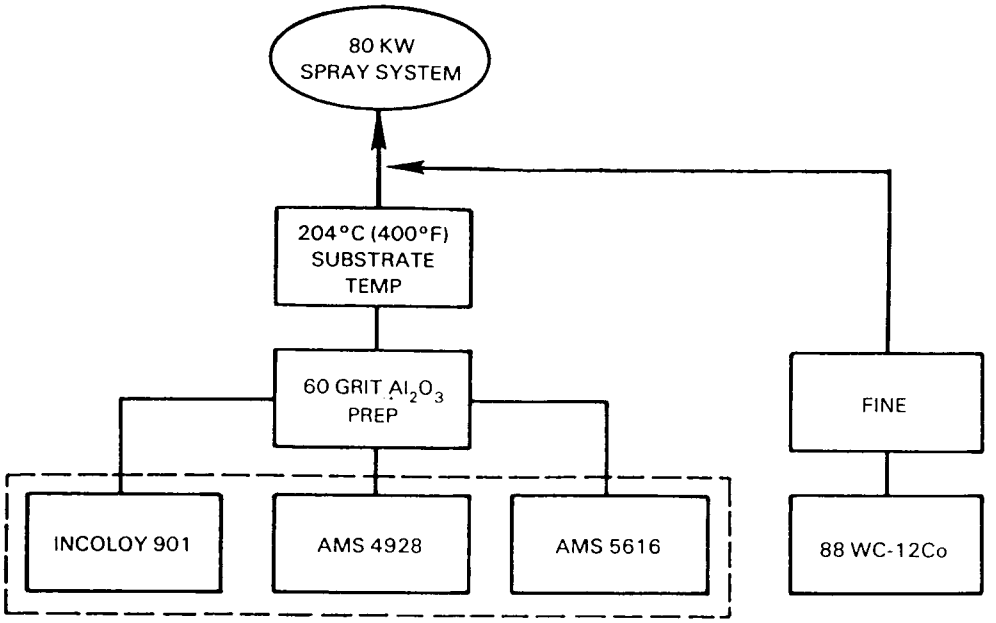

Figure 1f Evaluation of Substrate Alloy Variant

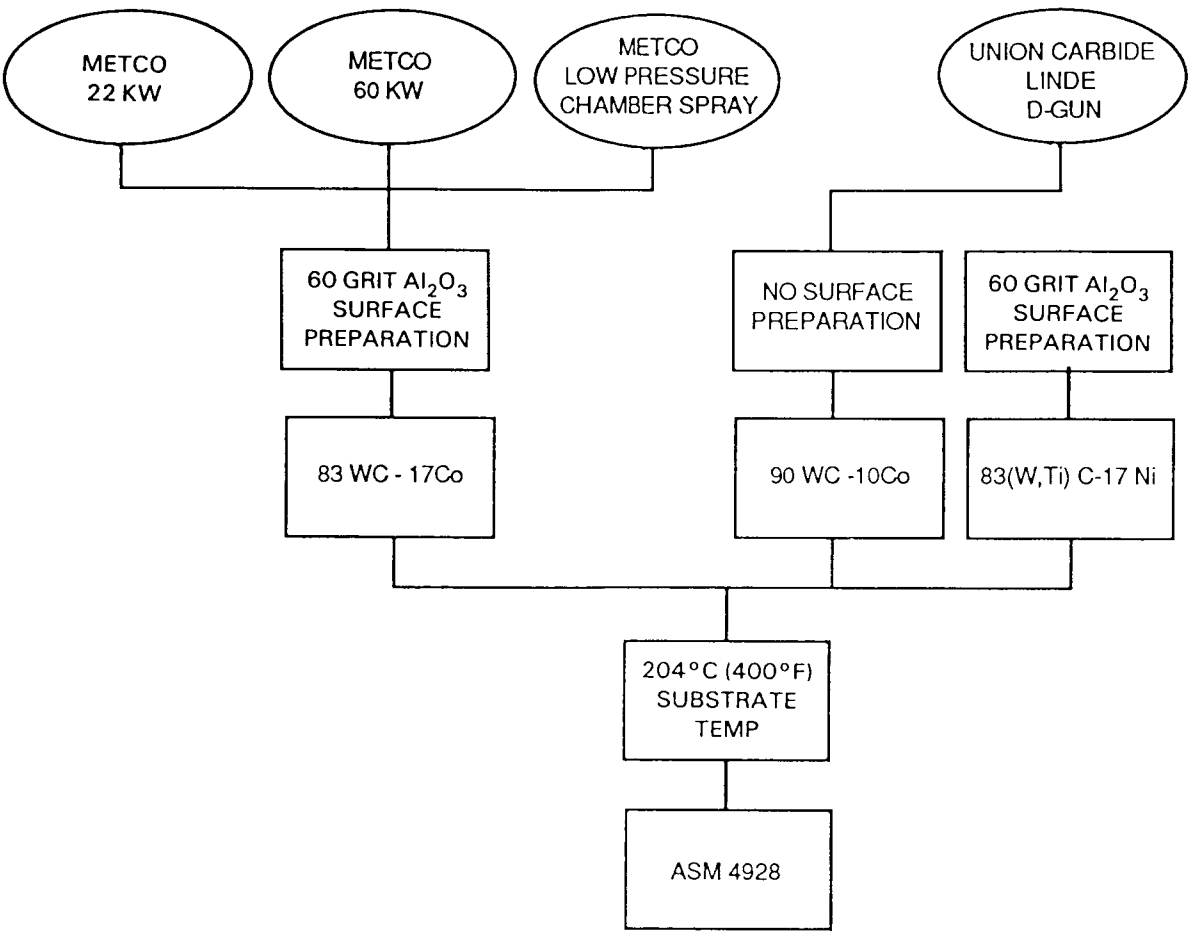

Figure 2 Additional Plasma Spray Coating Process Screening

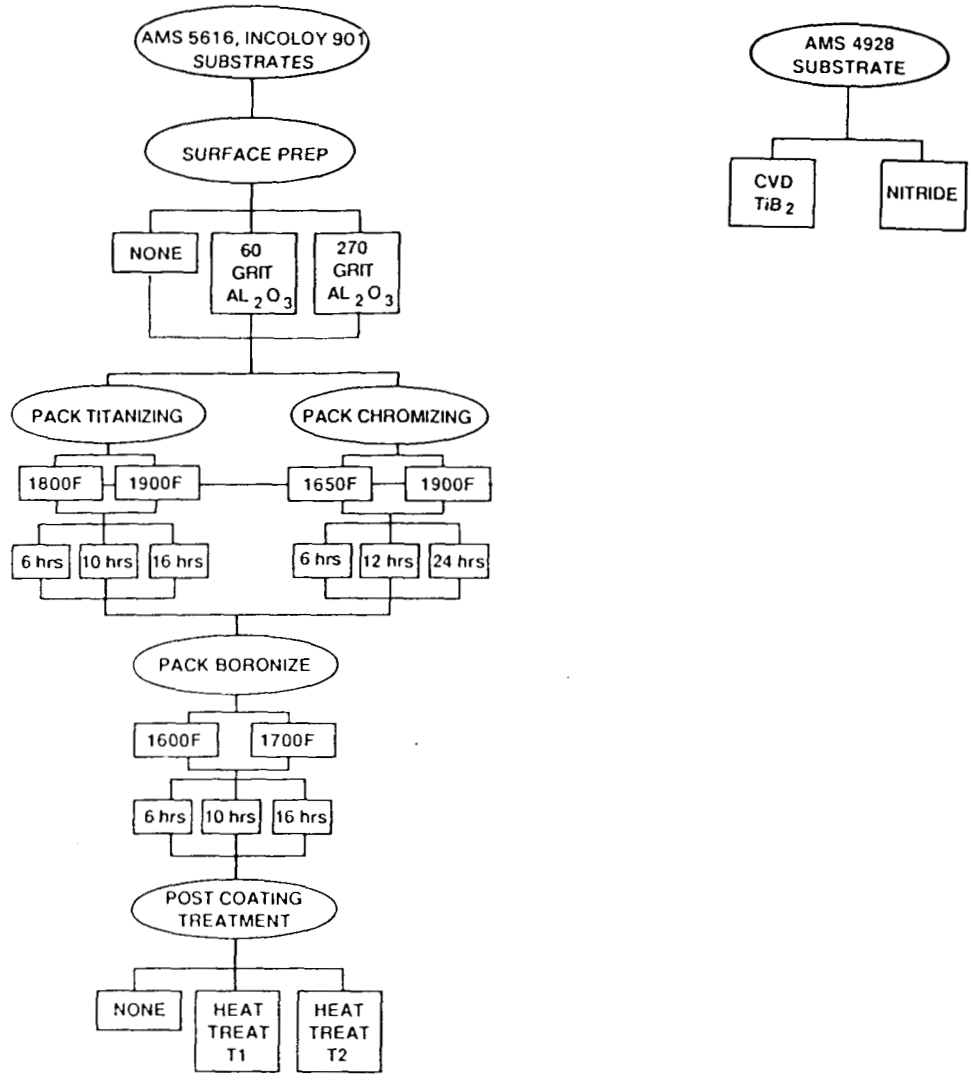

Figure 3 Diffusion Coating Process Screening

Source	Equipment
Pratt & Whitney	Plasmadyne SG100 spray gun, a high energy/high velocity thermal spray system.
Linde Div. of Union Carbide	Proprietary Detonation Gun System (D-Gun).
Metco, Inc.	Performed in air with Metco 7M high energy/high velocity system and in reduced atmosphere with low pressure plasma spray unit.
United Technologies Metal Products Division	Proprietary Gator-Gard system.

(2) Substrate and Powder Composition

Compositions of the alloys which were coated, as well as plasma spray powder specifications are listed in Tables I and II.

TABLE I
ALLOY SUBSTRATE COMPOSITIONS

Alloy Designation	Composition, Weight %
AMS 4928	Ti-6Al-4V
AMS 5616	Fe-13Cr-3W-2Ni-0.17C
Incoloy 901	Ni-34Fe-12.5Cr-6.0Mo-2.7Ti-0.1C-0.015B

TABLE II
PLASMA POWDER COMPOSITION

	Chemical Composition, Weight %						
Powder	Co	W	C	Ni	Al	Fe	Ti
AMS 7879 (coarse)	14.5	80.5	3.9	0.06	0.04	0.7	-
AMS 7879 (fine)	13.2	80.0	4.2	0.07	0.04	1.7	-
Metco 73F-NS-1	20.0	73.9	5.0	0.03	0.02	0.18	-
UCAR 205	0.1	53.6	7.9	16.2	0.01	-	20.2

Powders examined with the scanning electron microscope revealed various powder morphologies which, when sprayed, were expected to influence erosion resistance (Figure 4). The appearance and x-ray diffraction analysis of the powders were as follows:

	XRD, Vol %	Appearance
AMS 7879 (coarse)	70-75% WC 20% Co_3W_3C 5-10% $Co_3W_9C_4$	angular particles with a multifaceted surface structure
AMS 7879 (fine)	70-75% WC 25-30% Co_3W_3C 1% Co (cubic)	angular particles with an irregular surface structure
Metco 73F-NS-1	90% WC 10% Co (cubic)	composite aggregate, comprised of individual powder particles
UCAR 205	50-65% TiC 35% nickel solid solution, Ni_xC 1-2% WC	angular particles with a granular surface structure

Figure 4 Morphology of Plasma Spray Powders

(3) Powder Size

Particle size distribution of the powders is presented in Figure 5 and Appendix A. The subsieve technique, using a Leeds & Northrup Microtrac™ analyzer, determined the three dimensional powder size and the conventional sieve technique measured the particle size in two dimensions. These analyses indicated that the powders were generally less than 44 microns with the exception of coarse AMS 7879 which was intentionally chosen to evaluate the effect of large powder size on coating microstructure.

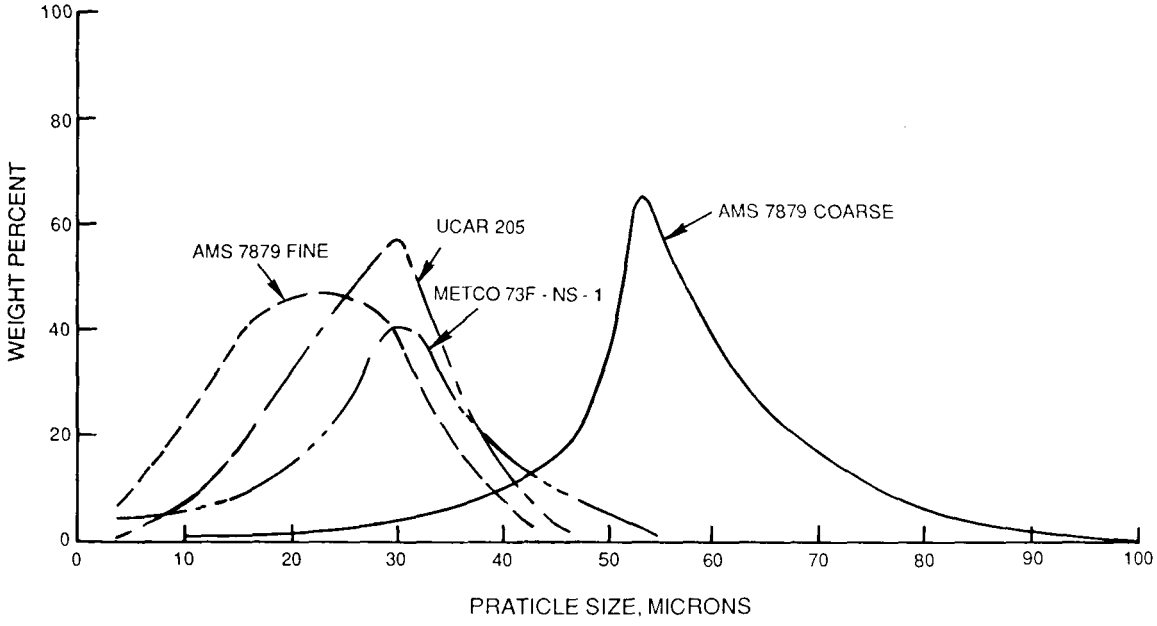

Figure 5 Particle Size Distributions of Plasma Spray Powders

(4) Surface Preparation

Plasma spray coatings typically require a pre-coating surface preparation to insure adequate coating/substrate bond strength. Three different abrasive blasting media sizes, 60, 90 and 240 grit, were examined to compare the relative amount of aluminum oxide grit entrapment and substrate surface roughening. These roughened conditions were also compared to the as-received surface condition.

(5) Substrate Coating Temperature

The effect of substrate temperature on coating quality was determined by preheating the substrate with the plasma gun. A preheat condition of 815°C (1500°F) was selected. No preheating resulted in a substrate coating temperature of approximately 205°C (400°F).

(6) Post Coating Heat Treatment

Subsequent to coating deposition, plasma coated specimens were subjected to the following thermal exposures to austenitize and temper AMS 5616 and to solution, stabilize, and precipitation heat treat Incoloy 901.

AMS 5616	980°C (1800°F)/1/2 hours + 565°C (1050°F)/2 hours
Incoloy 901:	1095°C (2000°F)/2hours + 790°C (1450°F)/4 hours + 730°C (1350°F)/24 hours

(7) Plasma Coating Analysis

Metallographic examination of coated specimens using Pratt and Whitney and Metco processes revealed that several of the coating parameters had a significant effect on coating microstructure. Specifically, the major differences in plasma spray coating microstructure were observed in the carbide phase morphology and distribution. A summary of metallographic analysis is presented below:

(a) Varying the substrate alloy had no apparent effect on the coating/substrate interface or coating microstructure.

(b) Varying the type of coating equipment had significant effects on the coating microstructure of plasma sprayed fine 88WC-12Co powder. Coatings applied with the Gator-Gard and Metco low pressure chamber process were characterized by a high concentration and uniform distribution of fine carbides, while coatings applied with an 80 KW gun (P&W and Linde) had a nonuniform distribution of discrete carbides. Use of a 35 KW spray system resulted in a coating with an intermediate concentration of descrete carbide particles (Figure 6). The amount of discrete carbide is believed to be related to the amount of thermal energy produced in the spray system. Higher energy systems, i.e. 80 KW, will produce a greater degree of splat structure and, hence, less discrete carbide. Plasma spray application of coarse 88WC-12Co powder resulted in a coating with a nonuniform distribution of discrete carbides.

(c) Varying the plasma spray powder composition resulted in differences in coating microstructure. Coatings applied with 88WC-12Co powder by P&W with a 80 KW gun were characterized by a nonuniform distribution of discrete carbides. Application of 83WC-17Co powder by Metco Inc. with a 60 KW gun resulted in a coating with a uniform distribution of discrete carbides. Metco recommended operating the plasma equipment at a 60 KW level to achieve a uniform coating microstructure. Application of 83(W,Ti)C-17Ni powder by P&W with an 80 KW gun resulted in a coating with an intermediate concentration of discrete carbide particles (Figure 7).

(d) Variations in surface preparation procedures resulted in no apparent differences in the level of interfacial oxides. However, as expected, differences were noted in the substrate surface roughness. In descending order from roughest to smoothest were surfaces prepared by (a) 60 grit Al_2O_3 @ 40 psi, (b) 90 grit Al_2O_3 @ 40 psi, (c) 240 grit Al_2O_3 @ 60 psi, (d) no surface preparation (Figure 8).

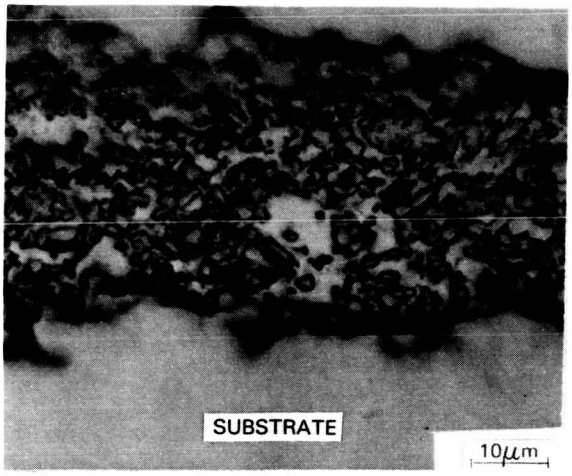

GATOR - GARD.

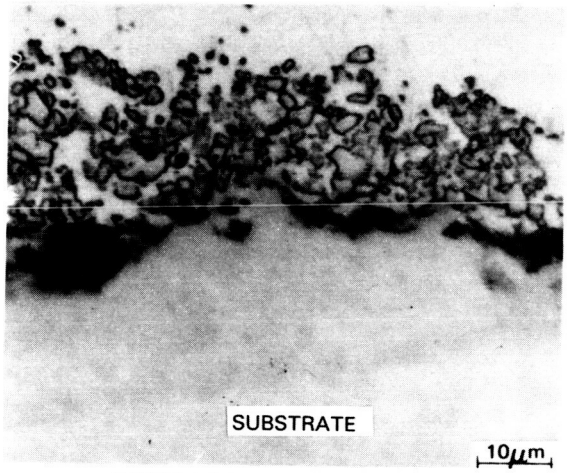

METCO LOW PRESSURE CHAMBER

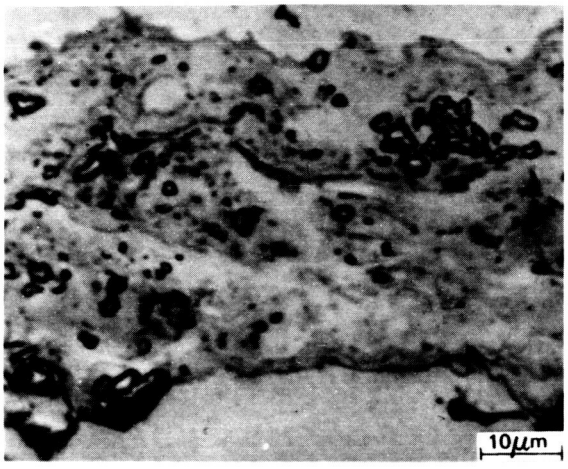

P&W 80 KW

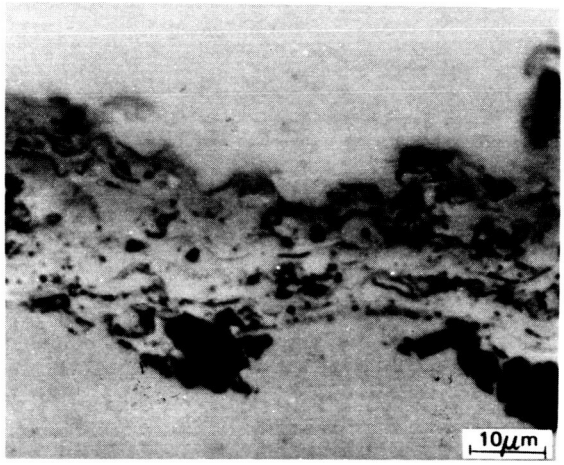

LINDE 80 KW

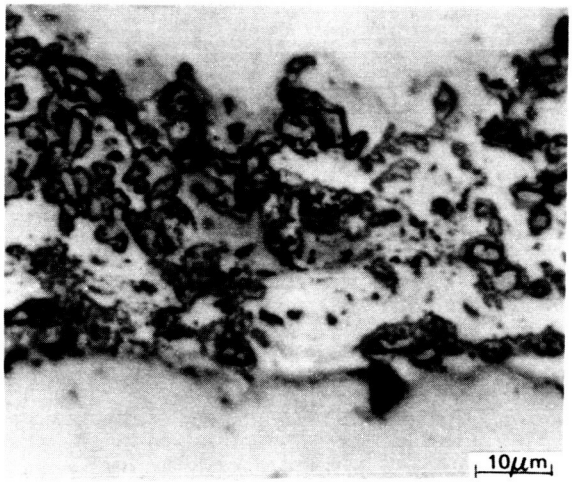

P&W 35 KW

Figure 6 Coating Microstructures of 88WC-12Co Powder Vary With Plasma Spray Process

88 WC - 12 Co
NON UNIFORM DISTRIBUTION OF CARBIDES

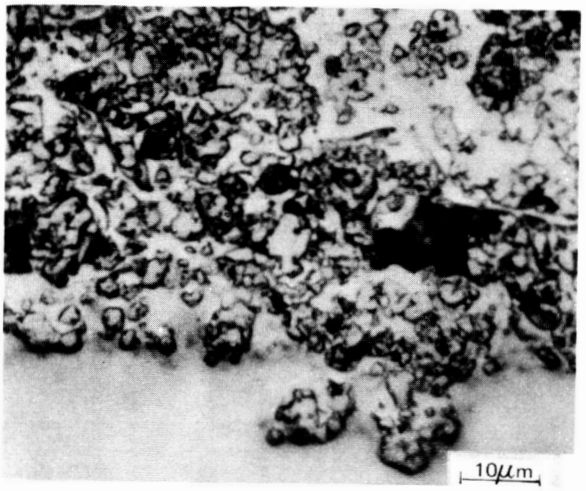

83 WC - 17 Co
UNIFORM DISTRIBUTION OF CARBIDES

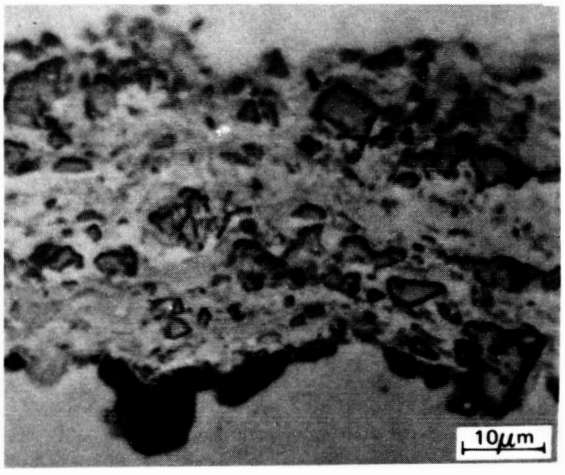

83(W,Ti)C - 17Ni
UNIFORMITY OF CARBIDES

Figure 7 Coating Microstructures of Different Powder Compositions Vary with the 80 KW Plasma Spray Process

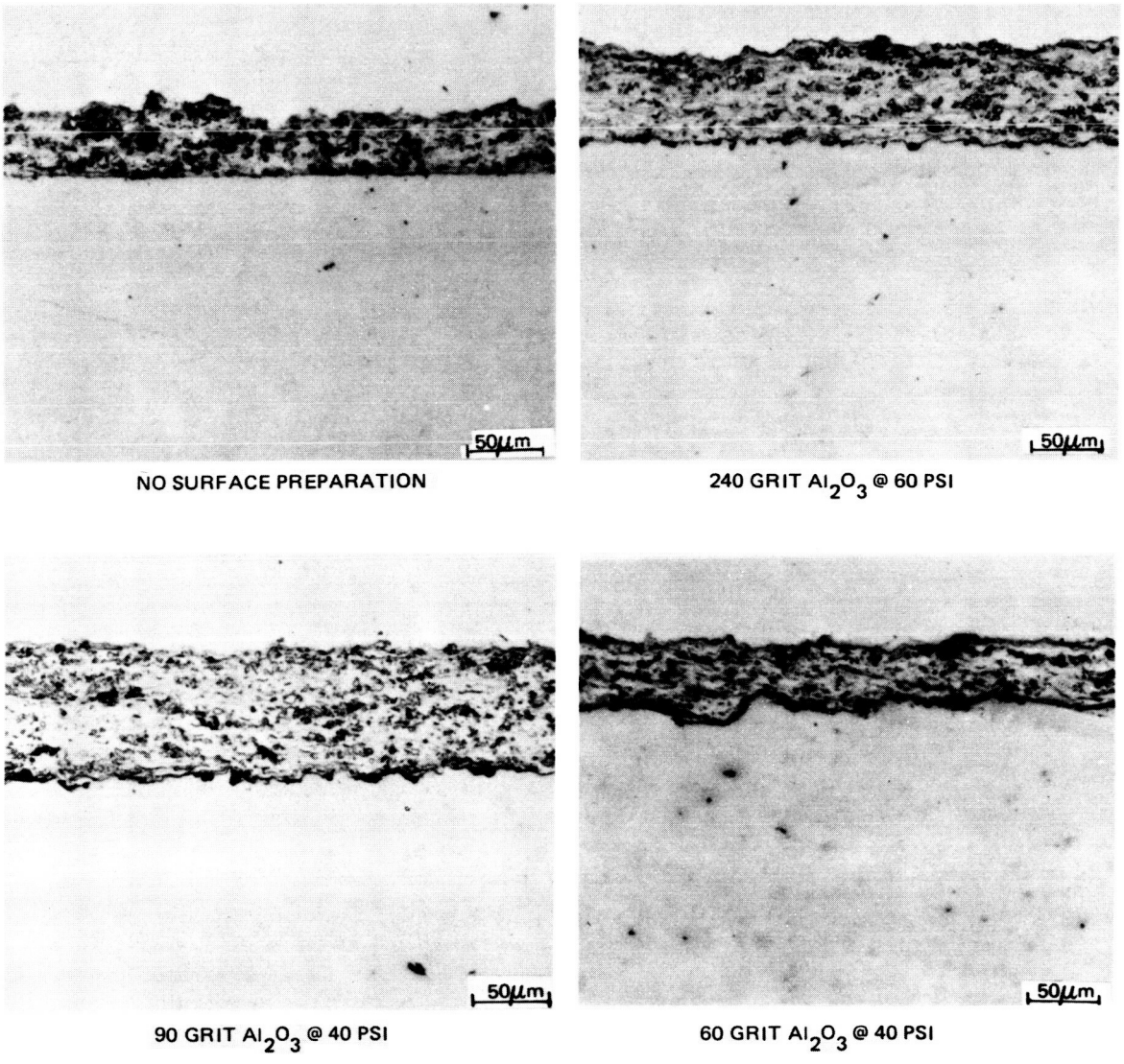

Figure 8 Comparison of Base Alloy Surface Preparation Prior to Application of 88WC-12Co Plasma Sprayed Powder Using P&W 80 KW Process

(e) Variations in substrate coating temperature of 205°C (400°F) and 815°C (1500°F) resulted in no apparent differences in either coating microstructure or interfacial oxide contamination.

Metallographic examination of plasma sprayed coating process parameters shown in Figure 2 revealed the following:

a) Detonation Gun application of 83(W,Ti)C-17Ni powder by the Linde Division of Union Carbide Corporation resulted in a coating with no apparent discrete carbides, whereas, the 90WC-10Co powder resulted in a coating containing a low concentration of discrete carbides (Figure 9).

b) Coating application by Metco Inc. of 83WC-17Co powder was performed under three conditions: (a) 22 KW, (b) 60 KW and (c) low pressure chamber spray system. Coatings applied with the 22 KW gun (standard parameters for the application of Metco 73F coating) had a varied distribution of large discrete carbides. Coatings applied with 60 KW and low pressure chamber spray processes had similar microstructures and contained a uniform distribution of smaller carbides (Figure 10). This microstructure was similar to that produced by the Gator-Gard process.

(B) Erosion Screening Test of Plasma Spray Coatings

According to the work plan, coating systems were to be selected for further evaluation in Task III based on the aforementioned metallographic examination. However, since the examinations provided no clear indications as to which coating systems would provide improved erosion resistance, a limited laboratory erosion test program was conducted using S.S. White Airbrasive test equipment to determine the effect of coating microstructure on erosion performance. This test equipment which is describd in more detail in Section III.B accelerates a small mass of abrasive particles at high velocity onto a fixed test specimen. The abrasive powder is placed in a pressurized hopper which is connected to a solenoid actuated vibrating unit. Powder from the hopper falls into an air stream which carries the particles through a nozzle to the specimen. Erosion resistance was determined by specimen weight and volume change as a function of erosion time and by the time required to erode through 25 microns (1 mil) of coating.

Testing of coated AMS 4928 test panels was performed at room temperature, with the panels inclined at a 20° impingement angle. Aluminum oxide (Al_2O_3), nominal 27 micron (1.1 mil) particle size, was used as the erosive medium and weight loss was measured after each nine second test interval. Additionally, the time to penetrate the coating was noted. The results of these tests indicated that those coatings containing a uniform dispersion of discrete carbides were most resistant to erosion.

Similar erosion tests were performed to determine the effect of pre-coat surface preparation and post-coat heat treatment on erosion resistance. Results indicated that these process variations had no significant effect on coating erosion resistance.

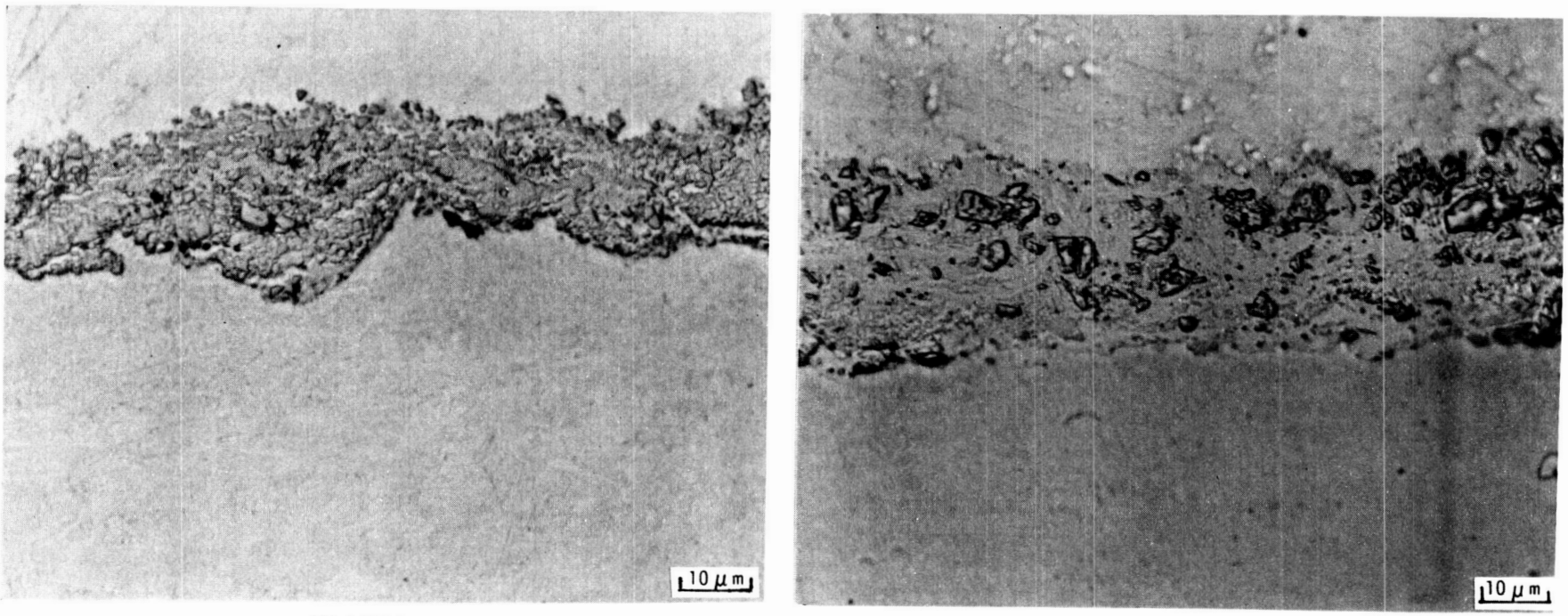

NO CARBIDES

LOW CONCENTRATION OF CARBIDES

Figure 9 Microstructure of 83(W,Ti)C-17Ni (left) and 90WC-10Co (right) Plasma Sprayed Powders by the Linde Division of Union Carbide Using the Detonation Gun Process

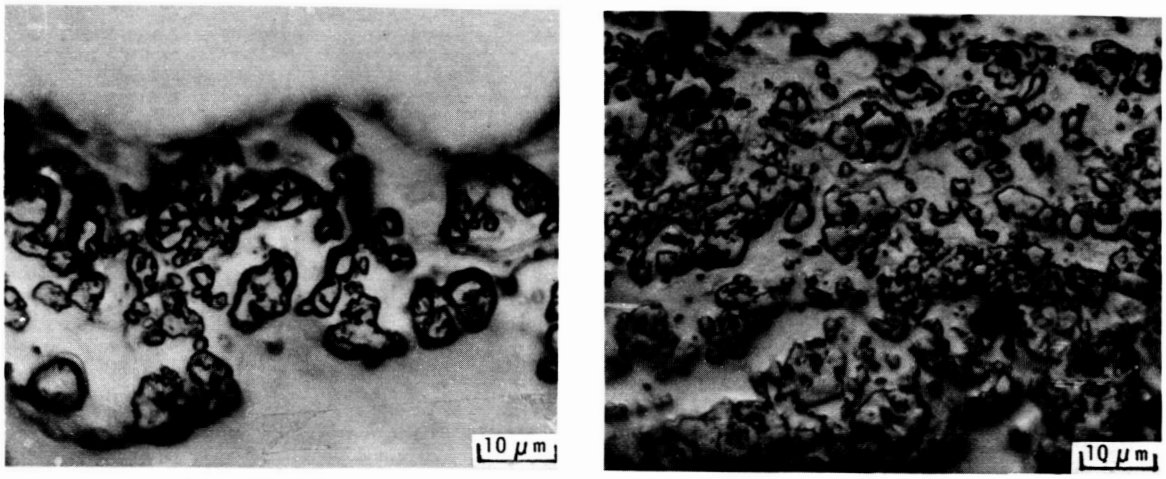

NONUNIFORM CARBIDES

UNIFORM CARBIDES

Figure 10 Microstructure of 83WC-17Co Powder Plasma Sprayed by Metco Inc. Using 22 KW (left) and 60 KW (right) Spray Conditions

(C) Diffusion Coatings on AMS 5616 AND Incoloy 901

(1) Substrate Compositions

Compositions of the two alloys investigated are presented in Section II.A.2.

(2) Pack Composition

Two basic coating systems were evaluated; (1) Cr+B and (2) Ti+B. These coatings were applied in two step processes: initial formation of a chromium or titanium rich layer followed by diffusing boron into these layers. Compositions of the three pack mixes, on a weight percent basis, were as follows:

Chromize: Al_2O_3-50Cr-5NH_4Cl
Titanize: TiO_2-30Ti-1NH_4Cl
Boronize: Al_2O_3-5B-1$NH_4F.HF$

(3) Pack Coating Cycle

Various pack coating temperatures from 870 - 1040°C (1600 - 1900°F) were evaluated to determine their effect on coating thickness and microstructures.

	Temperature	Time, hours
Chromize:	900°C (1650°F) and 1035°C (1900°F)	6, 12, 24
Titanize:	980°C (1800°F) and 1035°C (1900°F)	6, 10, 16
Boronize:	870°C (1600°F) and 925°C (1700°F)	6, 10, 16

(4) Surface Preparation

Pack diffusion coating required a pre-coating surface preparation. Two abrasive blasting media sizes, 60 and 220 grit Al_2O_3, were examined to compare the relative amount of grit entrapment and substrate surface roughening.

(5) Masking Techniques

Various masking techniques were evaluated to determine their effectiveness in preventing coating deposition on selected areas of the substrate which were to be protected during partial coating of the airfoil.

(6) Post Coating Heat Treatment

Following coating deposition, specimens were subjected to the following thermal exposures:

AMS 5616:	980°C (1800°)F/0.5 hours + 565°C (1050°F)/2hours
Incoloy 901:	1095°C (2000°F)/2hours + 790°C (1450°F)/4 hours + 730°C (1350°F)/24 hours

These exposures are the austenitize plus temper cycle for AMS 5616 and the solution, stabilization and precipitation cycle for Incoloy 901.

(7) Diffusion Coating Analysis

(a) Chromizing

Coating trials performed on AMS 5616 and Incoloy 901 produced coatings with thickness from 5.1 to 27.9 microns (0.2 - 1.1 mils) as shown in Figure 11.

A single phase chromized layer was formed on both alloy substrates. The coating which formed on AMS 5616 was relatively uniform in thickness, had a smooth outer surface and contained few entrapped pack mix particles (Figure 12). The coatings on Incoloy 901 were characterized by a variable coating thickness, rougher outer surface and a greater amount of entrapped pack powder. It is suspected that higher pack temperatures tended to trap more pack powder in the coating on Incoloy 901 (Figure 13).

(1) Greek Ascoloy

Examination of optical photomicrographs, elemental concentration profile traces and x-ray images indicated two distinct coating zones. Differences in the Cr content was the most notable feature between the two zones, although Ni and W gradients were detected. The maximum Cr content was 88 w/o in the outer zone and 22 w/o in the inner coating zone. (The nominal Cr content of AMS 5616 is 13 w/o). A region of W enrichment was presented at the outer/inner coating zone interface. Particles of aluminum oxide were detected in the coating and are probably entrapped pack powders (Figure 14).

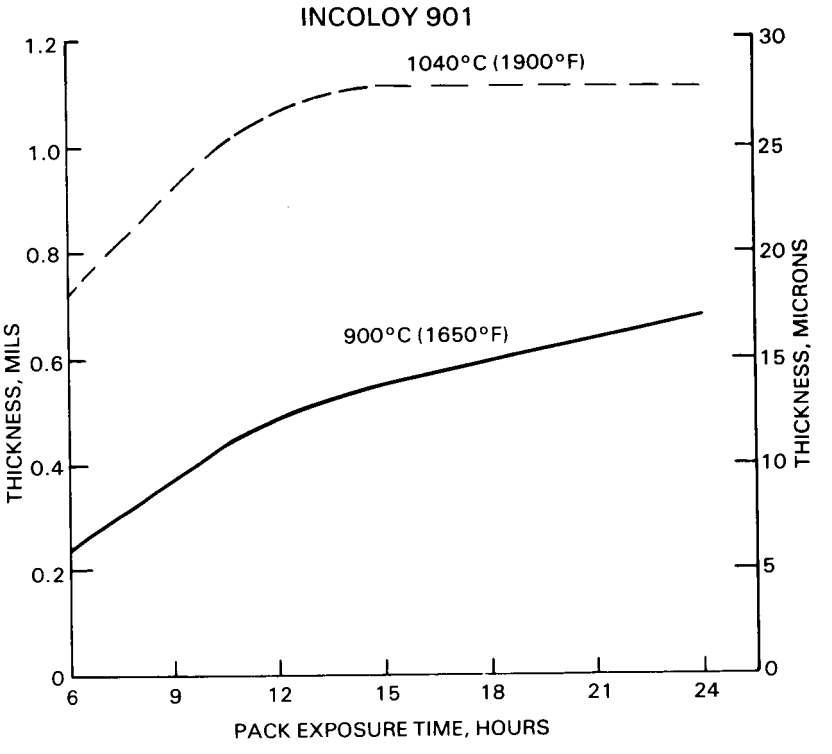

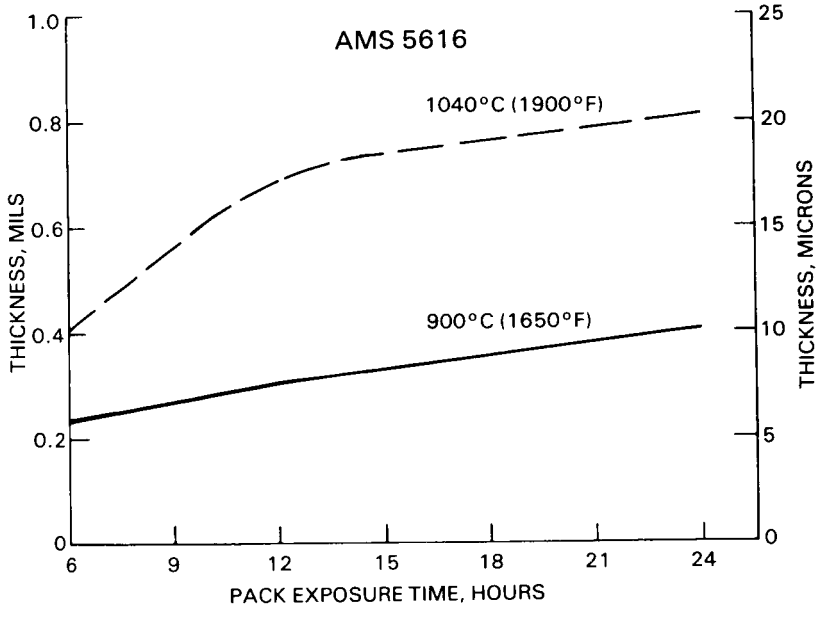

Figure 11 Chromize Coating Thickness on Incoloy 901 and AMS 5616

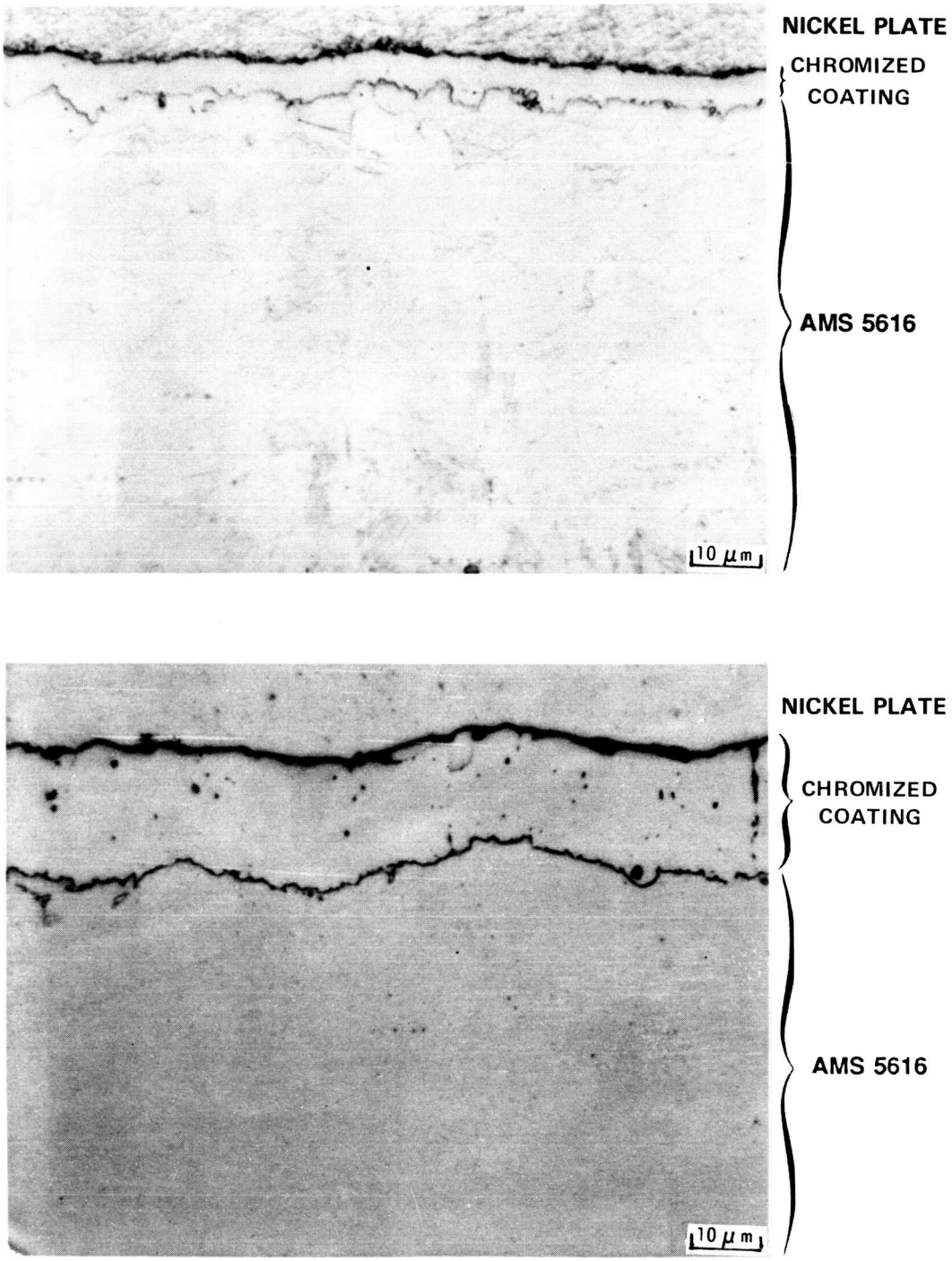

Figure 12 Coating Microstructures Following Pack Chromizing AMS 5616 at 900°C (1650°F)/6 hours (top) and 1040°C (1900°F)/24 hours (bottom) Etch: Villela's

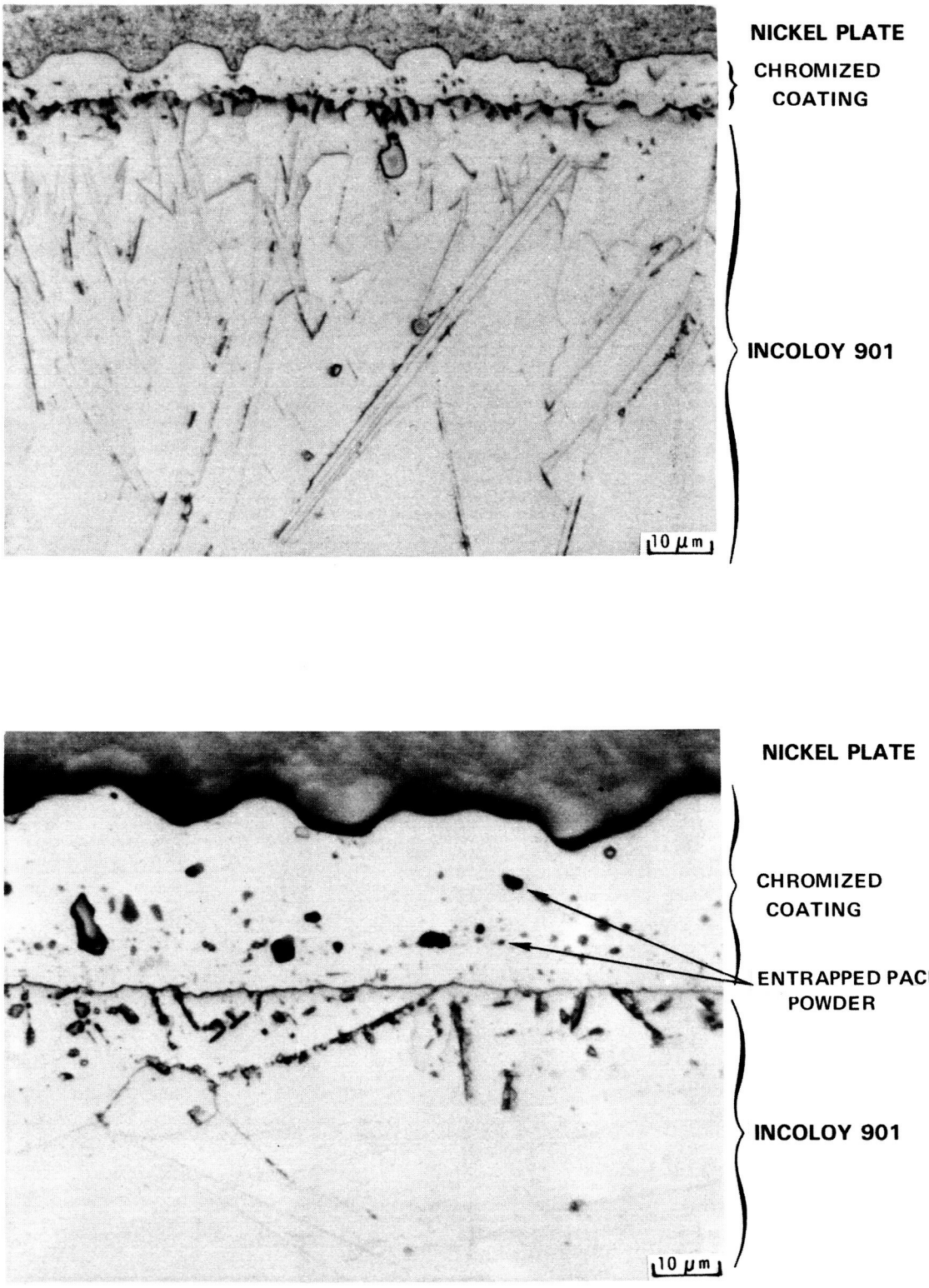

Figure 13 Coating Microstructures Following Pack Chromizing Incoloy 901 at 900°C (1650°F)/6 hours (top) and 1040°C (1900°F)/24 hours (bottom) Etch: Aqueous Ferric Chloride

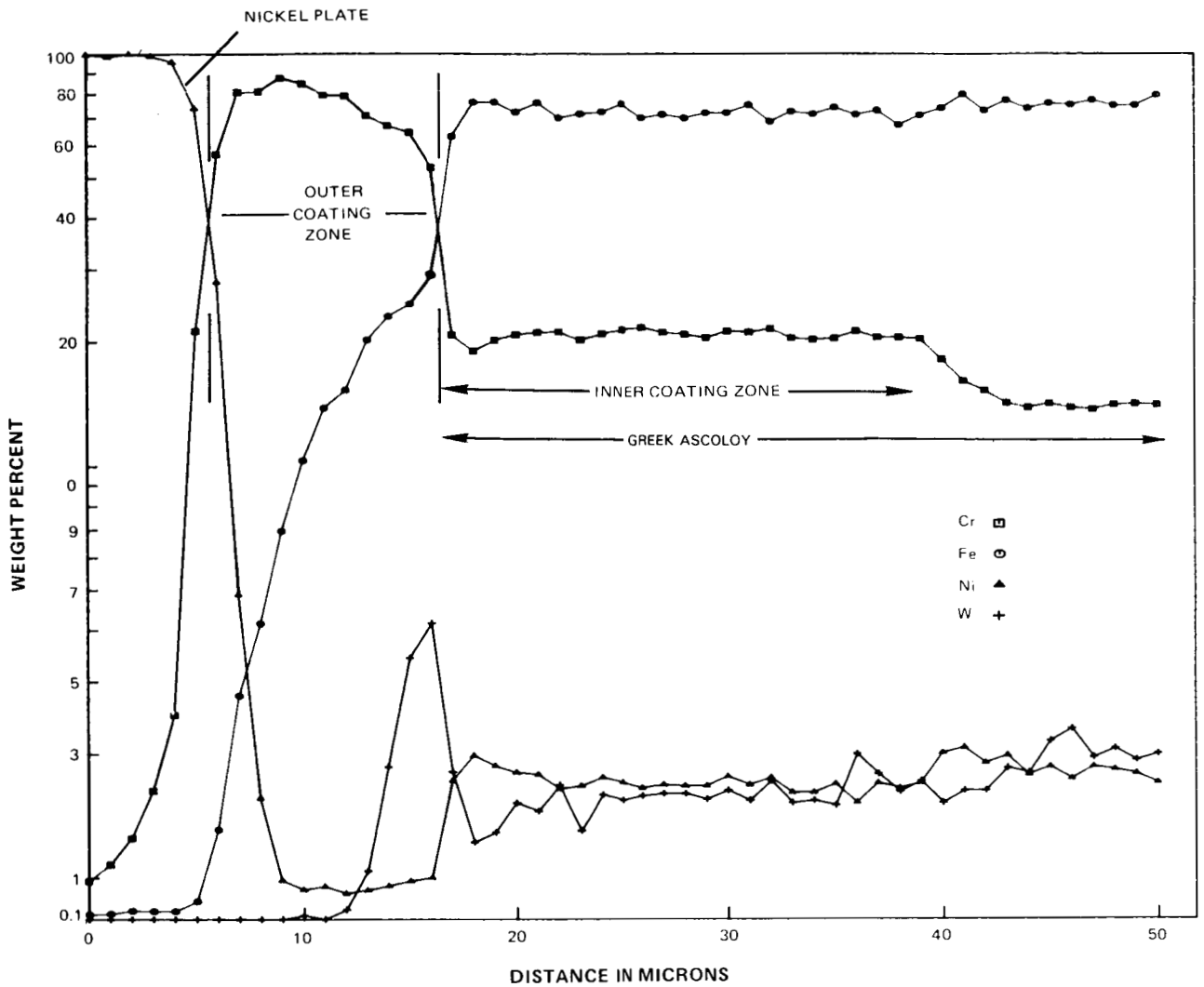

Figure 14 Electron Micrograph Concentration Profile Traces, Elemental X-Ray Images and Optical Photomicrograph of Chromized AMS 5616 Coating Cycle: 1040°C (1900°F) for Six Hours

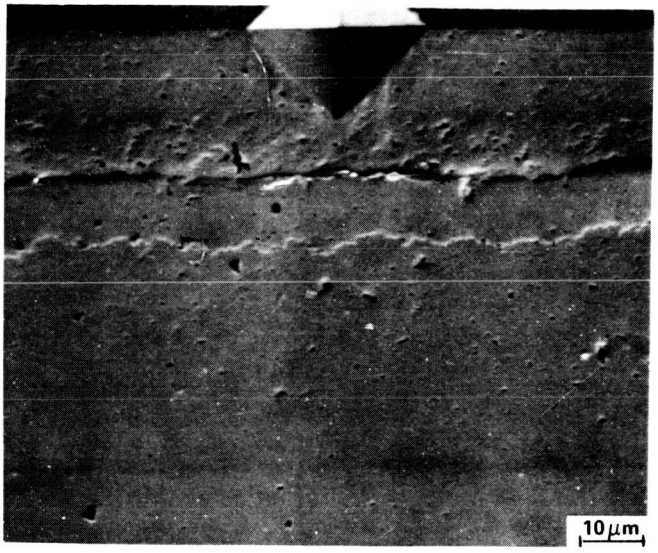

ELECTRON MICROGRAPH

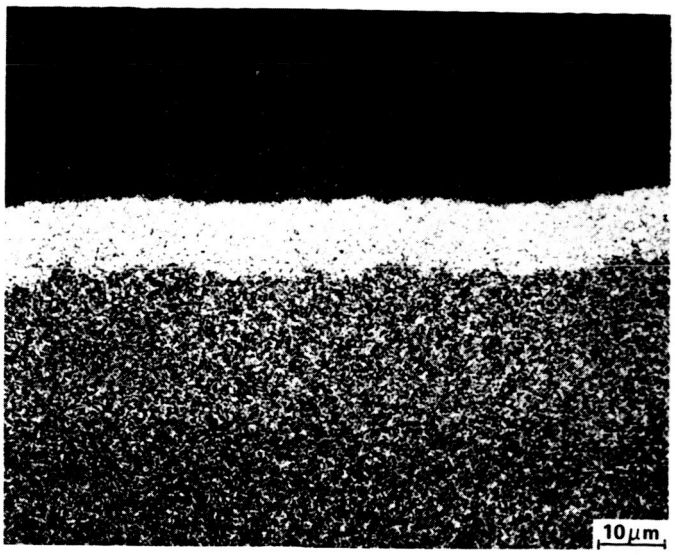

Cr X-RAY

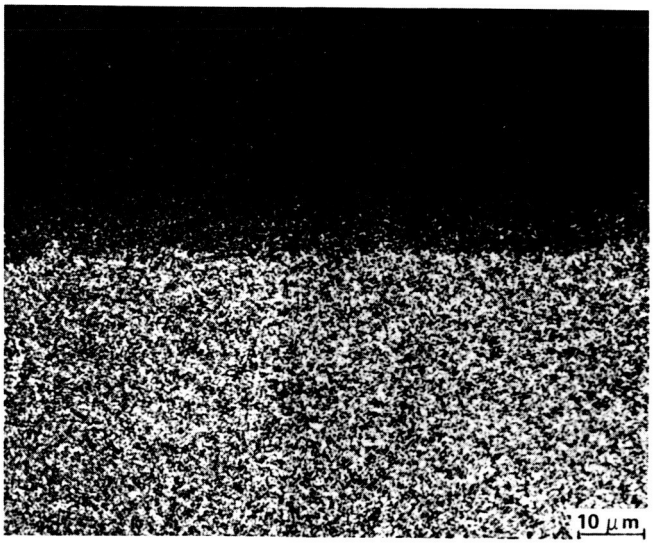

Fe X-RAY

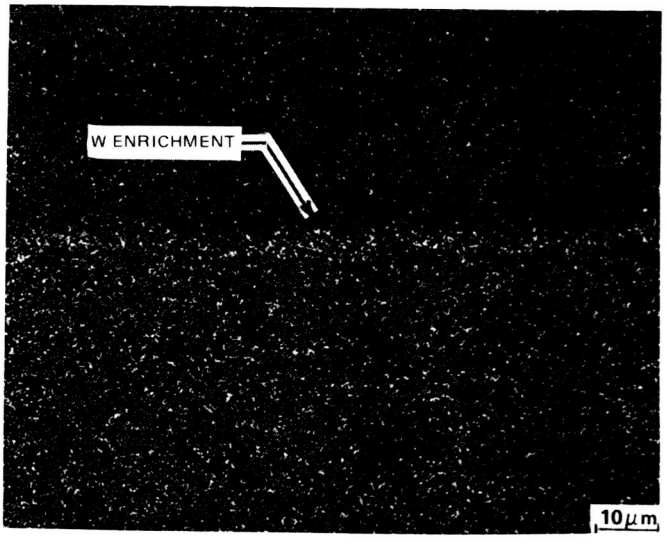

W X-RAY

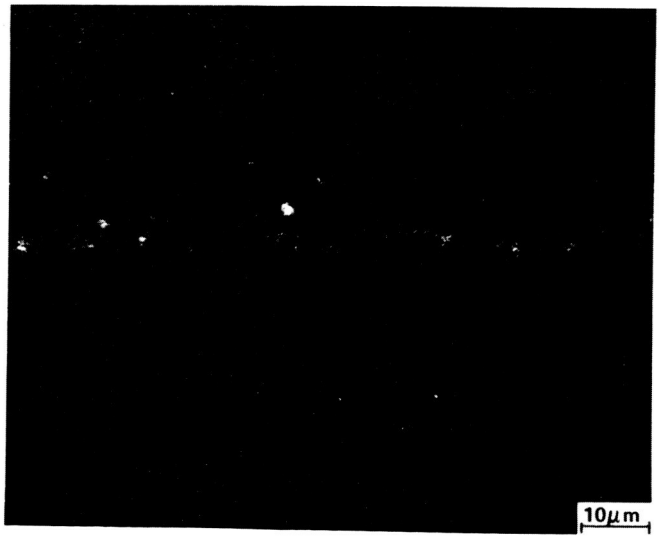

Al X-RAY

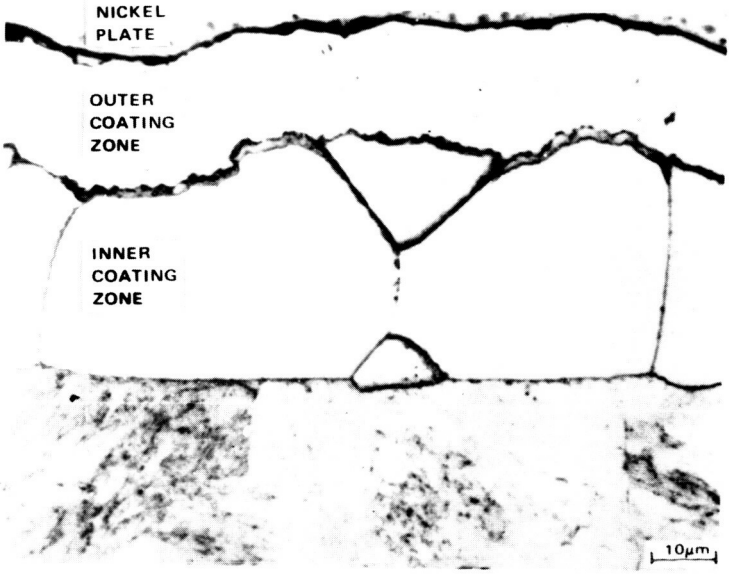

OPTICAL MICROGRAPH

(2) Incoloy 901

The chromium content ranged from a maximum of 92 w/o near the surface to a minimum of 72 w/o at the coating/substrate interface. Particles identified as aluminum oxide and a titanium enriched phase were present in the coating. Figure 15 presents concentration profile traces as well as elemental x-ray images of the coating. (The titanium spike in the concentration profile trace is due to a particle rather than a zone.)

(b) Titanizing

Coating trails were performed on AMS 5616 and Incoloy 901 substrates at 980°C (1800°F) and 1040°C (1900°F) for 6, 10 and 16 hours. A single phase coating, 2.5 to 5.1 microns (0.1 - 0.2 mils) in thickness, was formed on AMS 5616 (Figure 16). It was concluded that the time and temperature selections did not significantly affect coating thickness.

The titanized coating on Incoloy 901 consisted of at least two phases within two zones (Figure 17). One of the phases was larger and more acicular in the inner coating zone than in the outer zone. The thickness of the inner zone was slightly greater than that of the outer zone. Total coating thickness varied from 33 to 46 microns (1.3 - 1.8 mils) at 980°C (1800°F) and 46 to 53 microns (1.8 - 2.1 mils) at 1040°C (1900°F).

(1) Greek Ascoloy

This coating contained a maximum of 70 w/o titanium. A slight amount of substrate element diffusion into the coating was detected. Aluminum oxide particles were detected at the coating/substrate interface. Figure 18 presents concentration profile traces as well as elemental x-ray images.

(2) Incoloy 901

A complex coating was formed with an inner and outer coating zone, both of which contained titanium rich phases (Figures 19 and 20). Specific features of the coating are:

- o A 1-2 micron (0.4 - 0.8 mils) titanium rich layer at the coating surface
- o At least two distinct types of titanium rich particles in the outer coating zone
- o At least two distinct types of titanium rich phases in the outer coating zone
- o At least two different distinct types of titanium rich phases in the inner coating zone
- o A higher titanium content in the outer coating zone than in the inner coating zone.

PAGE _____ INTENTIONALLY BLANK

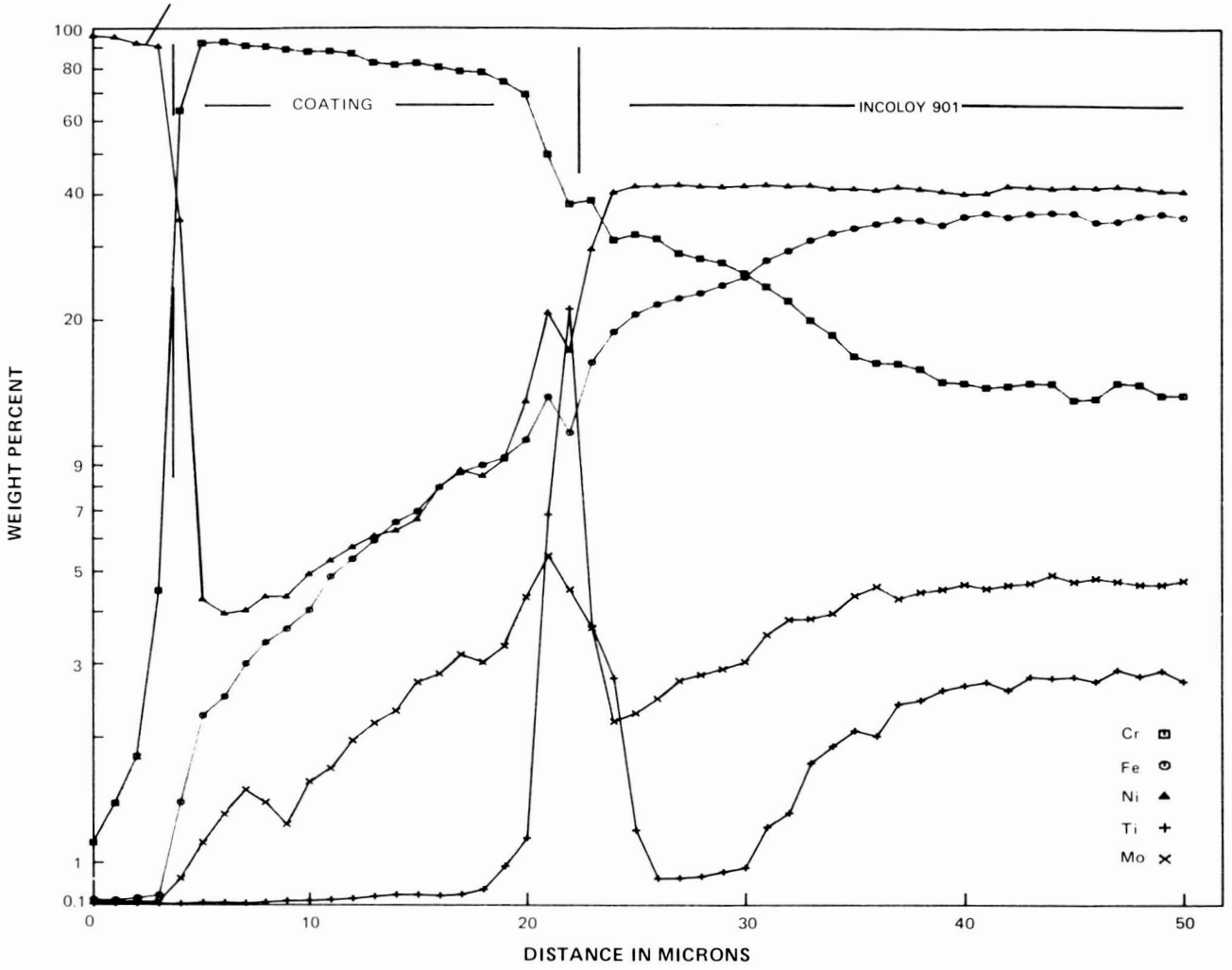

Figure 15 Electron Micrograph Concentration Profile Traces, Elemental X-Ray Images of Chromized Incoloy 901. Coating Cycle: 1040°C (1900°F) for Six Hours

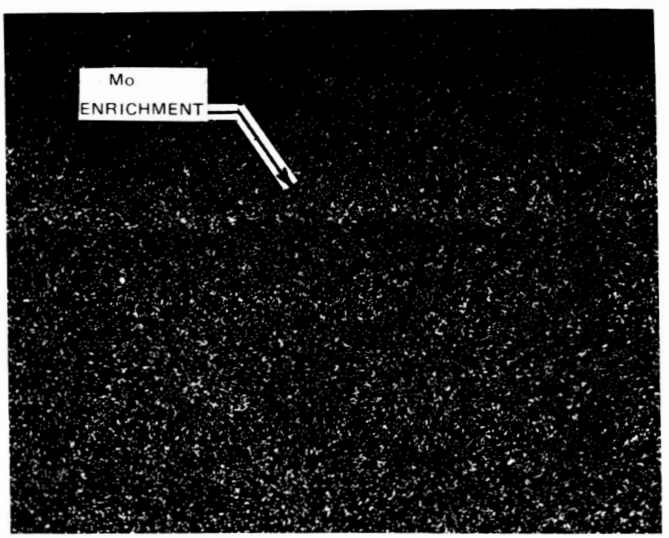

Mo X-RAY

COATING

ELECTRON MICROGRAPH

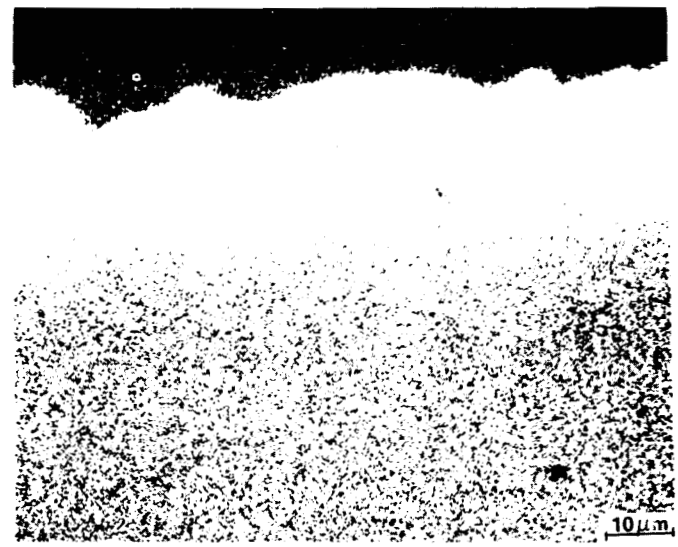

Cr X-RAY

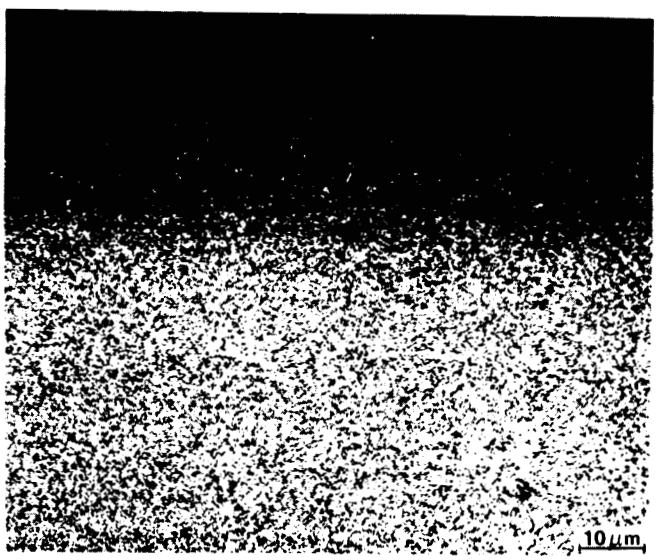

Fe X-RAY

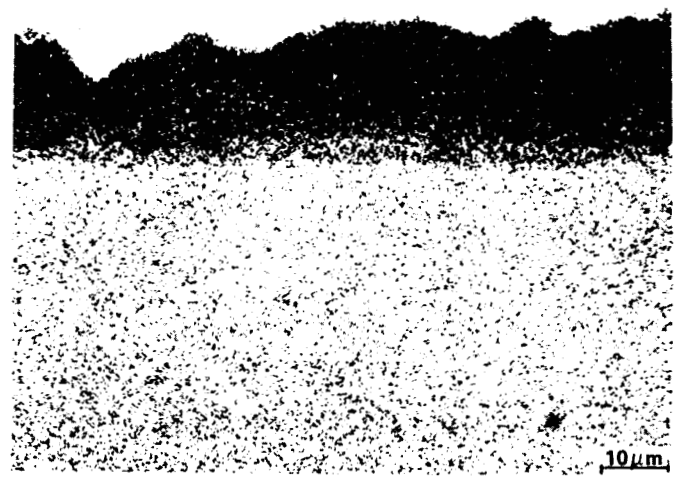

Ni X-RAY

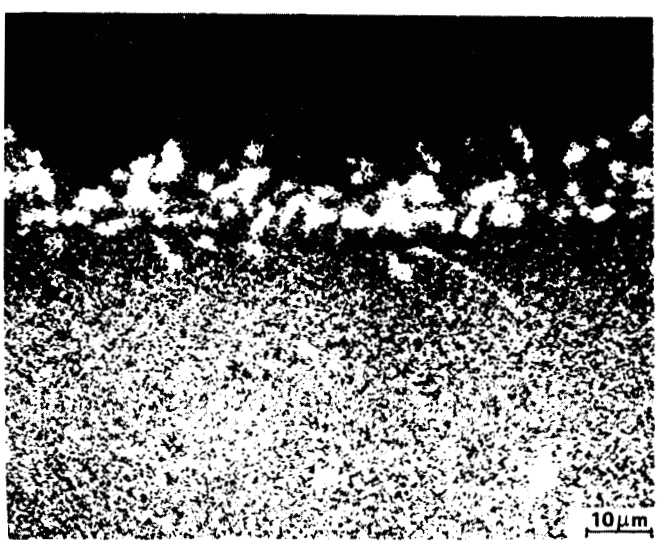

Ti X-RAY

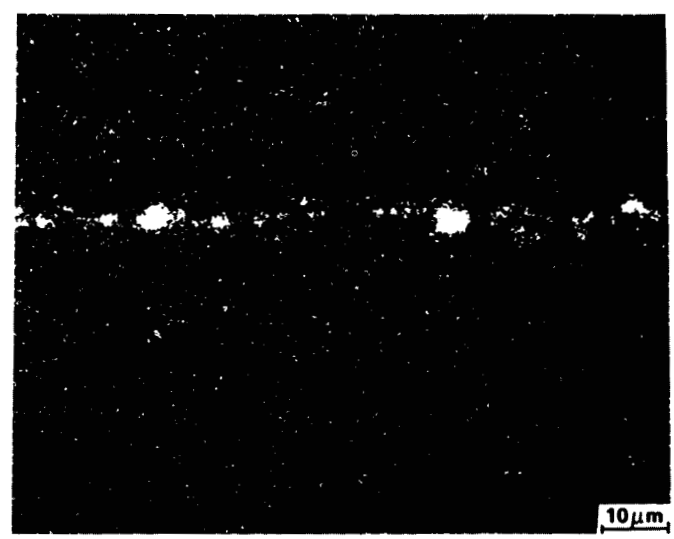

Al X-RAY

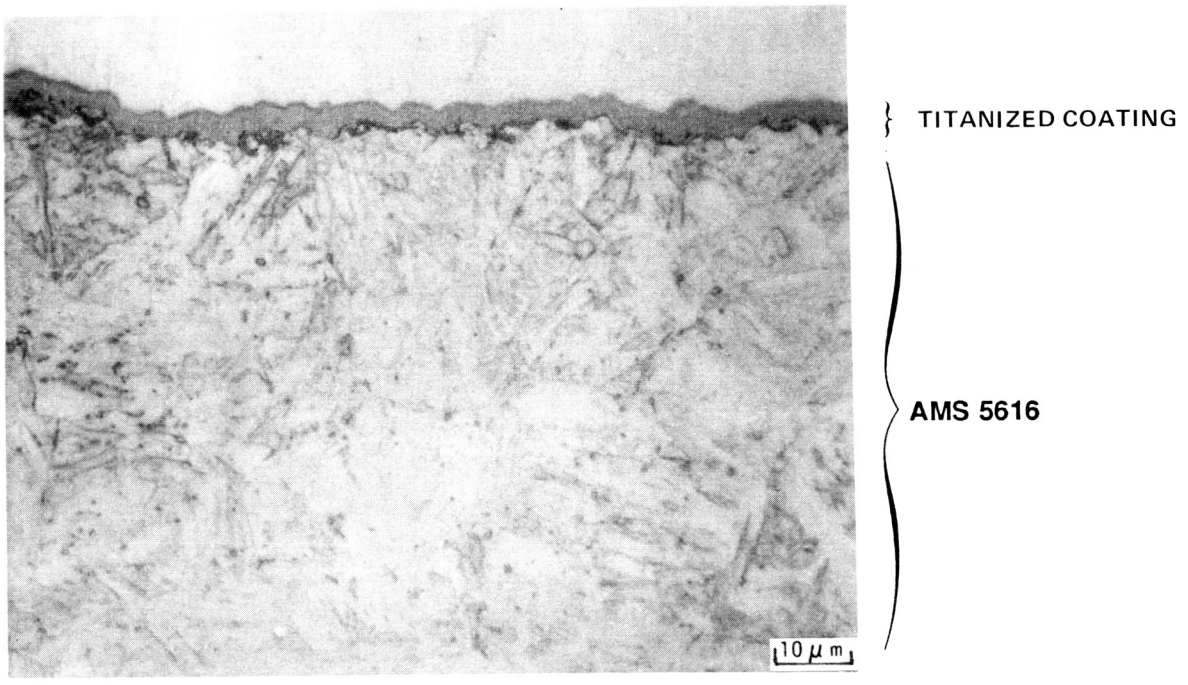

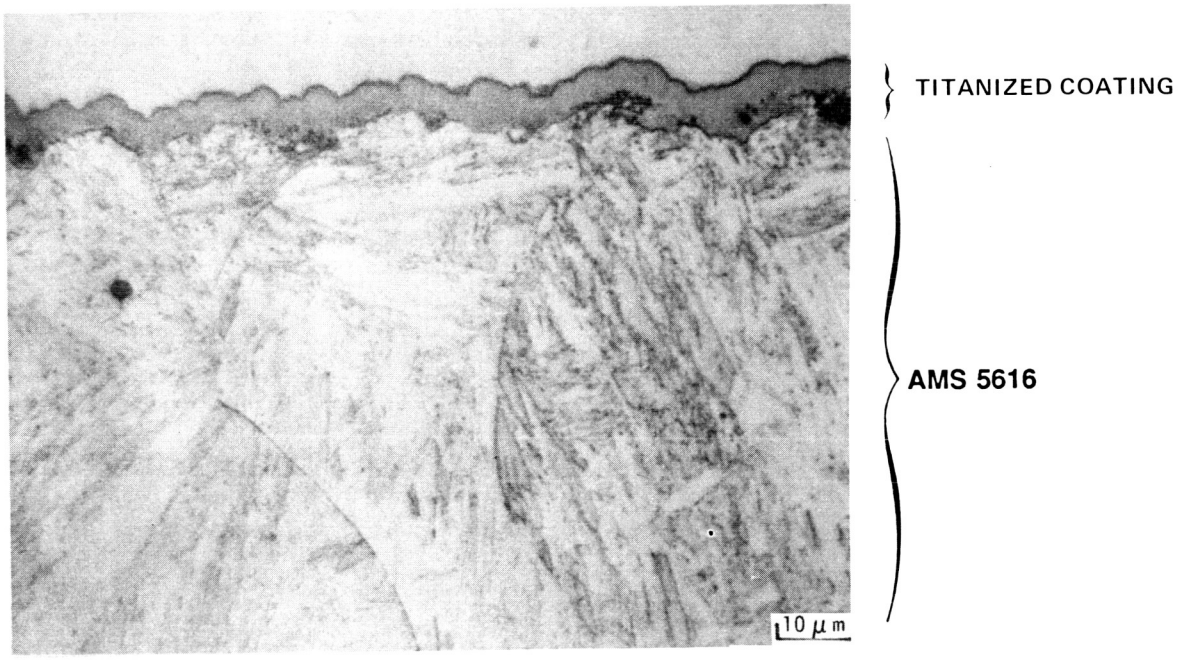

Figure 16 Coating Microstructures Following Pack Titanizing AMS 5616 at 980°C (1800°F)/6 hours (top) and 1040°C (1900°F)/24 hours (bottom) Etch: Villela's

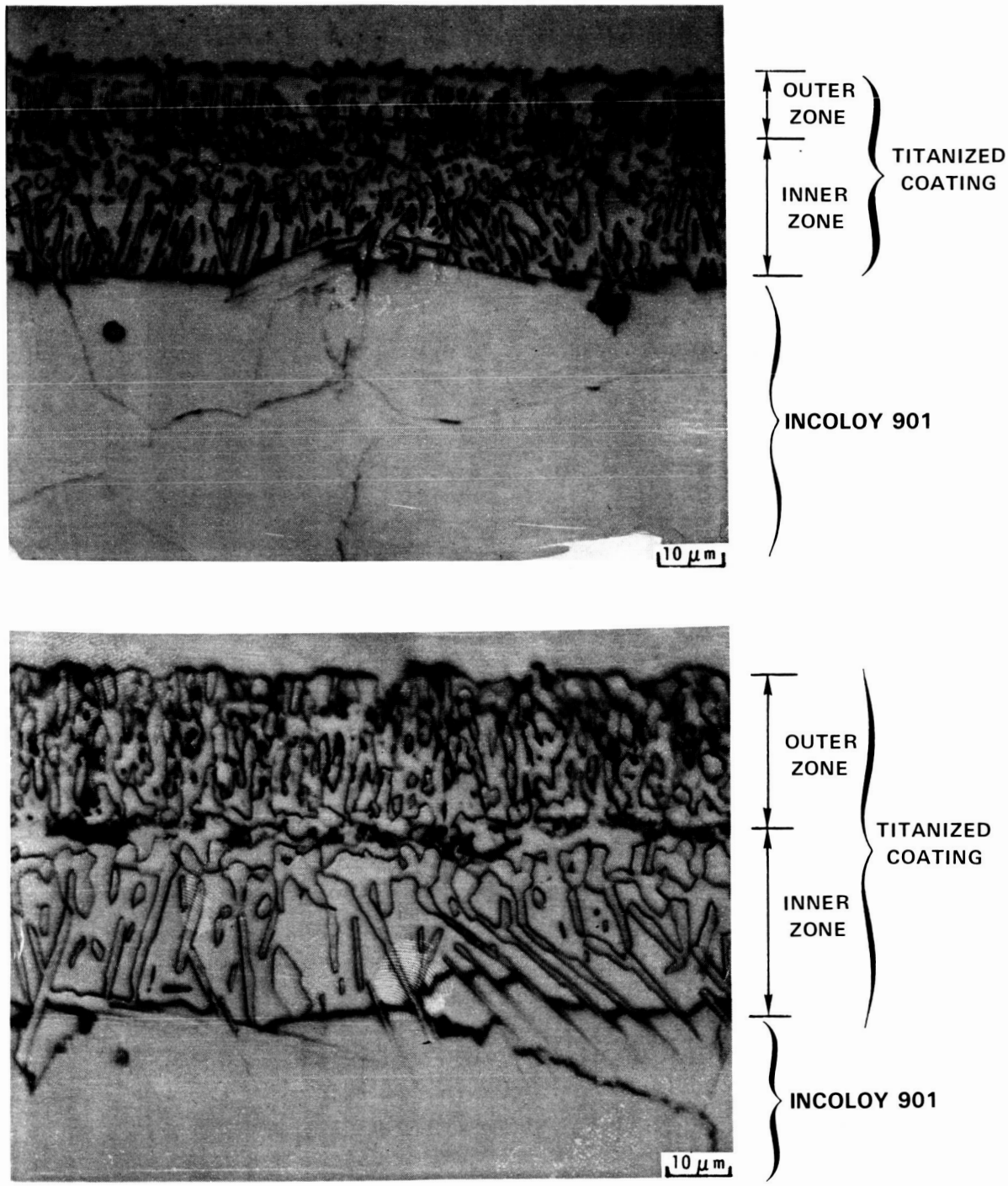

Figure 17 Coating Microstructures Following Pack Titanizing Incoloy 901 at 980°C (1800°F)/6 hours (top) and 1040°C (1900°F)/24 hours (bottom) Etch: Aqueous Ferric Chloride

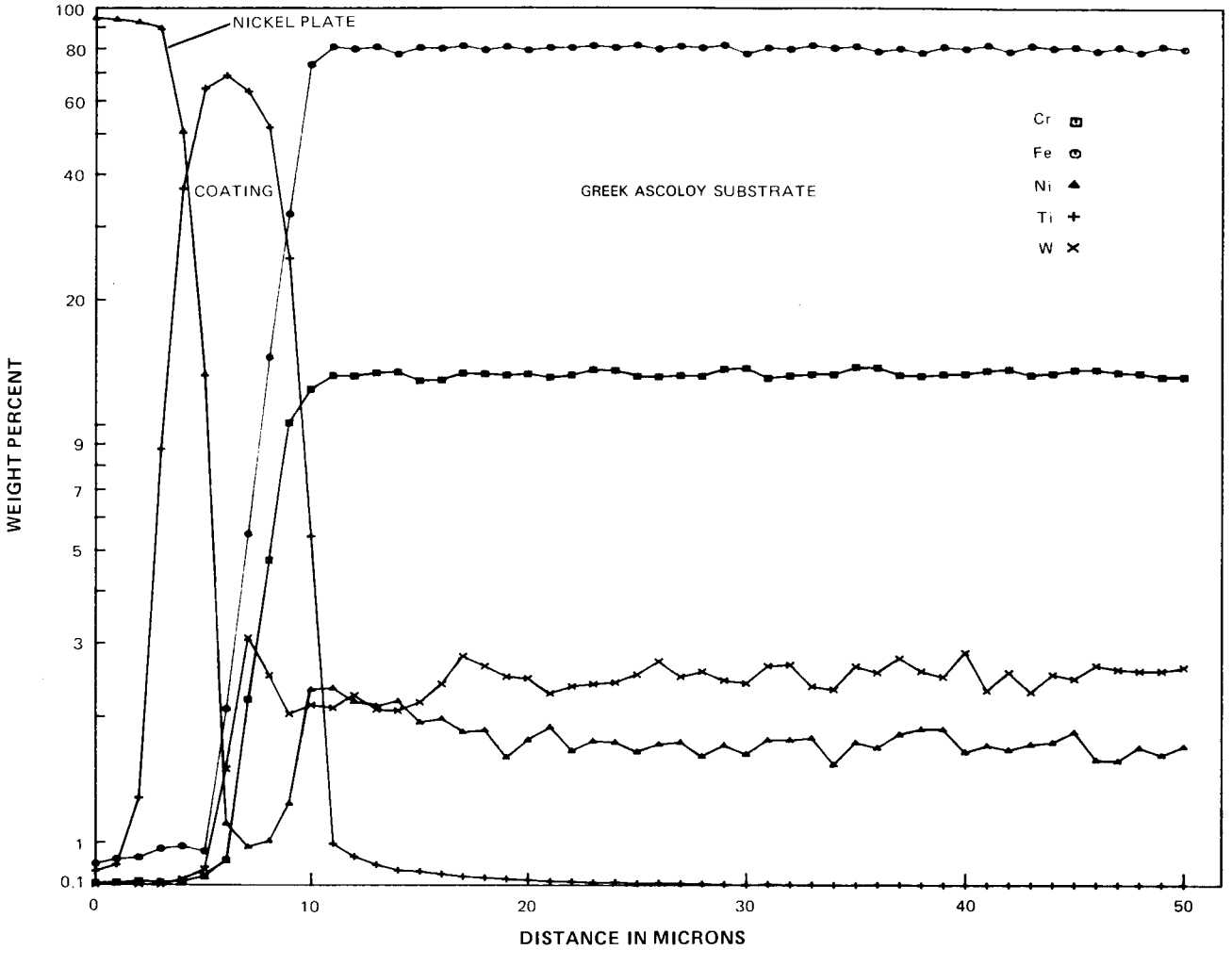

Figure 18 Electron Micrograph Concentration Profile Traces, Elemental X-Ray Images of Titanized AMS 5616. Coating Cycle: 1040°C (1900°F) for Six Hours

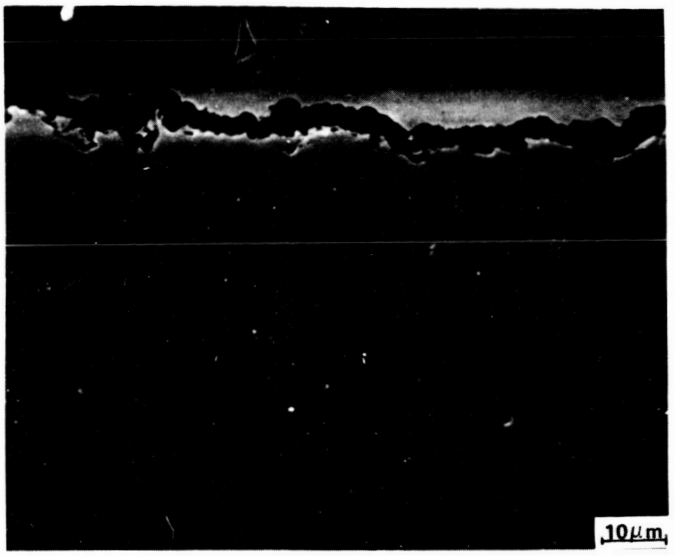

} COATING

ELECTRON MICROGRAPH

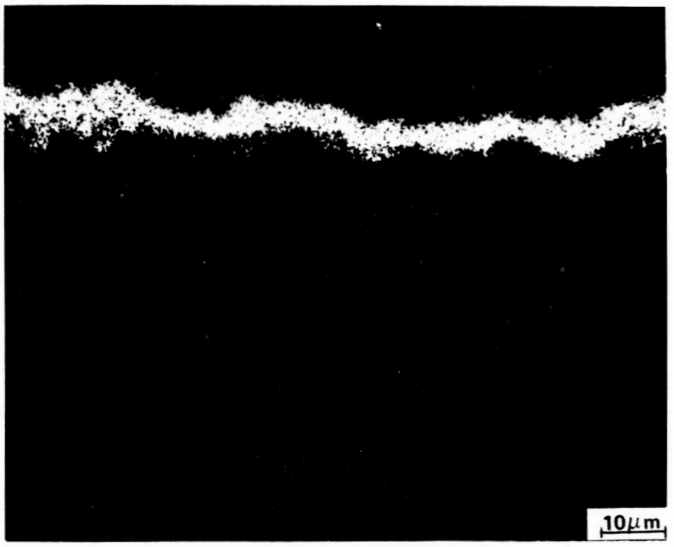

Ti X-RAY

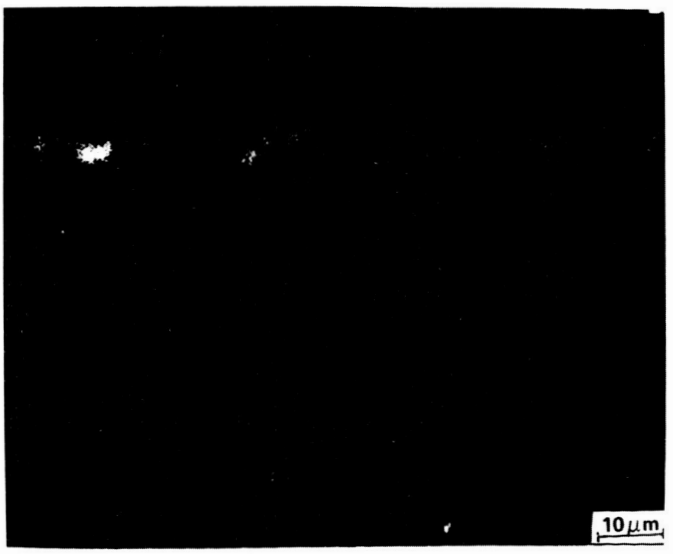

Al X-RAY

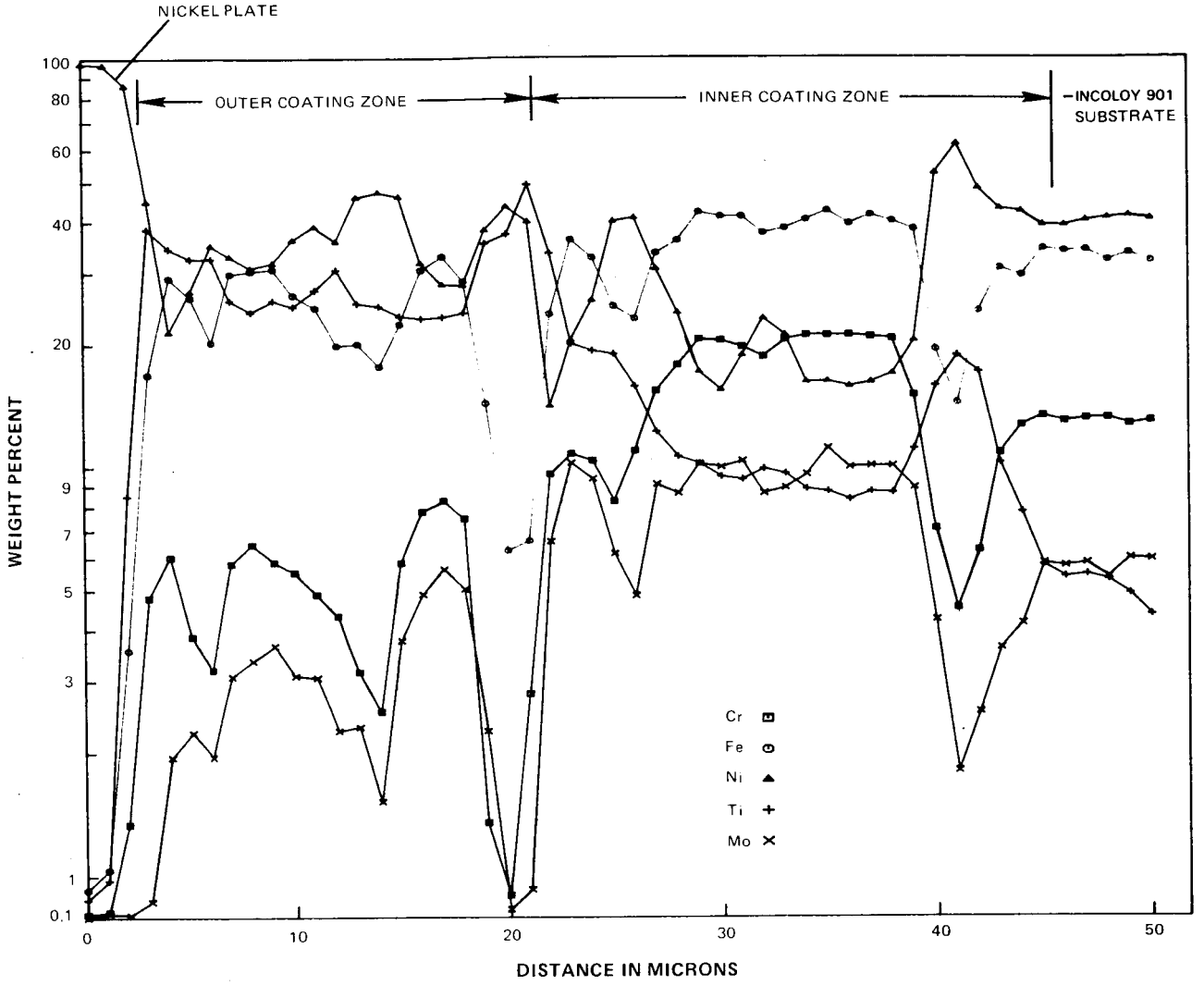

Figure 19 Electron Micrograph Concentration Profile Traces, Elemental X-Ray Images of Titanized Incoloy 901. Coating Cycle: 1040°C (1900°F) for Six Hours

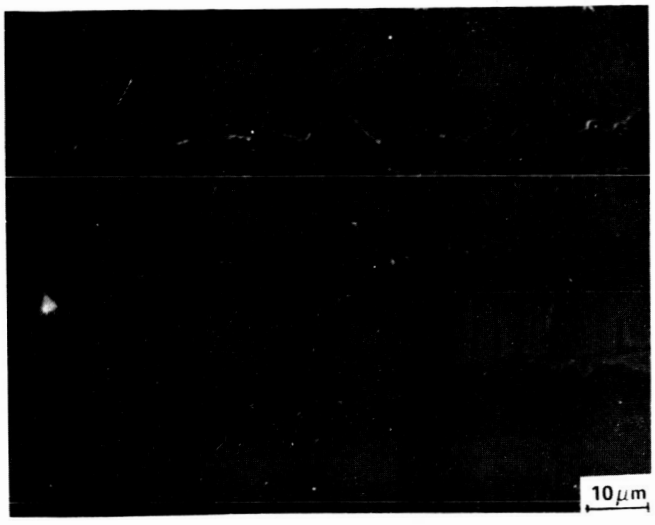

ELECTRON MICROGRAPH

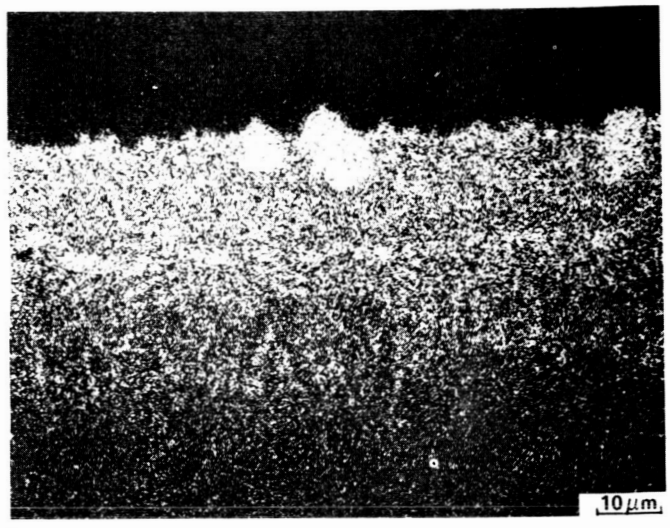

Ti X-RAY

Fe X-RAY

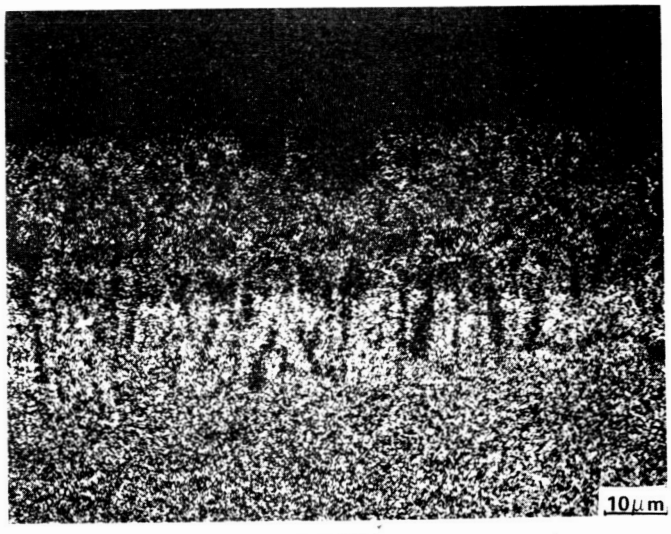

Cr X-RAY

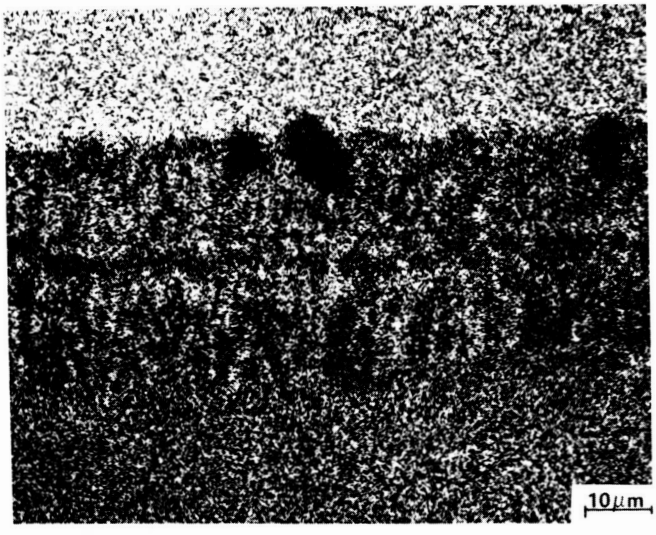

Ni X-RAY

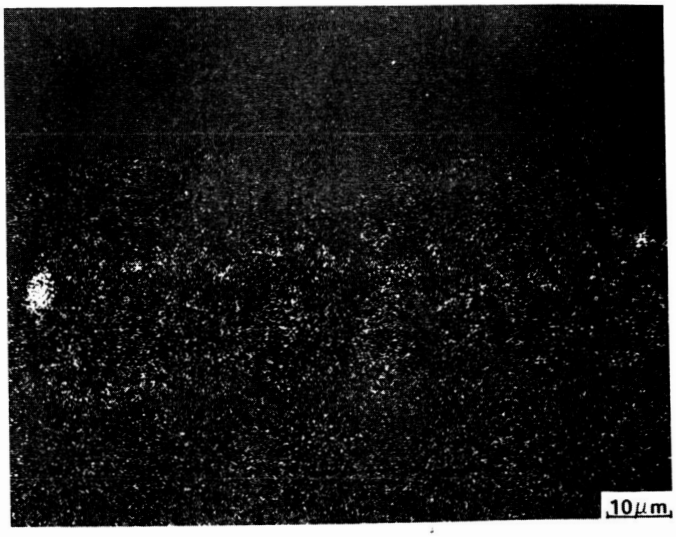

Mo X-RAY

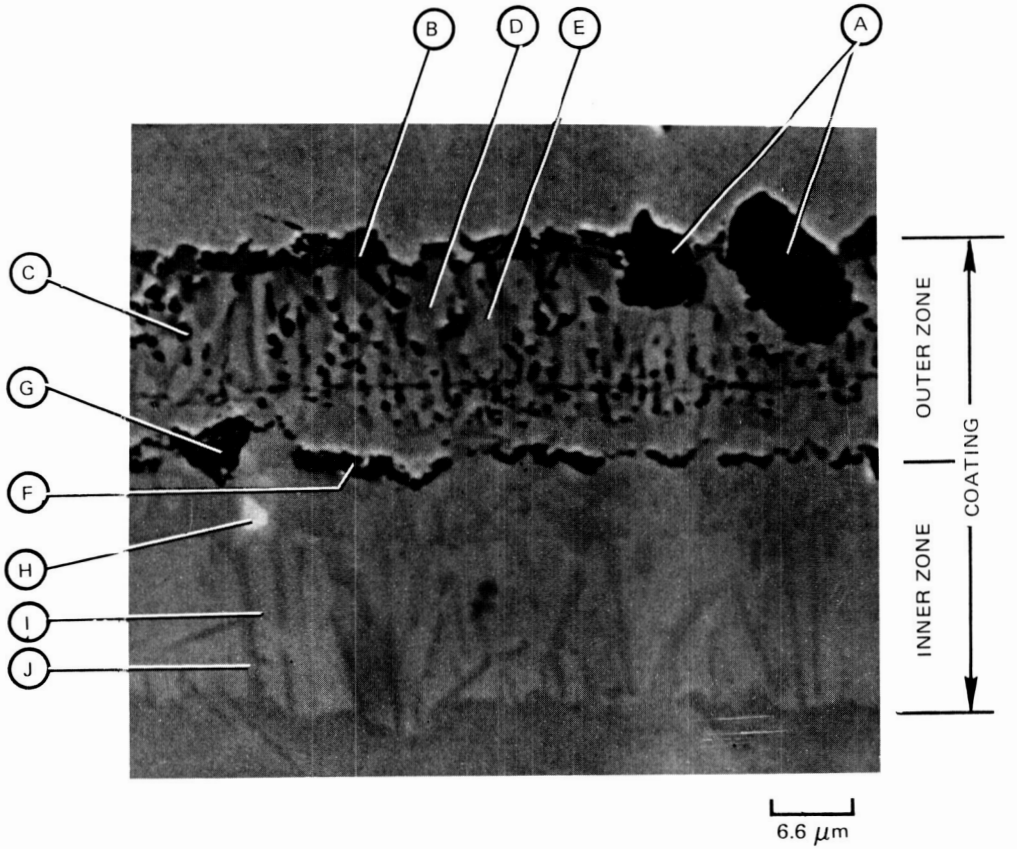

A. TITANIUM ENRICHED COATING PARTICLE
B. TITANIUM ENRICHED SURFACE LAYER
C. TITANIUM ENRICHED COATING PARTICLE
D. Ti, Fe, Ni ENRICHED PHASE
E. Ni, Ti ENRICHED PHASE
F. TITANIUM ENRICHED LAYER
G. Al., Ti ENRICHED PARTICLE
H. Mo ENRICHED PHASE
I. Fe, Cr, Ni, Ti ENRICHED PHASE
J. Ni, Ti ENRICHED PHASE

Figure 20 Electron Micrograph of Titanized Incoloy 901 Showing Location of Coating Phases

(c) Boronizing

Based on the coating microstructure and thickness obtained in the pack chromizing and titanizing trials, a 1040°C (1900°F)/6 hours cycle was chosen for processing both coatings on Greek Ascoloy and Incoloy 901 alloys prior to boronizing. Boronizing trials were conducted at 870°C (1600°F) and 925°C (1700°F). A metallographic examination of these specimens was then made which provided the following results:

(1) Greek Ascoloy

- Boron diffusion depths with chromized Greek Ascoloy ranged from 2.5 to 13 microns (0.1 to 0.5 mils) for boronizing cycles of 870°C (1600°F)/6 hours and 925°C (1700°F)/16 hours, respectively (Figure 21).

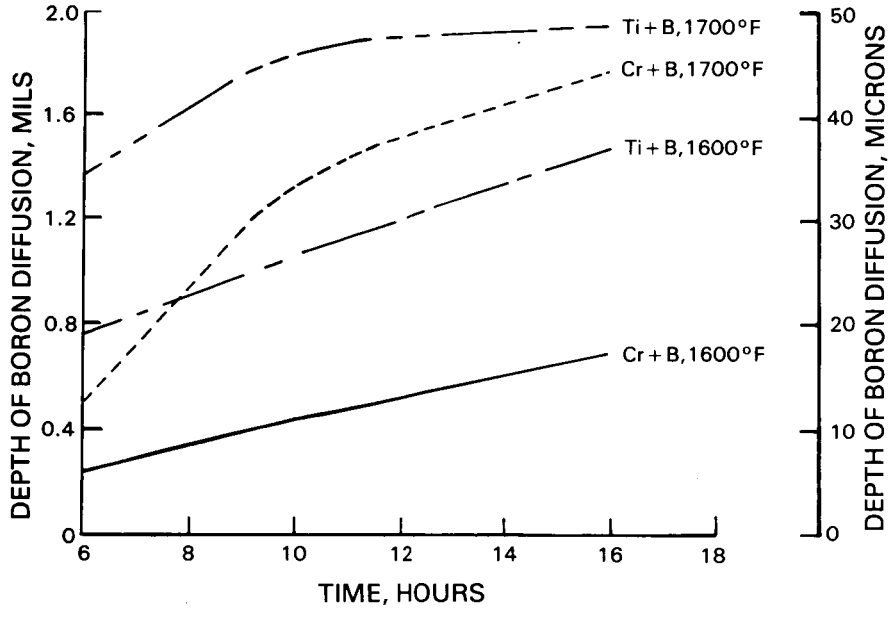

Figure 21 Mean Depth of Boron Diffusion Into Chromized AMS 5616

- While the initial chromized layer was single phase, the Cr+B coating on Greek Ascoloy consisted of two distinct zones (Figure 22). The two zone formation was attributed to a continued inward diffusion of chromium from the chromium enriched surface. The depth of boron diffusion did not exceed the thickness of the outer chromize zones on any of the trials.

- Within the inner zone, the precipitation of at least one additional phase was observed. Heat treatment investigations revealed that this phase was due to the thermal exposure during boronize processing (Figure 23) and not to boron diffusion throughout the entire chromize zone.

- The titanize coating on Greek Ascoloy exhibited no apparent changes in microstructure following boronizing, which is indicative of little or no boron diffusion.

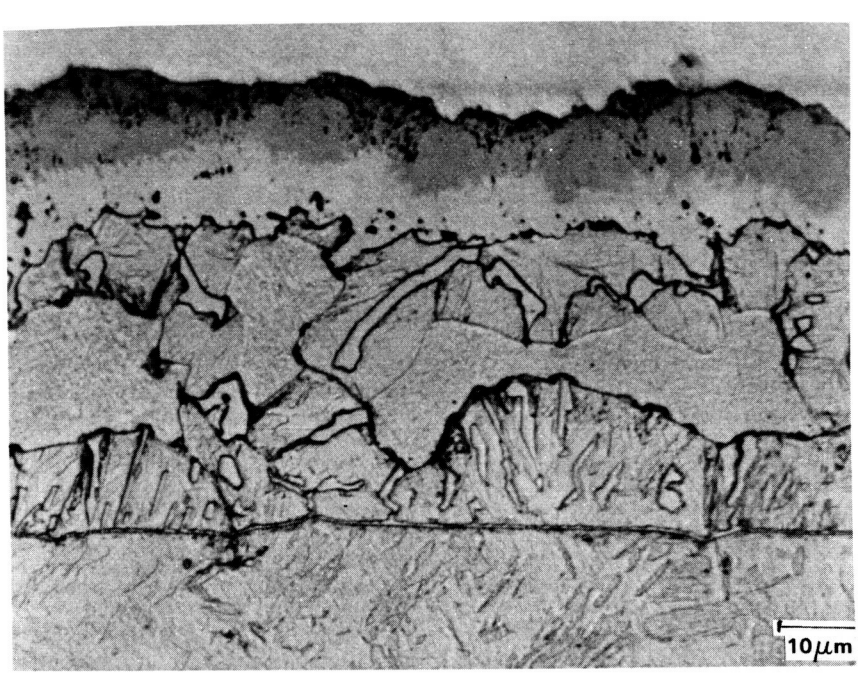

1035°C (1900°F)/6 HR CHROMIZE
925°C (1700°F)/10 HR BORONIZE

Figure 22 Microstructure of Chromize Plus Boronize Coating on AMS 5616
Etch: Villela's

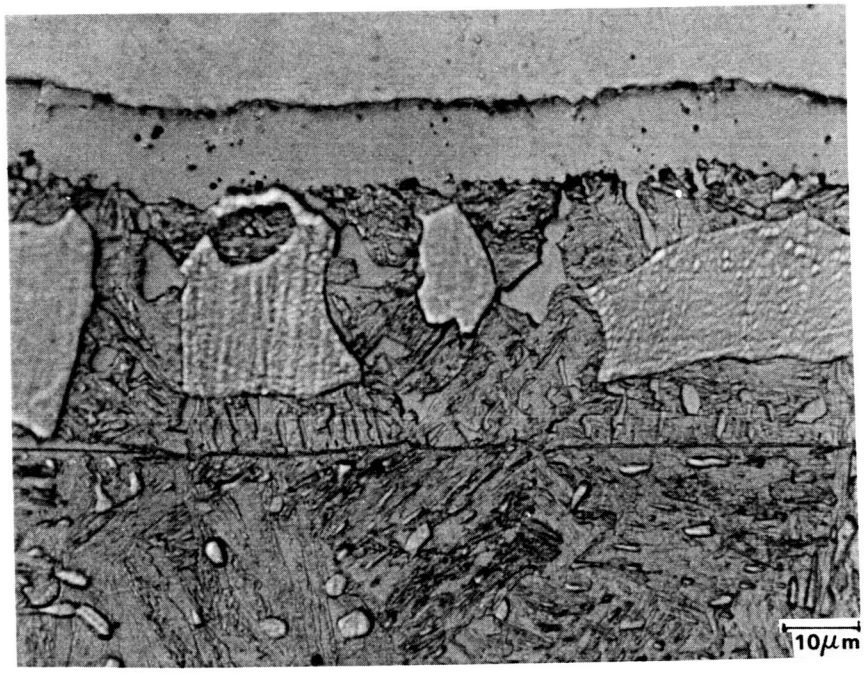

1035°C (1900°F)/6 HR CHROMIZE
925°C (1700°F)/HR HEAT TREATMENT

Figure 23 Microstructure of Heat Treated Chromize Coating on AMS 5616
Etch: Villela's

(2) Incoloy 901

- Boron diffusion depths into chromized Incoloy 901 ranged from 5 to 51 microns (0.2 - 2.0 mils) for boronizing cycles of 870°C (1600°F)/6 hours and 925°C (1700°F)/16 hours, respectively (Figure 24). The depth of boron diffusion did not exceed the thickness of the chromize coating with the 870°C (1600°F)/6 hours 870°C (1600°F)/10 hours and 927°C (1700°F)/6 hours coating trials (Figure 25).

- Boron diffusion depths into titanized Incoloy 901 ranged from 18 to 51 microns (0.7 to 2.0 mils) for boronizing cycles of 870°C (1600°F)/6 hours and 925°C (1700°F)/16 hours, respectively (Figure 24). The depth of boron diffusion exceeded the thickness of the titanize coating with the 927°C (1700°F)/16 hours coating cycle. There was no preferential boron diffusion along grain boundaries.

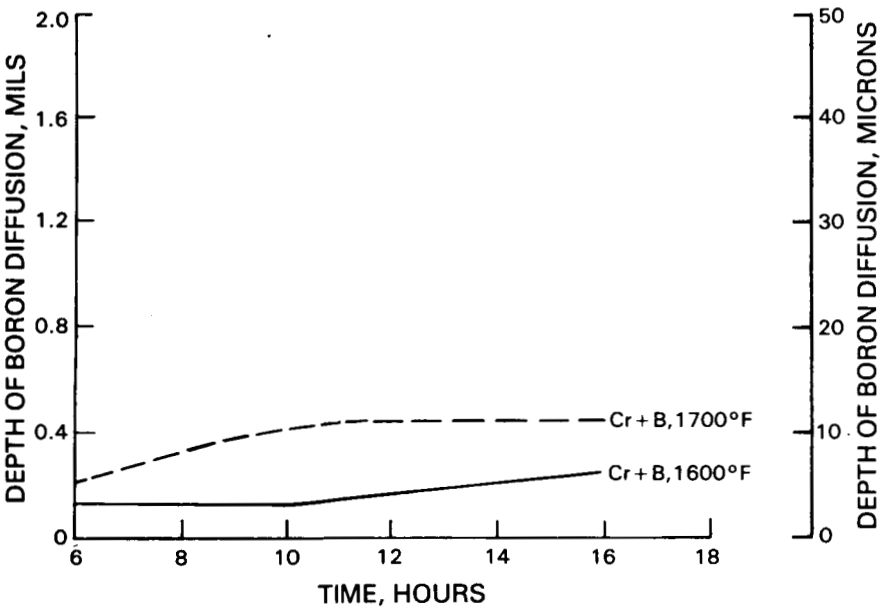

Figure 24 Mean Depth of Boron Diffusion Into Chromized AMS 5616 and Incoloy 901

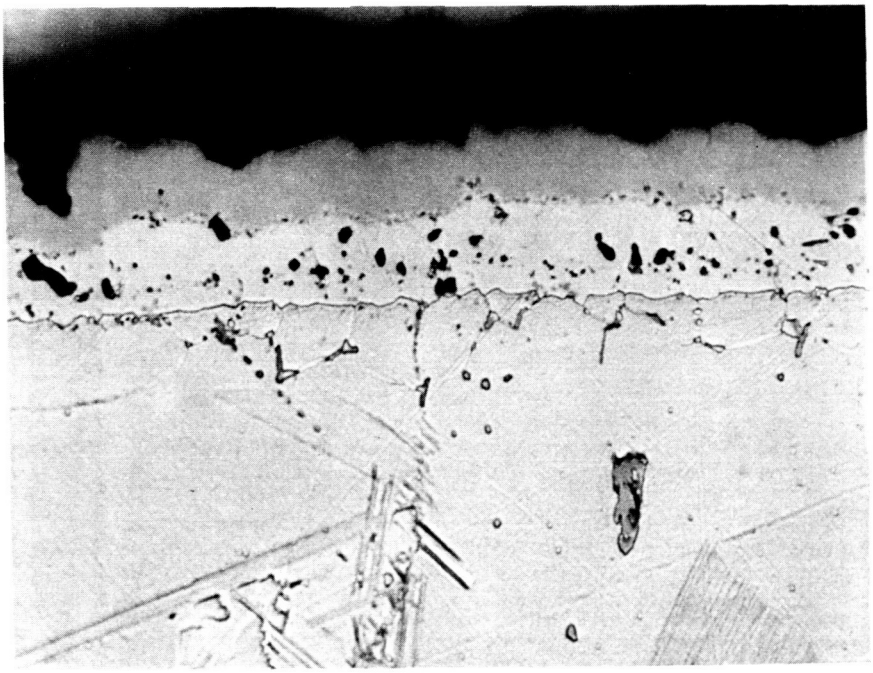

Figure 25 Microstructure of Incoloy 901 Showing Uniform Boron Diffusion Into Chromized Region
Etch: Aqueous Ferric Chloride

(D) Diffusion Coating on AMS 4928

(1) Coating Compositions and Temperatures Evaluated

(a) Nitride

Titanium alloy specimens were sent to Quality Heat Treating in Burbank, California for nitriding using a cyanide salt bath process.

Metallographic examination of processed specimens revealed no apparent nitride layer on the titanium alloy. Microhardness measurements indicated no measurable increase in alloy surface hardness within the outer 127 microns (5 mils). Therefore, this coating was eliminated from additional evaluations.

(b) CVD TiB_2

Application of chemical vapor deposited (CVD) titanium diboride (TiB_2) onto AMS 4928 was performed by Refractory Composites, Inc., Pacoima, California. Initial test specimens exhibited spallation of the TiB_2 coating. Metallographic examinations revealed a severely degraded coating/substrate interface which was deemed to be the cause of TiB_2 spallation. Process modifications by Refractory Composites did not result in acceptable coating adhesion. Thus, the CVD TiB_2 coating was not given further consideration.

No temperature variations were performed for nitriding or CVD TiB_2 as the vendors did not want to deviate from their standard coating parameters.

TASK III - LABORATORY EVALUATION OF COATINGS

Based on the microstructure analysis and screening erosion tests of Task II, coating systems were selected for further evaluation. The selected plasma spray and pack coating systems and application parameters that were evaluated are presented below and shown in Figure 26.

PLASMA SPRAY COATINGS ON AMS 4928, AMS 5616 and INCOLOY 901

Powder Composition	Coating Equipment	Vendor
88WC-12Co	35 KW	P&W
88WC-12Co	80 KW	P&W
88WC-12Co	Low pressure chamber	Metco Inc.
88WC-12Co	Gator-Gard	UTMP
83WC-17Co	60 KW	Metco Inc.
83WC-17Co	Low pressure chamber	Metco Inc.
90WC-10Co	Detonation Gun	Linde Div. of Union Carbide Corp.

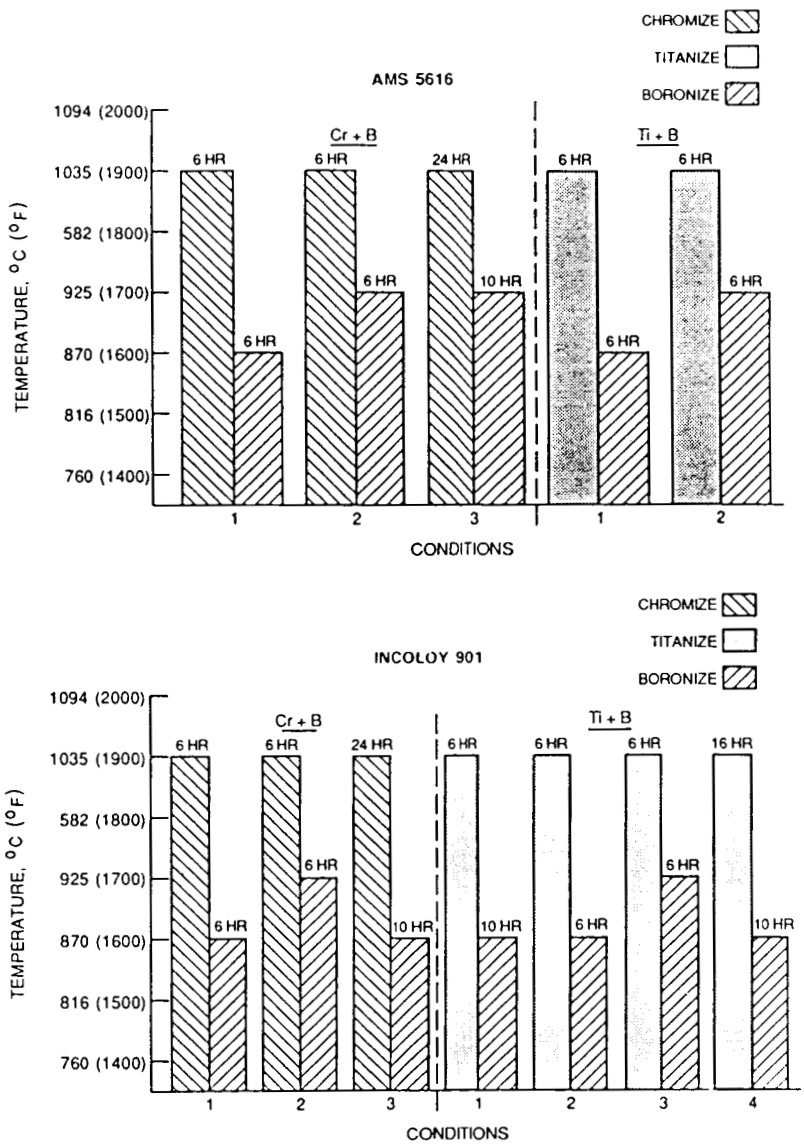

Figure 26 Diffusion Coating Parameters

In addition to these coating systems, further efforts were made to apply a TiB_2 coating onto AMS 4928. Sandia National Laboratories had disclosed the development of a CVD TiB_2 coating applicable to titanium alloys. However, we could not reach an agreement for them to coat specimens for evaluation.

Another system, commercially available and applicable to steel and metal alloys, was the BORAFUSE™ coating. This coating, produced by the Materials Development Corp., Medford, Ma, is applied by pack diffusion techniques and consists of a boron rich layer applied directly to the substrate at a temperature of 1500-1600°F.

All of the candidate coating systems on steel and nickel alloys were compared to electro-deposited TiB_2 which was the baseline system. The TiB_2 coating was applied by United Technologies Research Center from a molten salt bath.

Laboratory tests to characterize the coatings consisted of the following:

1) metallographic determination of coating microhardness and coating microstructure
2) room temperature erosion tests
3) high cycle fatigue tests

(A) Coating Structure and Hardness

Metallographic examination of all coating systems evaluated quality, morphology, uniformity (with respect to thickness and phase distribution) and the condition of the coating/substrate interface. The similarity of the coating microstructures to those observed in Task II was indicative of the repeatability of the coating process. Results of the metallographic analyses are discussed below and typical microstructures are shown in Figure 27.

(1) Plasma spray coating microstructures consisted of either a high concentration of discrete carbides or a low to intermediate concentration of discrete carbides.

(2) On Incoloy 901, Cr+B and Ti+B diffusion coatings exhibited a two zone microstructure, the outer zone being chromium-boron or titanium-boron rich, and the inner zone being chromium or titanium rich (Figure 28). On AMS 5616, the Cr+B coating was two zone, while the Ti+B coating was a thin, one zone structure.

(3) The Borafuse coating on both AMS 5616 and Incoloy 901 substrates exhibited a one zone, single phase microstructure (Figure 29).

(4) The electro-deposited TiB_2 coating exhibited a single zone columnar structure typical of electrodeposited coatings (Figure 30).

Coating microhardness was measured using a Leitz microhardness unit. The results are summarized in Tables III and IV.

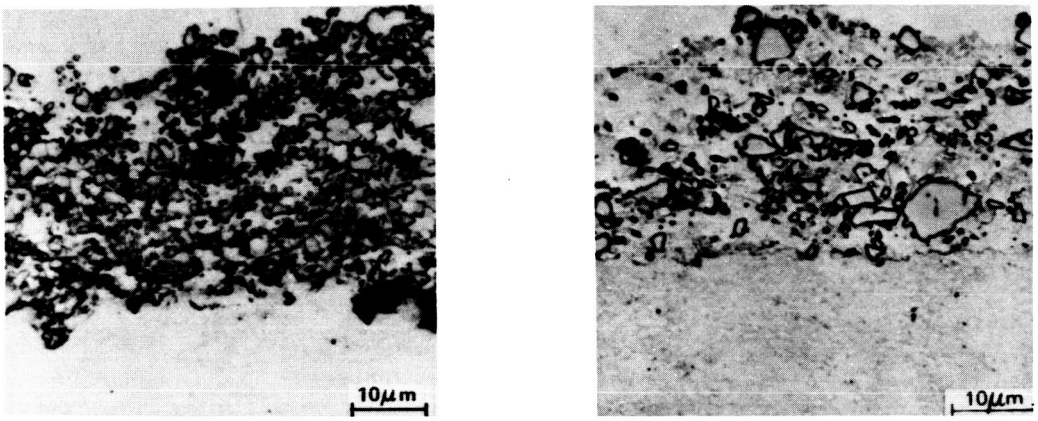

High concentration
of discrete carbides

Low concentration
of discrete carbides

Figure 27 Plasma Coating Microstructures

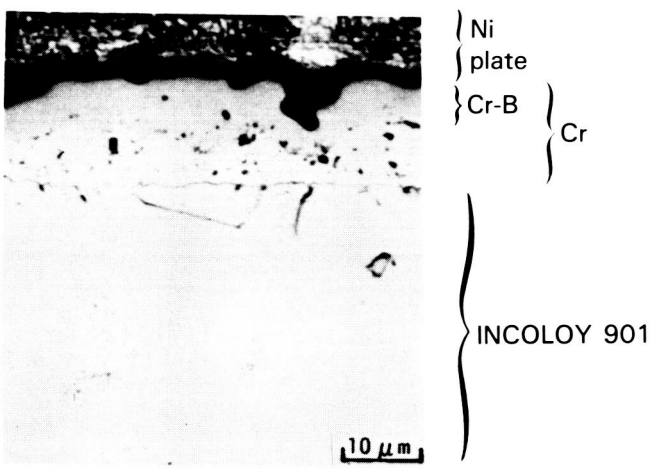

Figure 28 Microstructure of Cr+B Diffusion Coating on Incoloy 901

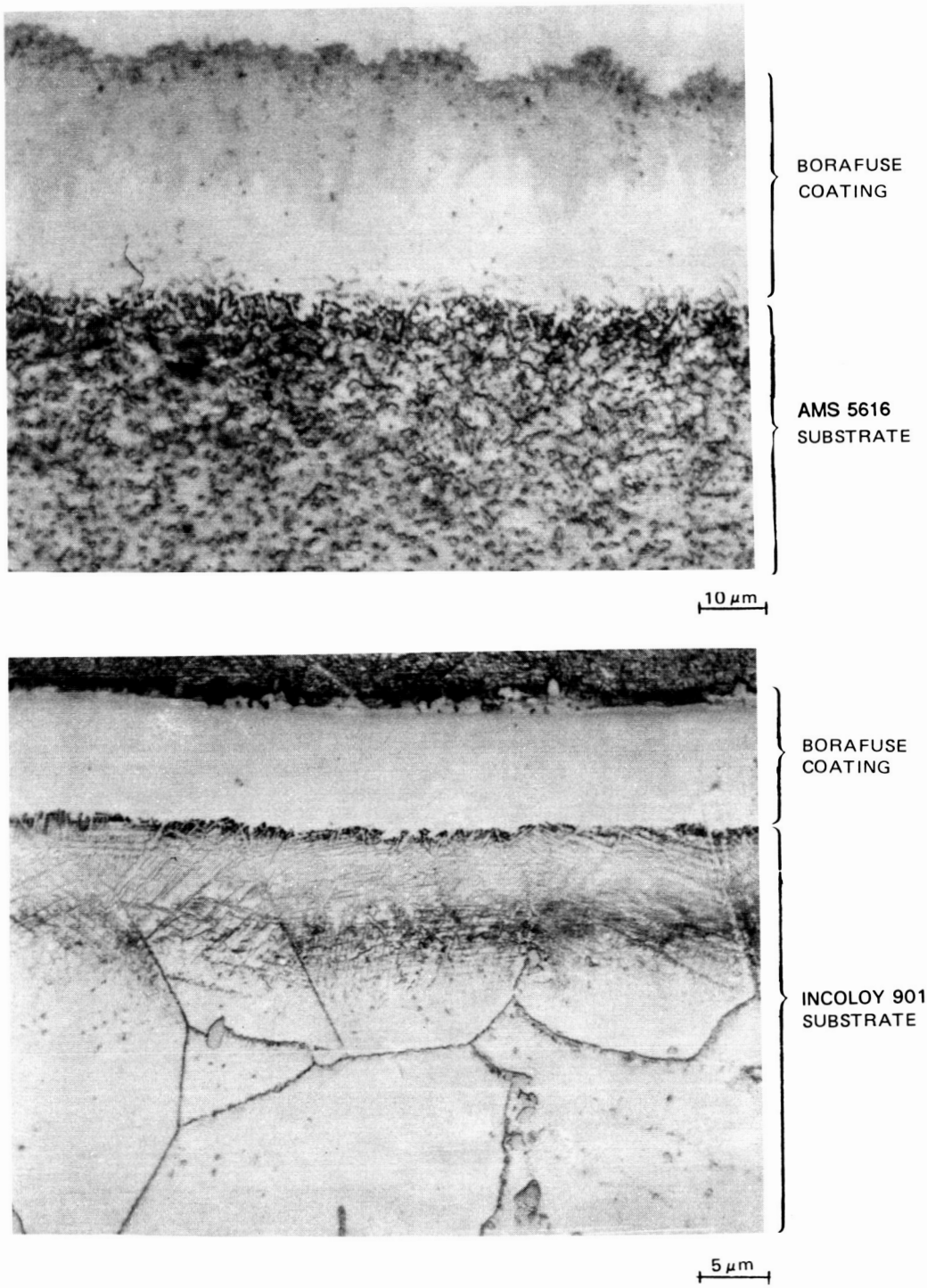

Figure 29 Borafuse Coating Applied to AMS 5616 and Incoloy 901

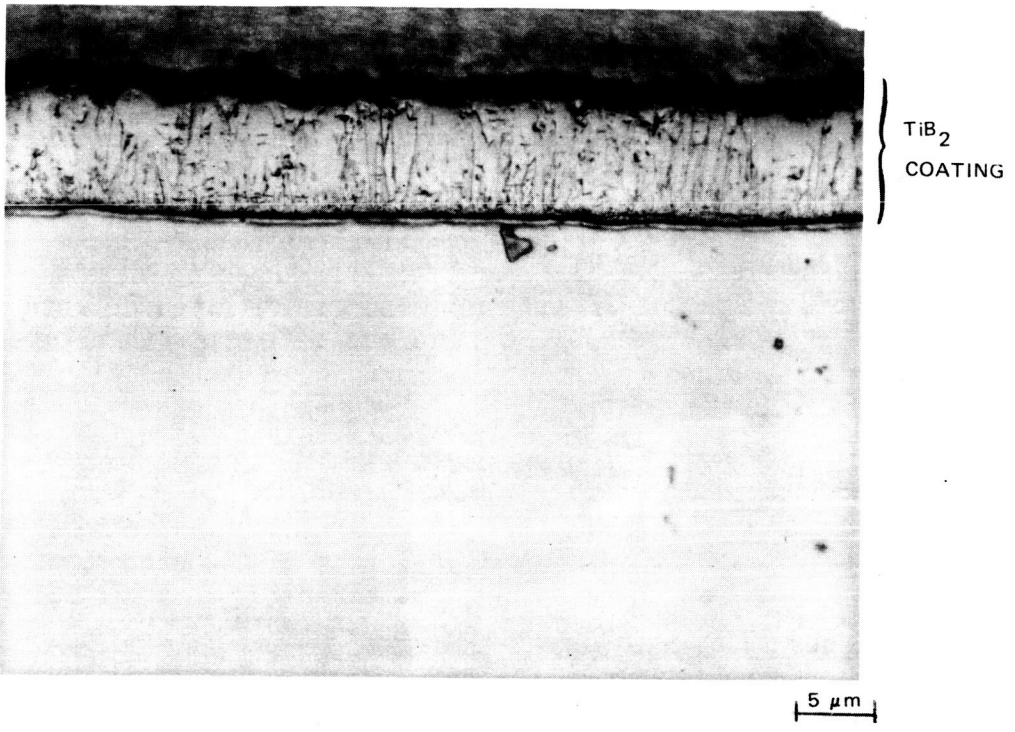

Figure 30 Electrodeposited TiB_2 on Incoloy 901

TABLE III
HARDNESS OF PLASMA SPRAY COATINGS

Powder Compostion	Coating Equipment	Microhardness Range (Vickers)
88WC-12Co	80 KW	980-1230
88WC-12Co	35 KW	870-1170
88WC-12Co	Gator-Gard	950-1220
88WC-12Co	Low Pressure Chamber	990-1150
83WC-17Co	60 KW	1190-1270
83WC-17Co	Low Pressure Chamber	1110-1290
90WC-10Co	Detonation Gun	1010-1170

TABLE IV
HARDNESS OF DIFFUSION AND ELECTRO-DEPOSITED COATINGS
ON AMS 5616 AND INCOLOY 901

Coating Type	Substrate	Microhardness Range (Vickers)
Diffusion		
Cr+B	AMS 5616	
chromize layer		200-370
chromize-boronize layer		1050-1150
Cr+B	Incoloy 901	
chromize layer		660-970
chromize-boronize layer		940-1180
Ti+B	Incoloy 901	
titanize layer		610-1060
titanize-boronize layer		1140-1350
Borafuse	AMS 5616	1400
Borafuse	Incoloy 901	1400
Electro-deposited		
TiB_2	AMS 5616	1400
TiB_2	Incoloy 901	1400

(B) Erosion Resistance

Erosion testing of coated test panels was performed using an S.S. White Airbrasive Unit (Figure 31). Testing was performed at three abrasive impingement angles; 20, 45 and 90 degrees. Two tests were performed per coating per alloy. Evaluation of the test data revealed the following:

(1) Plasma spray coating microstructures characterized by high concentrations of discrete carbides exhibited superior erosion resistance compared to those with low discrete carbide concentrations (Figures 32 - 34). Coatings which contained a high concentration of discrete carbides improved erosion resistance at a 20° impingement angle by 2.5-3X compared to the uncoated condition. At the 90° impingement angle, all plasma applied coatings exhibited little improvement relative to the uncoated baseline.

(2) Cr+B diffusion coatings on Incoloy 901 exhibited an improvement of approximately 15X at a 20° impingement angle, as compared to the uncoated condition. The Borafuse coating exhibited an improvement of approximately 1.5X while the Ti+B coating showed no improvement in erosion resistance. Erosion at a 90° impingement angle resulted in a 12X improvement for Cr+B and no improvement with the Ti+B and Borafuse coatings.

(3) Cr+B diffusion coatings on AMS 5616 exhibited an improvement of approximately 4.5X at a 20° impingement angle, as compared to the uncoated condition. Borafuse coated specimens exhibited an improvement of approximately 1.5X. Specimens coated with Ti+B showed no improvement in erosion resistance. At 90°, a 2.3X improvement was noted for Cr+B and no improvement for the Ti+B and Borafuse coatings.

(4) Electro-deposited TiB_2 was the most erosion resistant coating on both AMS 5616 and Incoloy 901 alloys (Figure 35). The TiB_2 coating exhibited minimal weight and volume losses throughout the duration of the tests. This erosion behavior was exhibited at all three abrasive impingement angles. As was previously noted, electro-deposited TiB_2 was included for baseline comparisons only. Previous field service evaluations on compressor airfoils performed by Pratt & Whitney revealed that electro-deposited TiB_2 experienced significant chipping on airfoil leading edges which disrupts laminar airflow.

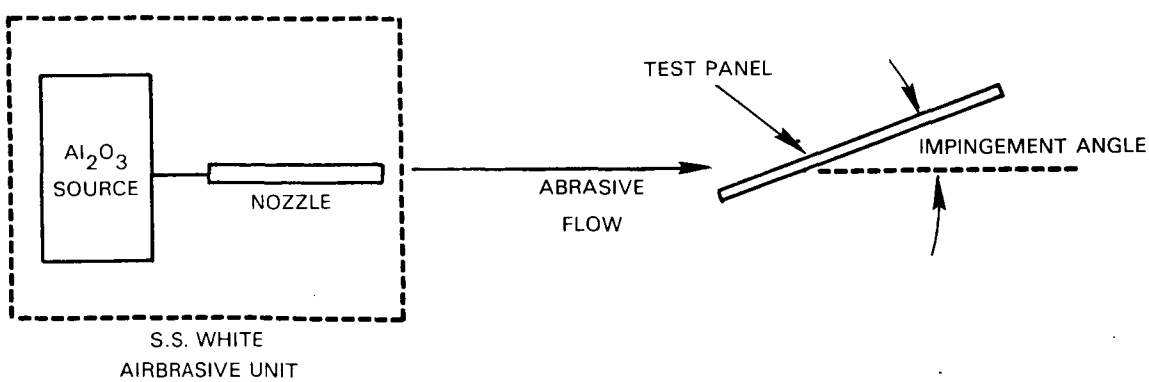

Figure 31 Schematic of Panel Erosion Test

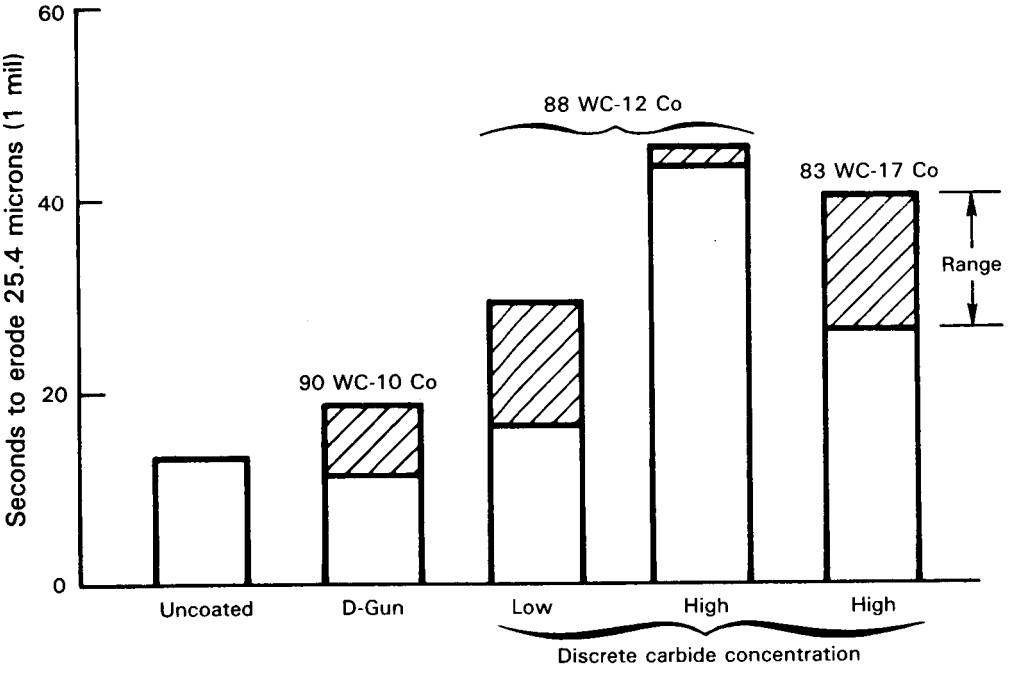

Figure 32 Plasma Coating Erosion Resistance on AMS 4928 at a 20° Impingement Angle

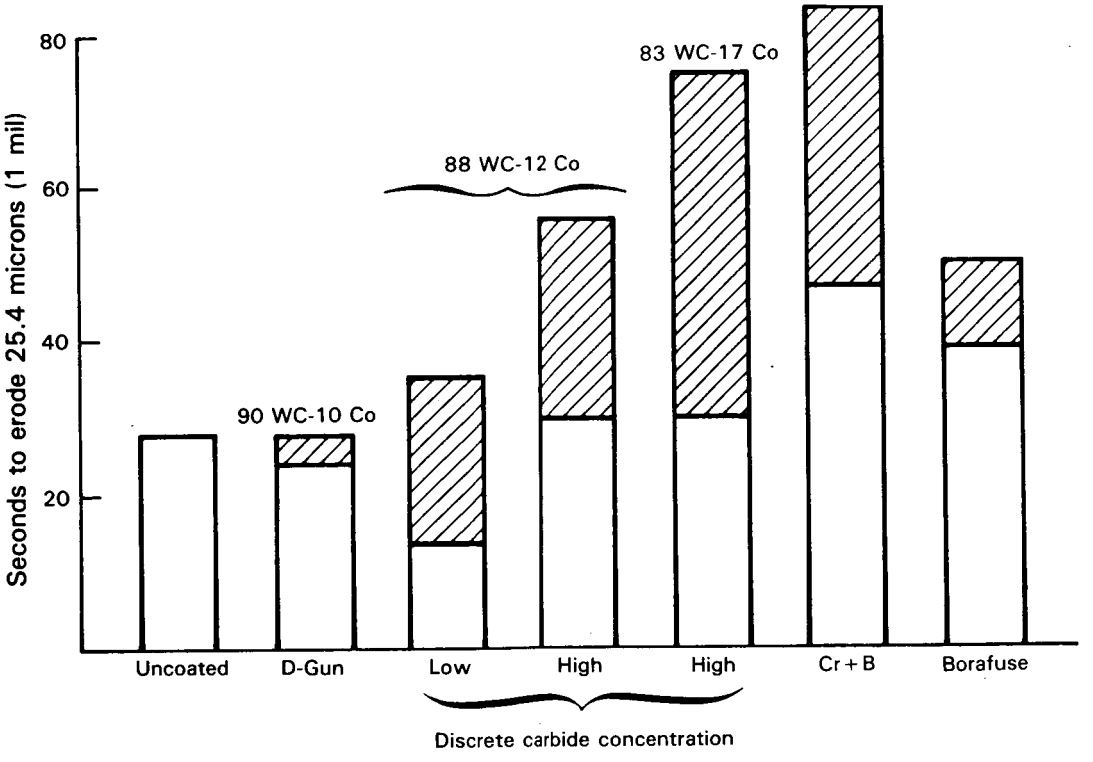

Figure 33 Plasma Coating Erosion Resistance on AMS 5616 at a 20° Impingement Angle

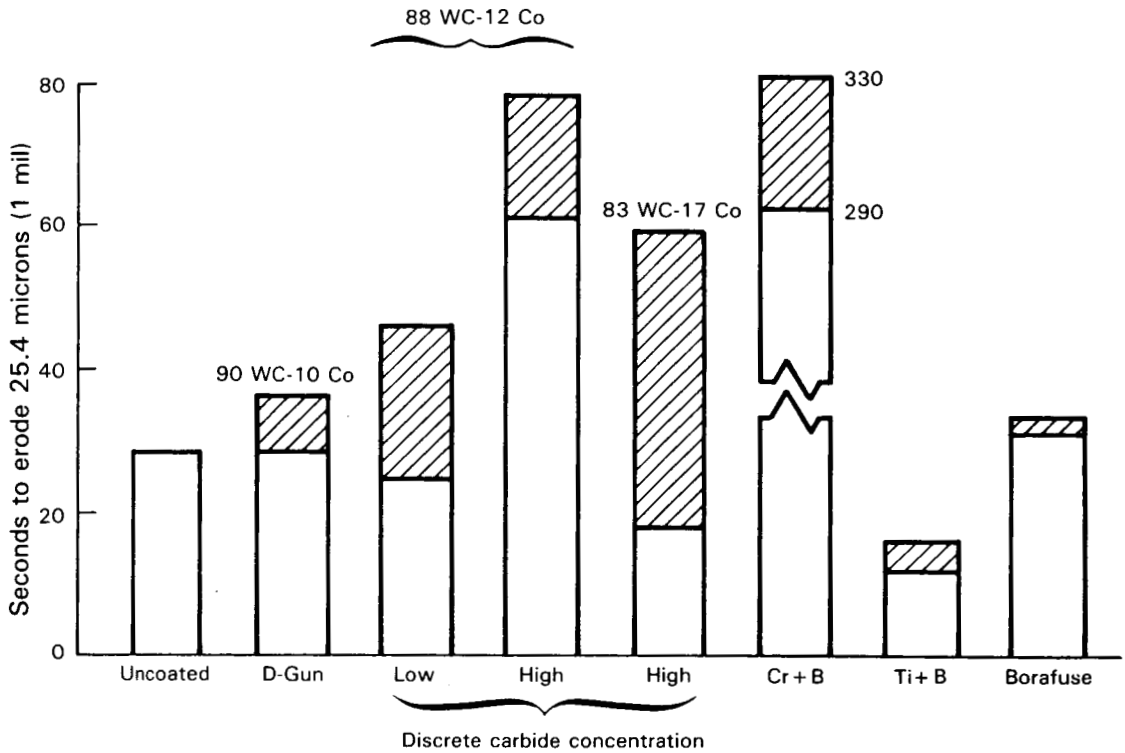

Figure 34 Coating Erosion Resistance on Incoloy 901 at a 20° Impingement Angle

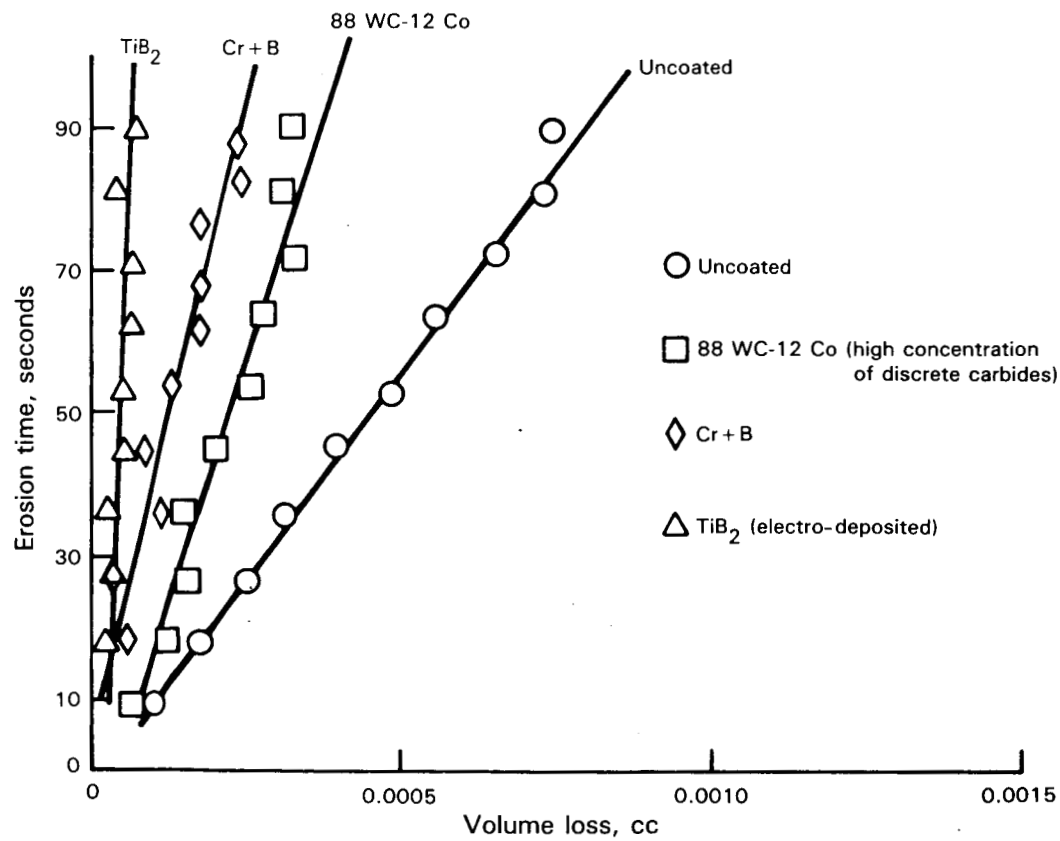

Figure 35 Coating Erosion Resistance on AMS 5616 at a 20° Impingement Angle

(C) High Cycle Fatigue

The following coating systems, in addition to baseline uncoated specimens, were evaluated in high cycle fatigue testing:

Alloy	Coating System
AMS 4928	Uncoated
AMS 4928	Gator-Gard applied 88WC-12Co powder
AMS 4928	Low pressure chamber sprayed 88WC-12Co powder
Incoloy 901	Uncoated
Incoloy 901	Cr+B diffusion coating
Incoloy 901	Ti+B diffusion coating
Incoloy 901	Gator-Gard applied 88WC-12Co powder
AMS 5616	Uncoated
AMS 5616	Cr+B diffusion coating
AMS 5616	Gator-Gard applied 88WC-12Co powder

During Task III, high cycle fatigue testing of five coatings and a baseline uncoated alloy was performed to more clearly define the behavior of candidate coatings. These HCF tests utilized a tapered Krouse specimen (Figure 36) which was coated on the entire gage section surface. Tests were conducted at room temperature using a frequency of 30 Hz. The required specimen deflection was applied using an adjustable eccentric pin connected to the loading arm. Data from HCF tests are shown in Figure 37 and indicated the following:

1) Significant HCF strength reductions and differences were observed for plasma spray coatings on AMS 4928 although the same 88WC-12Co powder lot was sprayed by both vendors and the coatings were similar in microstructure and microhardness.

2) AMS 5616 also exhibited reduced HCF strength for the coatings evaluated.

3) Incoloy 901 exhibited a lower than expected baseline HCF strength. Post test metallography revealed the base alloy to be of typical microstructure and microhardness. All coated specimens showed strengths higher than the baseline.

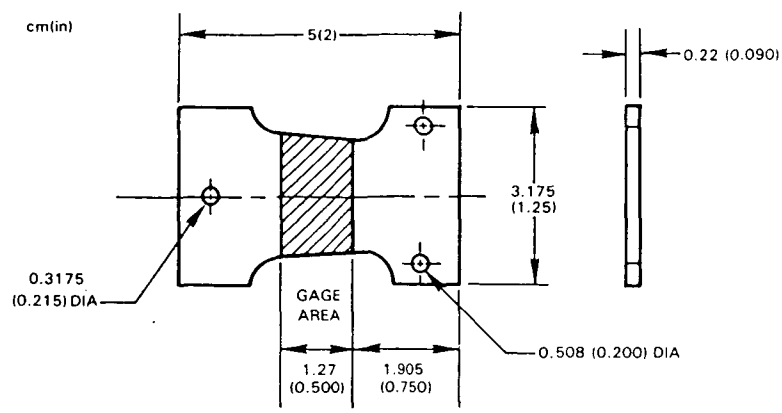

Figure 36 Tapered Krouse High Cycle Fatigue Test Specimen

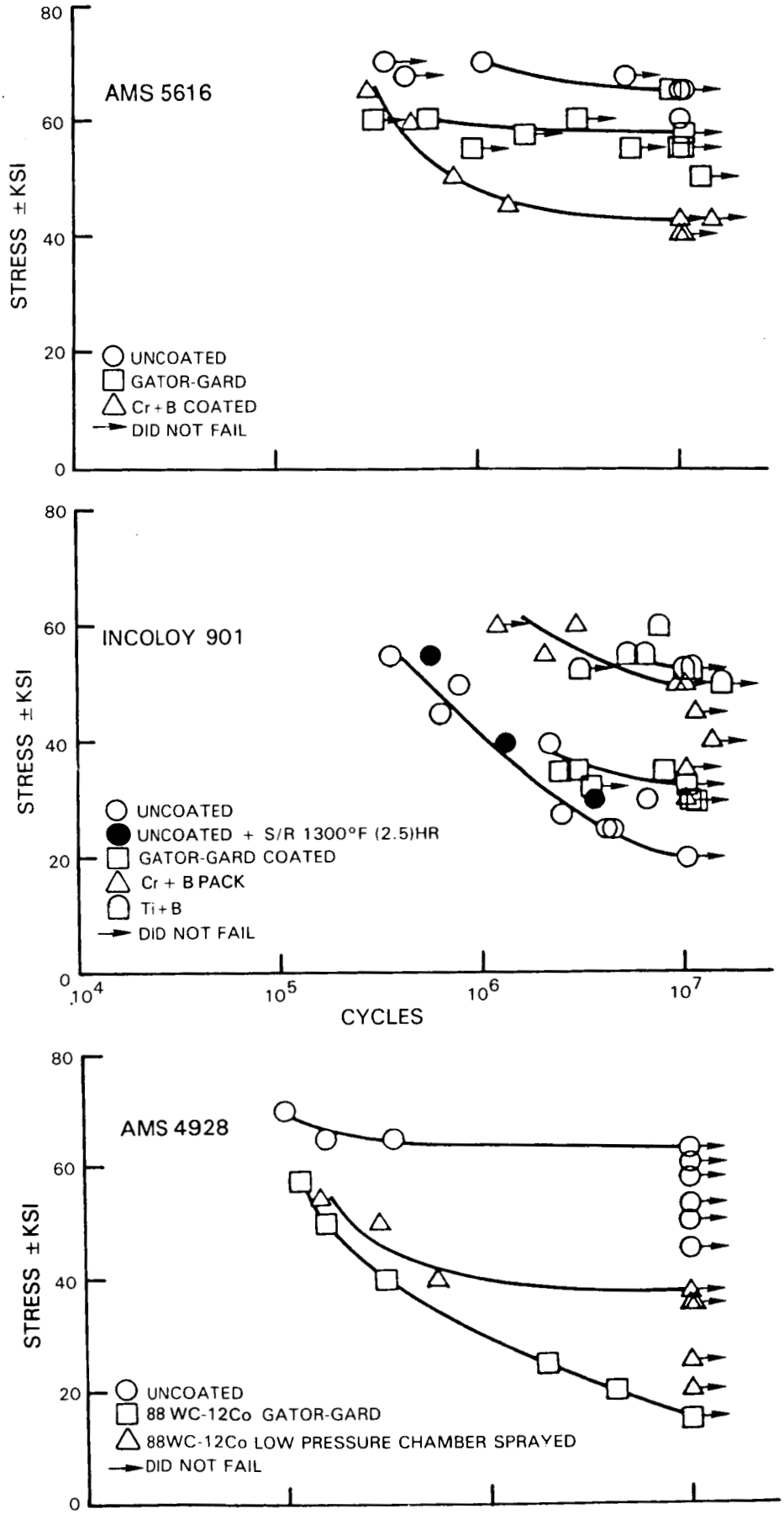

Figure 37 Room Temperature HCF Test Results

Based on the results of the erosion and high cycle fatigue tests, and metallographic examinations of the coating/substrate combinations, the following systems were selected for Task V and Task VI investigations.

(a) Coatings applied to AMS 4928

(1) 88WC-12Co powder, applied by the Gator-Gard plasma spray system
(2) 83WC-17Co powder, applied by the 60 KW plasma spray system

(b) Coatings applied to AMS 5616

(1) 83WC-17Co powder, applied by the 60 KW plasma spray system
(2) Chromium-boron diffusion coating, applied by a 1035°C(1900°F)/6 hr chromize cycle plus 925°C(1700°F)/10 hr boronize cycle

(c) Coatings applied to Incoloy 901

(1) 83WC-17Co powder, applied by the 60 KW plasma spray system
(2) 88WC-12Co powder, applied by the low pressure chamber spray (LPCS) plasma spray system
(3) 90WC-10Co powder, applied by the Linde D-Gun spray system
(4) Chromium-boron diffusion coating, applied by a 1035°C(1900°F)/6 hr chromize cycle plus 870°C(1600°F)/6 hr boronize cycle

The plasma coatings, with the exception of the D-Gun applied 90WC-10Co powder, have microstructures which are characterized by a high concentration of discrete carbides. This type of structure was found to provide the most erosion resistance. The D-Gun applied coating is commercially available and is presently used on a number of aircraft engine components as a wear resistant hardface coating, e.g. on fan blade midspan shrouds. Thus, it was included for component evaluations. The diffusion coating cycles selected represent coating systems which provided maximum erosion resistance with the most cost effective coating cycle.

TASK IV - DESIGN ANALYSIS AND COMPONENT/COATING SYSTEMS SELECTION

(A) Systems Selection

Compressor blade designs were evaluated to select the specific blade stages to demonstrate the effectiveness of the erosion resistant coatings. The selection was based on an analytical airfoil evaluation for (1) critical vibration modes and nodals during engine operation, (2) effects of coatings on airfoil fatigue strength, and 3) blade areas most prone to erosion blade designs were selected from current JT8D and JT9D engine models and included two configurations each of steel, nickel and titanium based alloys (AMS 5616, Incoloy 901, and AMS 4928, respectively).

Six airfoil stages were selected after an analytical evaluation of the vibration history, vibration modes and stress distributions of all JT8D and JT9D high pressure compressor stages. These evaluations coupled with high cycle fatigue test data of uncoated airfoils defined the airfoil surface to be coated in order to provide the desired erosion resistance to the blade without compromising component mechanical properties. The airfoil stages and coating systems are listed in Table V.

TABLE V
AIRFOIL STAGES AND COATING SYSTEMS

Airfoil Substrate	Coating System	Engine/Rotor Stage	Airfoil Quantities Coated
AMS 4928	(a) 83WC-17Co powder 60 KW plasma system	JT9D/7	16
		JT8D/8	44
	(b) 88WC-12Co powder Gator-Gard plasma system	JT9D/7	16
		JT8D/8	24
AMS 5616	a) 83WC-17Co powder 60 KW plasma system	JT8D/10	36
		JT8D/12	16
	(b) Cr + B Pack diffusion system	JT8D/10	24
		JT8D/12	24
Incoloy 901	(a) 83WC-17Co powder 60 KW plasma system	JT9D/14	36
		JT9D/15	16
	(b) 88WC-12Co powder Low pressure plasma system	JT9D/14	6
		JT9D/15	6
	(c) 90WC-10Co D-Gun system	JT9D/14	6
		JT9D/15	6
	(d) Cr+B Pack diffusion system	JT9D/14	14
		JT9D/15	14

Application of the erosion resistant coating was to be made to the outer 50% of the airfoil based upon the following:

1) Engine service history that indicated significant airfoil erosion occurred at the outer 50% of the airfoil.

2) The analytical evaluations of airfoil vibration and stress distributions indicated that at least the outer 50% of the blade span could be coated without compromising blade high cycle fatigue strength (Figure 38).

3) Standarized coating coverage to the outer 50% of each airfoil would simplify coating processing and minimize any possible application errors.

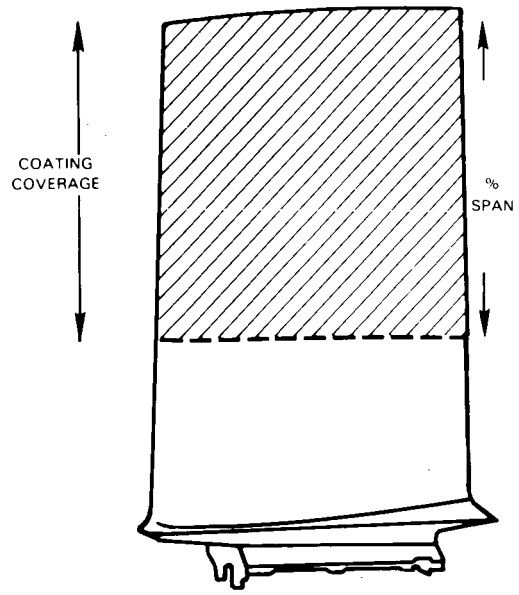

ENGINE MODEL	ROTOR STAGE	MAXIMUM ALLOWED COATING COVERAGE, % SPAN*
JT8D	8	73
	10	76
	12	60
JT9D	7	59
	14	59
	15	75

* SEE ADJACENT SKETCH

Figure 38 Airfoil Coating Coverage as Determined by an Analytical Evaluation of Airfoil Vibration and Stress Characteristics

TASK V AIRFOIL COATING OPTIMIZATION

Coatings were applied to the six compressor blade stages selected in Task IV. The coating application processes were optimized. Post coat AMS 4928, AMS 5616 and Incoloy 901 finishing techniques were employed to produce coatings with a 20-30AA surface finish. Measurements of the surface finish were made at selected airfoil locations to ascertain the uniformity of the finishing process. Metallographic examination was performed to measure the extent of coating removal.

(A) Coating Application

Plasma spray coatings were applied to the convex and concave airfoil surfaces to a target thickness of 25 to 64 microns (1-2.5 mils). The coatings were feathered out within 2.5 mm (0.1") of the 50% span location. A metal shadow and/or tape mask was used to prevent coating application onto the lower region of the blade. The selection of the particular type of mask was left to the discretion of the vendor; all masks appeared acceptable. Masking the lower portion of the airfoils being coated with the Cr+B systems required a different type of masking system, i.e., one that could withstand the 1035°C (1900°F)/6 hr chromize cycle and the 870-925°C (1600-1700°F)/6-10 hr boronize cycle. Investigations were conducted using various types of commercially available masking systems, e.g. M1 and M7, manufactured by Alloy Surfaces Co., as well as thin metal foils, such as nickel. Metallographic examination of Cr+B coated specimens which were masked by these systems revealed that only nickel foil was successful in preventing deposition of chromium or boron. However, use of nickel foil during the chromize cycle resulted in localized diffusion bonding of the foil to the airfoil surface with undesirable degradation of the substrate material in the affected zones. Bonding of the mask to the substrate did not occur during the boronize process. Application of a parting agent to the substrate beneath the nickel foil resulted in reduced instances of bonding of the mask to the airfoil.

Due to the inability to define an acceptable masking system for use during the chromize cycle, as well as the desire to increase the corrosion resistance of the steel compressor blades, the entire AMS 5616 airfoil surface was chromized. During the boronize cycle, the nickel foil mask was applied to prevent the formation of Cr+B coating on the high stress regions of the airfoil.

(B) Coating Thickness

Metallographic sections were made at three locations on at least one blade of each coating system of each rotor stage. Examination of these sections indicated that the coating microstructures were similar to those observed in Task III. The Gator-Gard, 60 KW and low pressure chamber sprayed coatings were characterized by a high concentration of small discrete carbides, while the D-Gun applied coatings had a non-uniform distribution of coarse discrete carbides. The Cr+B coatings on both AMS 5616 and IN 901 were characterized by two layers: a Cr+B rich outer layer and a Cr rich inner layer. Examination of the coatings to determine thickness distribution and uniformity indicated that the plasma coating vendors were generally able to maintain the target 25 - 64 micron (1 - 2.5 mil) coating thickness (Figure 39), with the exception being the JT9D 15th stage blades coated by Metco with the 60 KW system which exhibited significant variations from the target thickness. The plasma spray process with the greatest degree of coating uniformity was the Gator-Gard coating process, followed by the D-Gun, 60 KW and low pressure chamber spray processes.

The pack diffusion Cr+B system was superior to the plasma spray coatings in maintaining coating thickness uniformity, although the process was not capable of meeting the minimum target thickness of 25 microns (1 mil).

(C) Surface Finish

Aerodynamic analytical evaluations have indicated that a high pressure compressor airfoil surface finish of 20-30AA is desired in order to maintain required performance levels (Figure 40). Therefore, surface finishing efforts were directed towards defining processing procedures to produce the desired degree of surface smoothness. As the coatings, by their nature, are hard, it was anticipated that techniques to improve their surface finish would need to be, by neccesity, very aggressive. Two finishing techniques were evaluated; 1) abrasive tumbling and 2) overcoating with SermeTel W, a corrosion resistant coating applied to ferrous alloys and manufactured by SermeTel, Inc. Surface texture measurements using a 0.010" cutoff, and peak counts at 50 and 250 microinch levels) were made at various airfoil locations with a Bendix Profilometer.

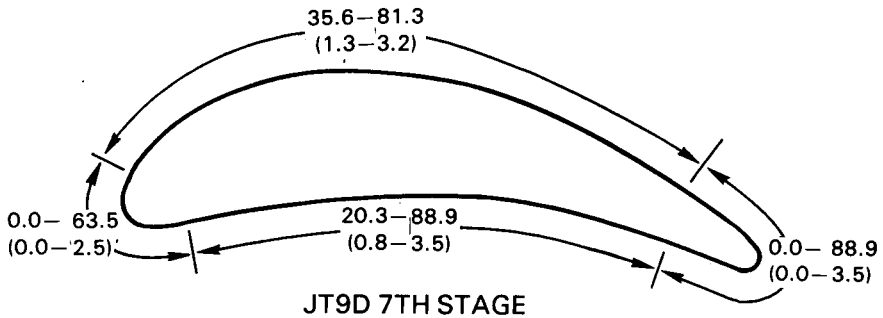

JT9D 7TH STAGE
METCO 83WC-17Co, 60KW

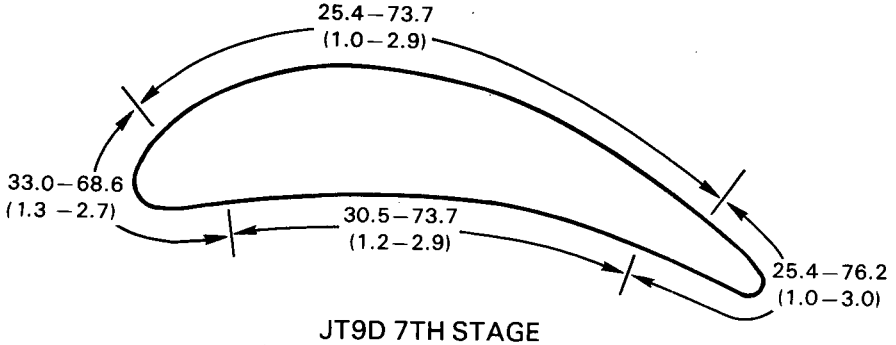

JT9D 7TH STAGE
UTMP 88WC-12C0, GATOR-GARD

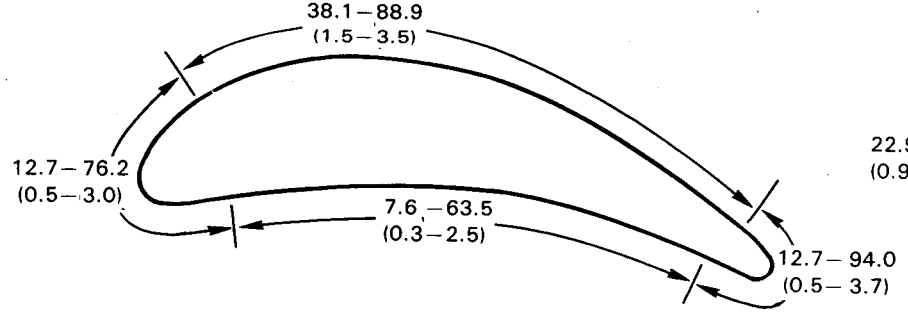

JT8D 8TH STAGE
METCO 83WC–17Co, 60 KW

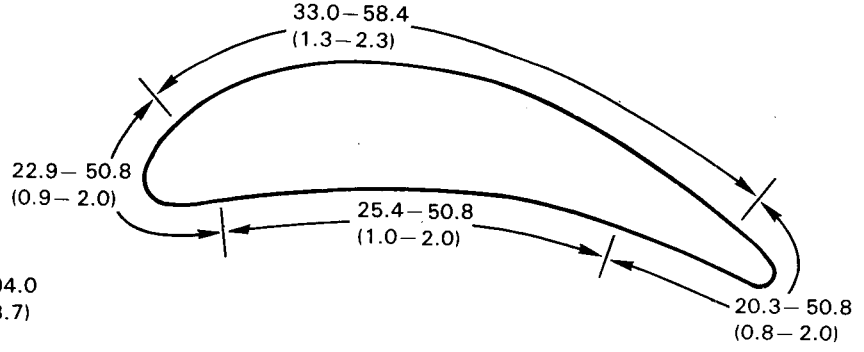

JT8D 8TH STAGE
UTMP 88WC-12Co, GATOR-GARD

Figure 39 Thickness Schematics of Plasma Sprayed and Diffusion Applied Coatings. Thickness in Microns (mils)

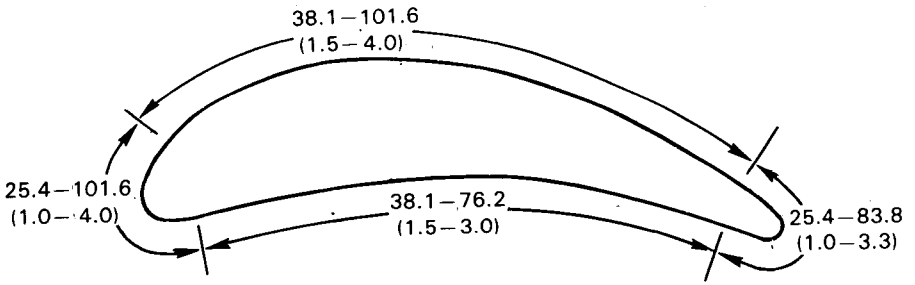

JT8D 10TH STAGE
METCO 83WC-17Co, 60KW

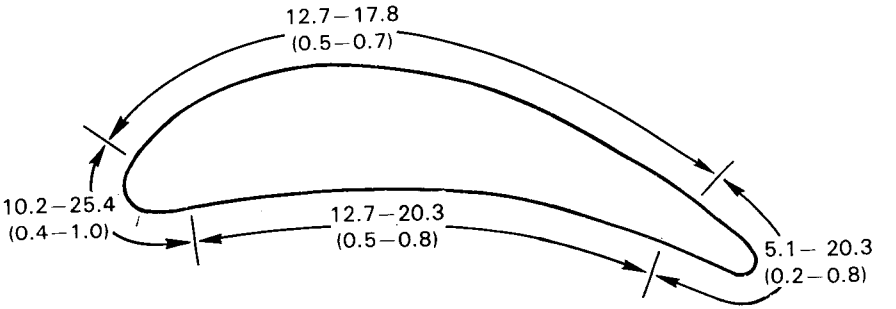

JT8D 10TH STAGE
P&W Cr + B

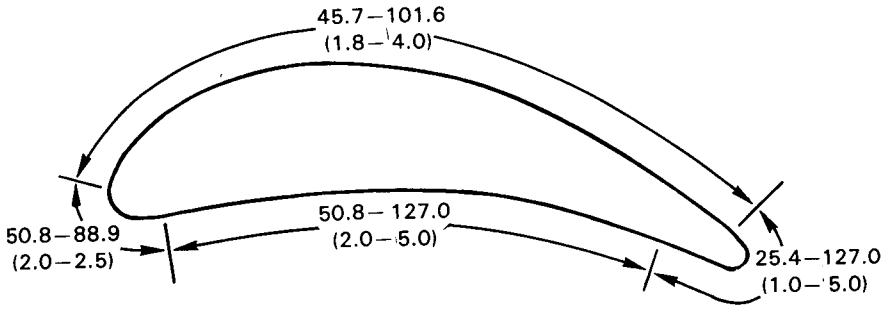

JT8D 12TH STAGE
METCO 83WC-17Co, 60 KW

Figure 39 (Continued)

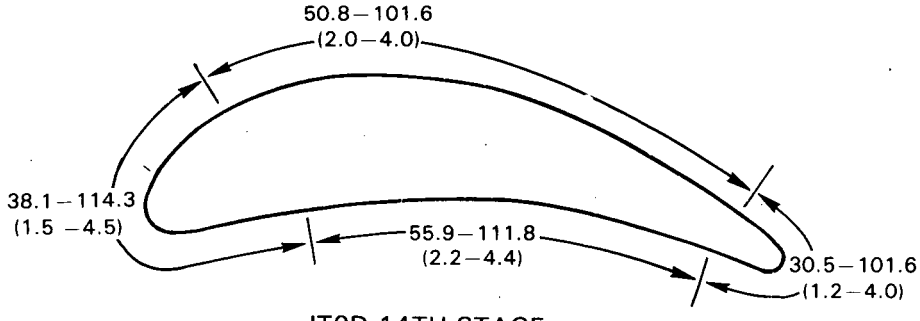

JT9D 14TH STAGE
METCO 83WC-17Co, 60KW

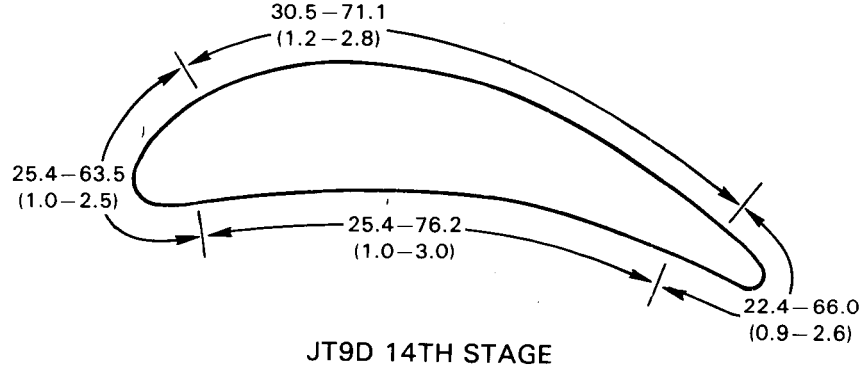

JT9D 14TH STAGE
UTMP 88WC-12Co, GATOR-GARD

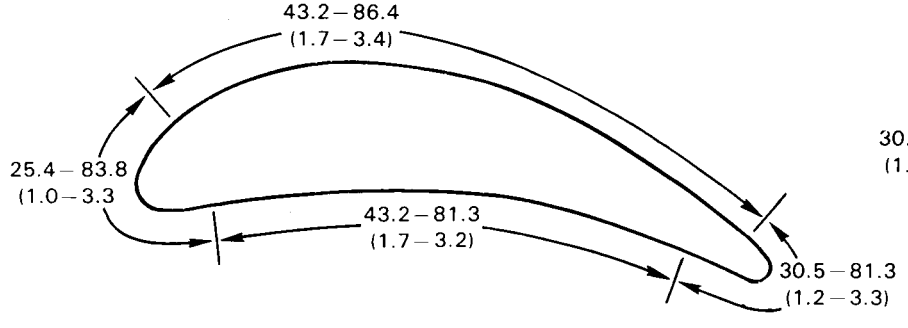

JT9D 14TH STAGE
UNION CARBIDE 90WC-10Co, D-GUN

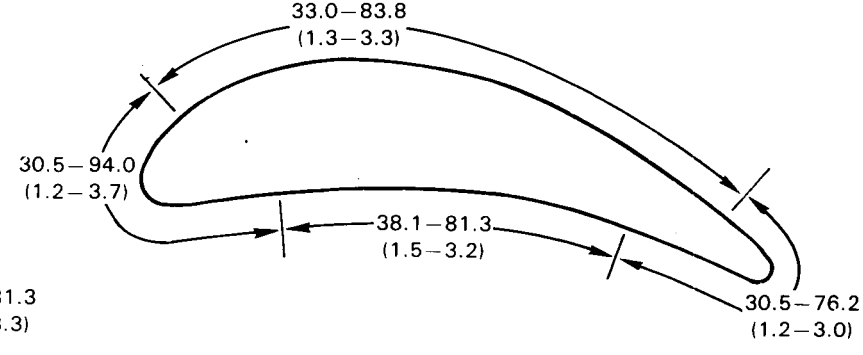

JT9D 14TH STAGE
METCO 88WC-12Co, LOW PRESSURE CHAMBER

Figure 39 (Continued)

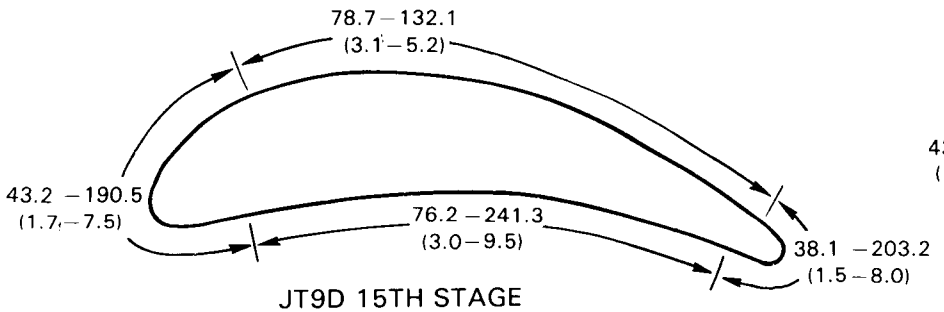

JT9D 15TH STAGE
METCO 83WC-17Co, 60KW

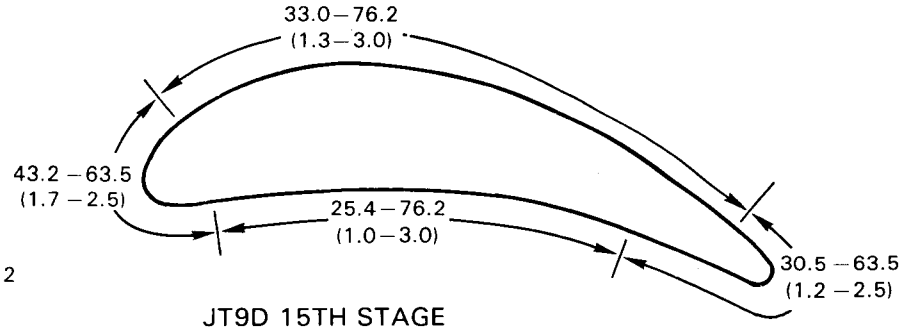

JT9D 15TH STAGE
UNION CARBIDE 90WC-10Co, D-GUN

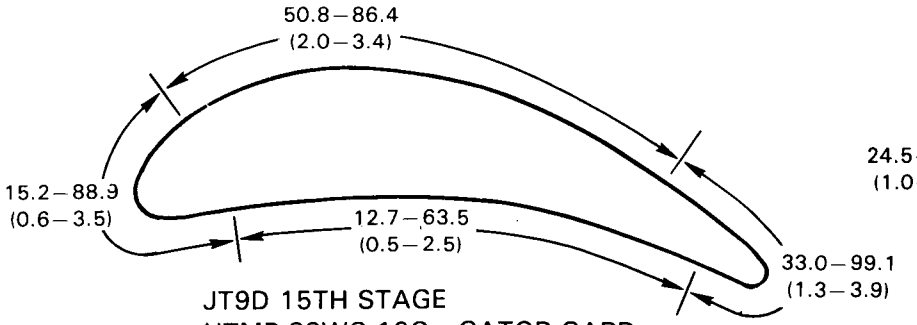

JT9D 15TH STAGE
UTMP 88WC-12Co, GATOR-GARD

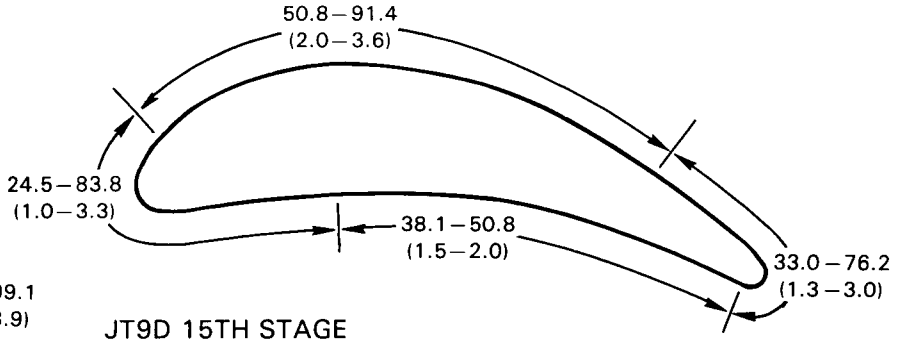

JT9D 15TH STAGE
METCO 88WC-12Co, LOW PRESSURE CHAMBER

Figure 39 (Continued)

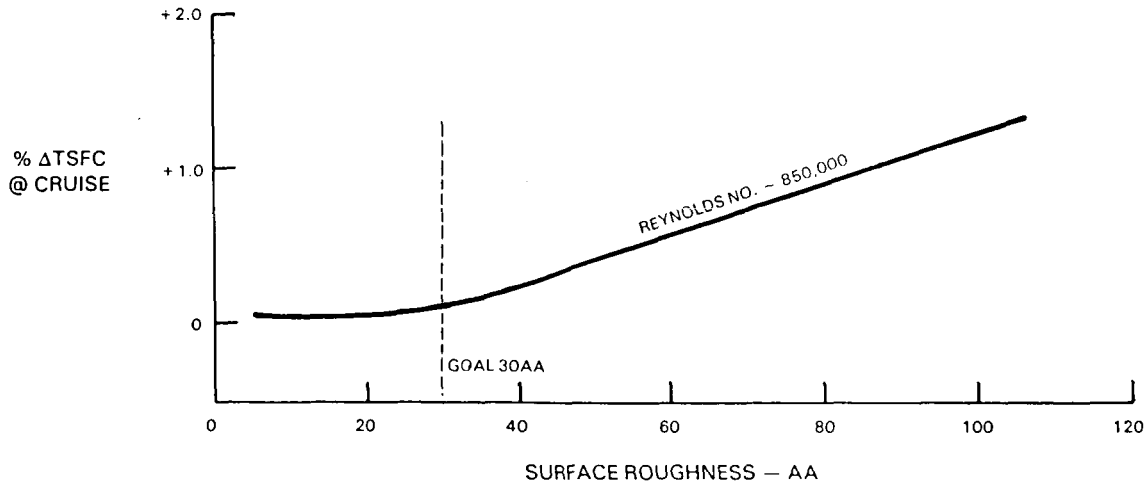

Figure 40 Effect of Airfoil Surface Roughness on Typical HPC Performance

Surface finishing efforts concentrated on evaluating the effects of different types and sizes of polishing media and the effect of process time. Table VI presents the polishing media evaluated. A Harperize mass media polishing system, manufactured by the Harper Co., East Hartford, Ct., was utilized for this evaluation. This centrifugal finishing system is commonly used for mechanical deburring and surface finishing of all types of metallic components. The equipment consists of two drums mounted on a turret which rotates at a high speed in one direction while the drums rotate more slowly in the opposite direction. Parts are loaded into the drums along with the polishing media, water and a lubricating compound. In the evaluation conducted, the rotation of the turret created a centrifugal force of 15 g's. This force compacts the polishing media into a tight mass which then slides against the coated airfoil, removing roughness and producing a smooth surface texture.

TABLE VI
ABRASIVE FINISHING MEDIA EVALUATED ON COATED AIRFOILS

Description	Nominal Size
Fused Aluminum Oxide	ANSI Mesh Size 00
Triangular Aluminum Oxide	150 grit
Triangular Shape Vitrified Bonded Silicon Carbide	150 grit
Triangular Shape Vitrified Fused Aluminum Oxide	32 grit
Triangular Shape Plastic Bonded Quartz	Mesh 2.05 cm (13/16") x 0.94 cm (3/8") x 1.27 cm (1/2")
Fused Aluminum Oxide	ANSI Mesh Size 10
Fused Aluminum Oxide	ANSI Mesh Size 6

In order to maintain the required coating thickness at the airfoil leading and trailing edge surfaces and the airfoil tip, a masking fixture was developed to protect the coating on these surfaces during the finishing process (Figure 41). Coatings on the edges and corners are more prone to material removal than the coating on flat portions of the airfoil surface. Thus, the masking fixture was designed to limit leading and trailing edge wear and permit the coating on the airfoil to be exposed to the polishing action of the abrasive finishing process. Additionally, the fixture prevented removal of material on the load bearing root surfaces.

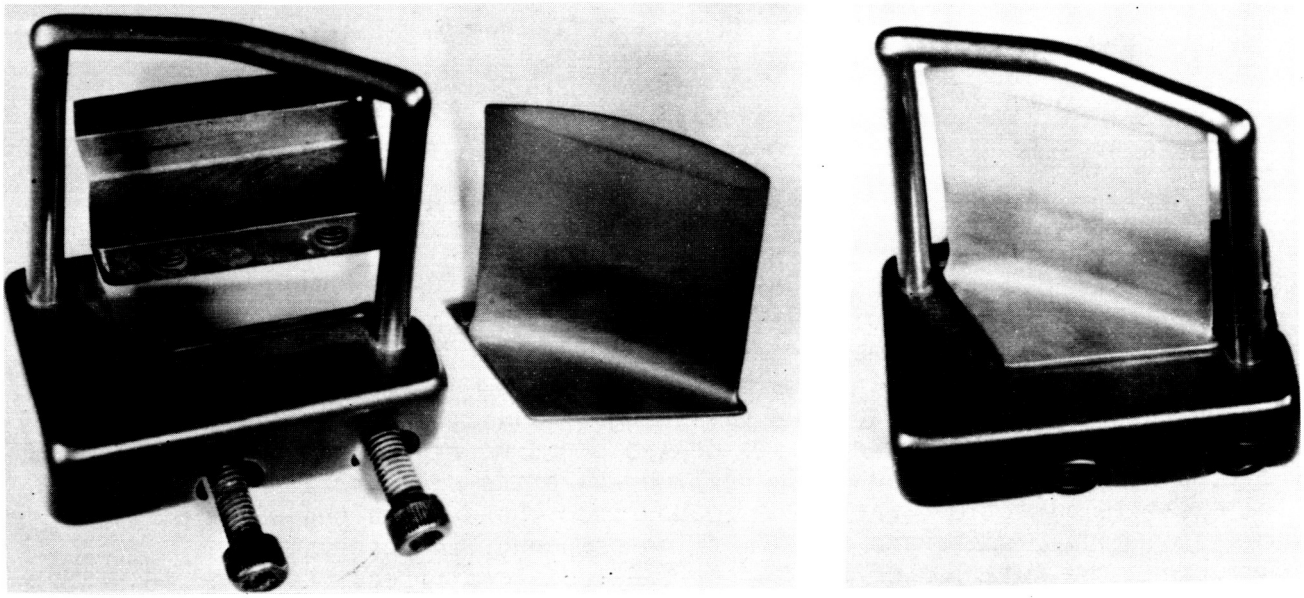

Figure 41 Fixture to Limit Media Wear at Leading and Trailing Edges

Surface finishing evaluations were conducted on Gator-Gard and Cr+B coatings as representative of the plasma and pack coatings, respectively. Finishing efforts on the plasma applied coating indicated that regardless of the polishing media used, there was a significant decrease in coating surface roughness during the first 30 minutes of the process. Additional decreases in roughness proceeded at a much slower rate and, in most cases, reduction to the 20-30AA requirement was not achieved.

It was determined that media size played an important role in the finishing process. Since improvement in surface texture is attributed to material removal caused by abrasive wear, and wear rates are a function of applied force, greater wear of the coating and therefore greater reduction in surface roughness can be achieved by utilizing polishing procedures which apply higher forces to the coating. At a given force, a more massive polishing media resulted in greater surface smoothing than a smaller polishing media. Data obtained on two different polishing media shapes showed different effects on surface roughness as a function of time (Figure 42).

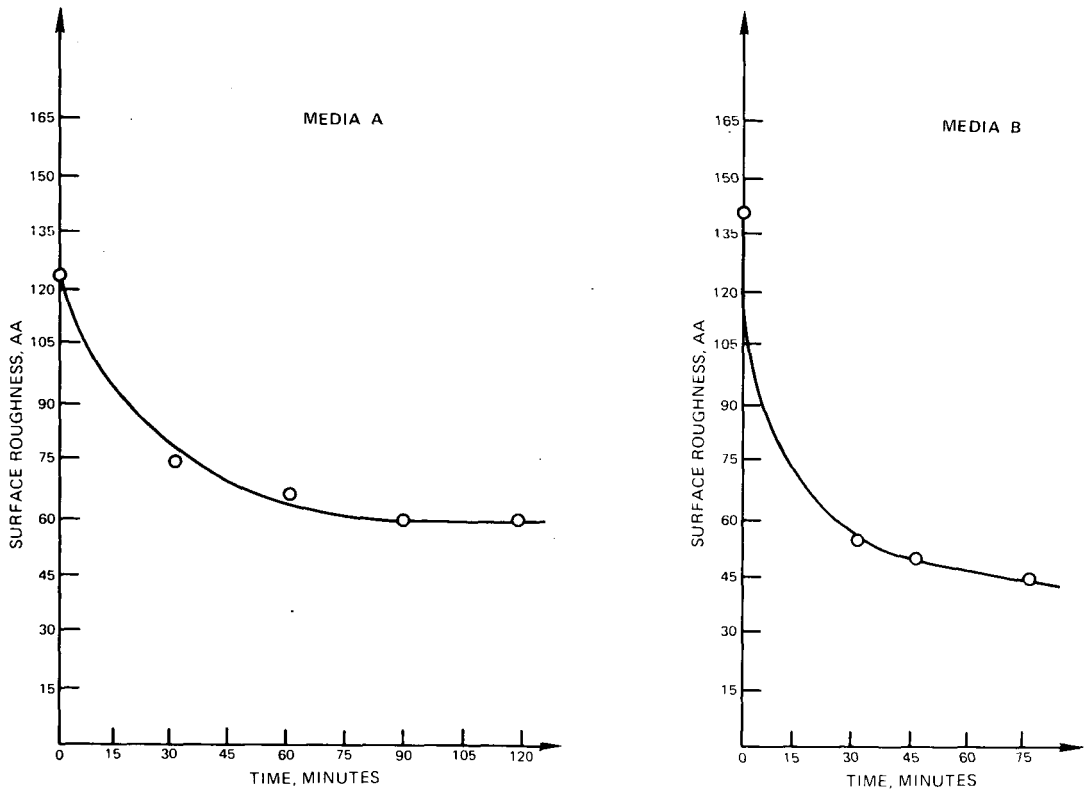

Figure 42 Surface Texture as a Function of Polishing Media and Process Time. Left, random shaped Al_2O_3 chip. Right, triangular shaped Al_2O_3 chip.

These tests showed that the vitrified fused aluminum oxide polishing chip produced the required 20-30AA surface roughness on the plasma sprayed coating. The Harperize process, used for all polishing media experiments, consisted of 60 minutes of tumbling at 15 g's. Surface texture measurements taken at five locations on convex and concave surfaces of Gator-Gard coated airfoils subjected to this process are shown in Figure 43. The media finishing operation resulted in the removal of coating surface asperities with only scratches, remnants of the aggressive Harperize treatment, remaining (Figure 44).

Surface finishing investigations of Cr+B coated Incoloy 901 revealed that the 20-30AA surface texture (Figure 45) was achieved by using a Harperize treatment consisting of 30 minutes, a force of 15 g's and a randon shaped fused aluminum oxide chip.

Metallographic examination of both plasma sprayed and diffusion applied coatings on airfoils after surface finishing to the 20-30AA level indicated that the coating thickness was still within the desired range.

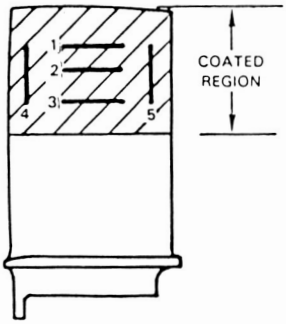

Condition	Average Surface Roughness, AA (0.010" Cutoff)	Peak Counts 50μ"	250μ"
As Coated			
Concave Airfoil	132	211	96
Convex Airfoil	121	198	94
Coated and Media Finished			
Concave Airfoil	24	69	1
Convex Airfoil	19	55	2

Figure 43 Surface Texture Measurements on Plasma Coated and Media Finished JT9D 15th Stage Airfoils. Airfoil schematic indicates measurement locations.

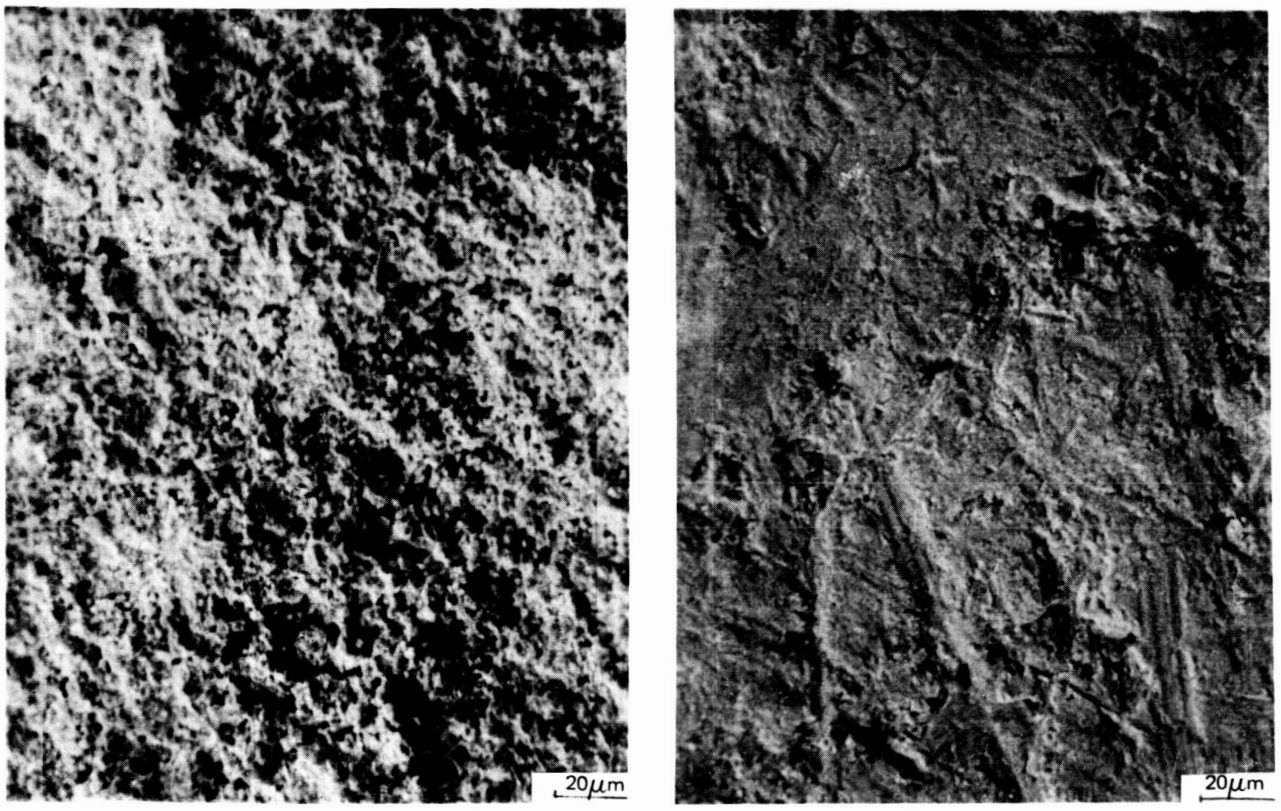

Figure 44 Scanning Electron Microscope (SEM) Showing Coating Surfaces As-Sprayed (left) and After Media Finishing (right).

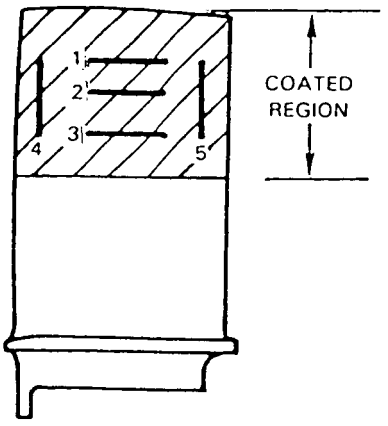

Condition	Average Surface Roughness, AA (0.010" Cutoff)	Peak Counts 50 μ"	250μ"
As Coated			
Concave Airfoil	35	145	12
Convex Airfoil	38	173	13
Coated and Media Finished			
Concave Airfoil	14	44	1
Convex Airfoil	15	59	2

Figure 45 Surface Texture Measurements on Cr+B Diffusion Coated and Media Finished JT9D 15th Stage Airfoils. Airfoil schematic indicates measurement locations.

Ferrous materials, such as AMS 5616, are used for compressor airfoils and are susceptible to corrosion degradation in the engine environment. Thus, ferrous alloys require the use of a corrosion resistant coating. SermeTel W is a coating composed of aluminum particles dispersed in an inorganic binder and is used in the aircraft industry to prevent corrosion degradation of ferrous alloys. Plasma coated airfoils were submitted to SermeTel Inc. to evaluate their ability to apply SermeTel W over the erosion resistant coating and thereby produce a 20-30AA surface finish. SermeTel Inc. utilized two proprietary processes in this evaluation, SermeTel 5375 and SermeTel 5380. Surface texture measurements of the SermeTel processed airfoils indicated that the SermeTel 5380 provided the 20-30AA finish (Figure 46). Metallographic examination of the SermeTel 5380 coating over the plasma applied coating indicated the SermeTel W coating to be typically 25 microns (1 mil) in thickness. SermeTel coatings were applied to the entire airfoil to provide total corrosion protection.

TASK VI COMPONENT FABRICATION AND TEST

The coated airfoils were subjected to rig erosion testing at temperatures and erosive particle velocities which were believed to approximate the levels encountered during engine operation. Volume and chord losses were measured as a function of test time, and airfoil profiles were made before and after erosion testing to precisely locate those areas being eroded and the extent to which they were eroded. High cycle fatigue testing was also conducted and the coated airfoil fatigue strength was compared to the uncoated fatigue strength.

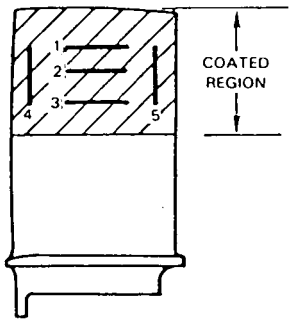

Condition	Average Surface Roughness, AA (0.010" Cutoff)	Peak Counts 50 μ"	250μ"
As Coated			
Concave Airfoil	132	212	96
Convex Airfoil	121	199	94
Finished Per Sermetel 5375			
Concave Airfoil	35	51	8
Convex Airfoil	25	36	3
Finished Per Sermetel 5380			
Concave Airfoil	26	27	4
Convex Airfoil	25	27	4

Figure 46 Surface Texture Measurements on Plasma Sprayed Coated and SermeTel W Overcoated JT9D 15th Stage Airfoils. Airfoil schematic indicates measurement locations.

(A) High Temperature Erosion Testing

Erosion testing was performed in a high velocity burner rig which injected alumina particles, Al_2O_3, nominal 20 micron (0.8 mil) diameter, into the gas stream. The angular shaped abrasive powder was injected into the burner's instrument collar between the primary and secondary combustors at four locations, 90° apart. Transport of a controlled amount of Al_2O_3 to the instrument collar was accomplished using a Sylco Plasma Spray Powder Feeder and argon carrier gas. The specimen holder was designed to permit variability in abrasive impingement angle, specimen height in the erosive stream and nozzle-to-specimen distance (Figures 47 and 48).

Erosion test parameters were chosen to simulate engine operating conditions, i.e., temperature airfoil/airstream impingement angle, and airstream velocity. High amounts of Al_2O_3 were injected into the gas stream to accelerate the rate of chord loss. In a four hour test, the blade chord loss generally met or exceeded the Engine Overhaul Manual limits. The erosion test parameters used to evaluate the JT8D eighth stage and JT9D seventh stage airfoils were as follows:

Parameter	Test Conditions JT8D 8th	JT9D 7th
Gas velocity	225m/sec (740 ft/sec)	225m/sec (740 ft/sec)
Gas temperature	374°C(705°F)	374°C (705°F)
Nozzle to specimen distance	25 cm (10 in.)	25 cm (10 in.)
Abrasive powder feed rate	5.2 g/min (0.01 lb/min)	5.0 g/min (0.01 lb/min)
Air angle	34°	32°

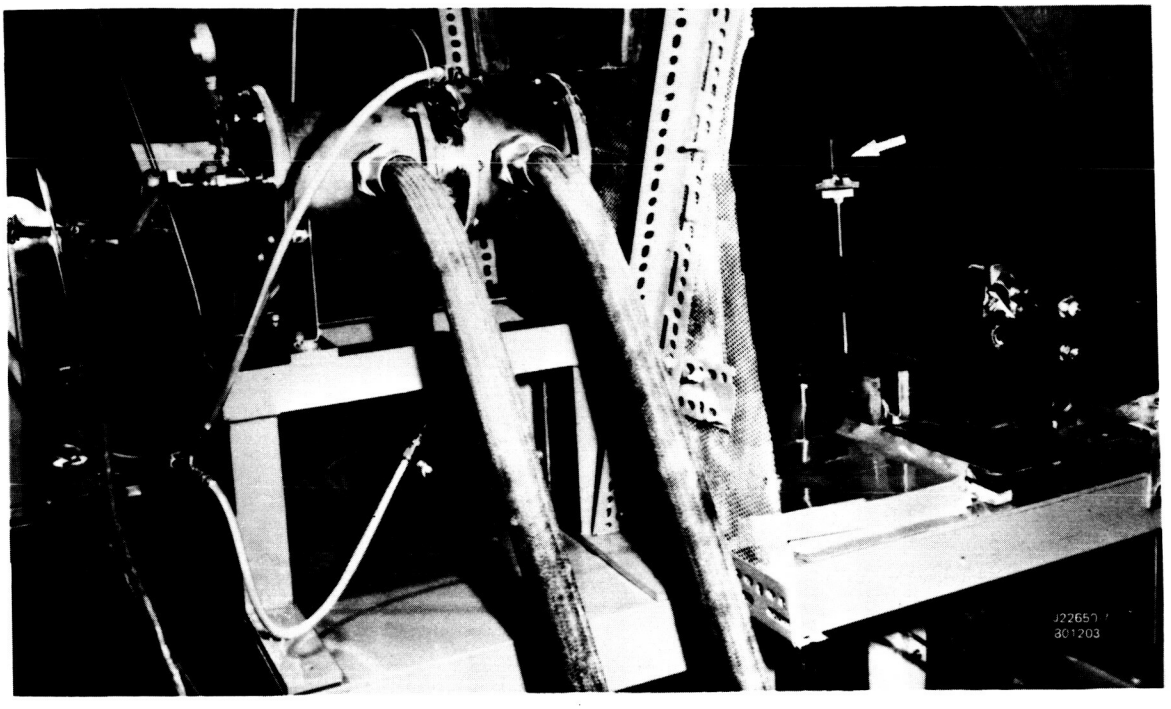

Figure 47 Erosion Test Facility Showing Burner Rig and Airfoil Test Specimen (arrow)

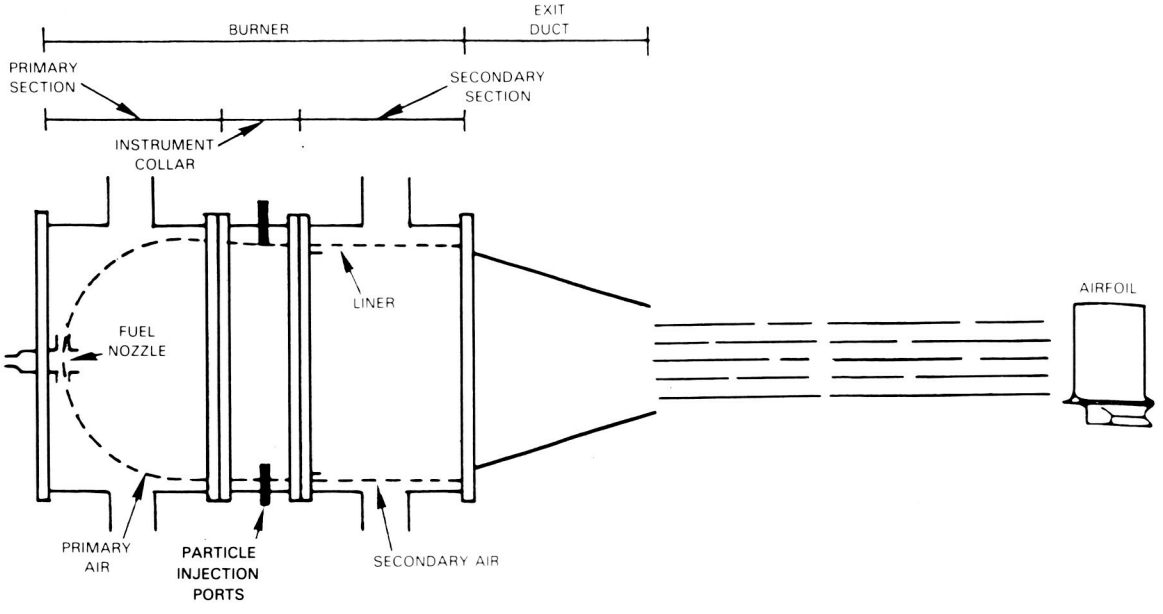

Figure 48 Schematic of Airfoil Burner Rig

The air angle is defined as the angle which the air stream makes with the disk face (Figure 49). A section of compressor disk was utilized as the specimen holder. During the test, weight, volume and chord loss measurements for the uncoated and coated airfoil were recorded after each hour of test. Volume loss measurements were made in accordance with ASTM specification C20-80. Chord measurements were made using a modified dial gauge which allowed airfoil chord dimension determinations at any spanwise location (Figure 50). Uncoated airfoils were tested as the baseline condition.

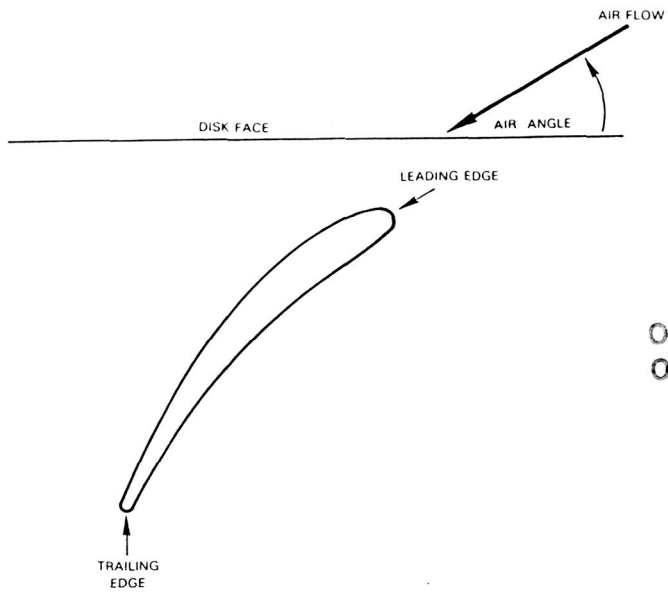

Figure 49 Schematic Showing Relationship of Airfoil and Airflow

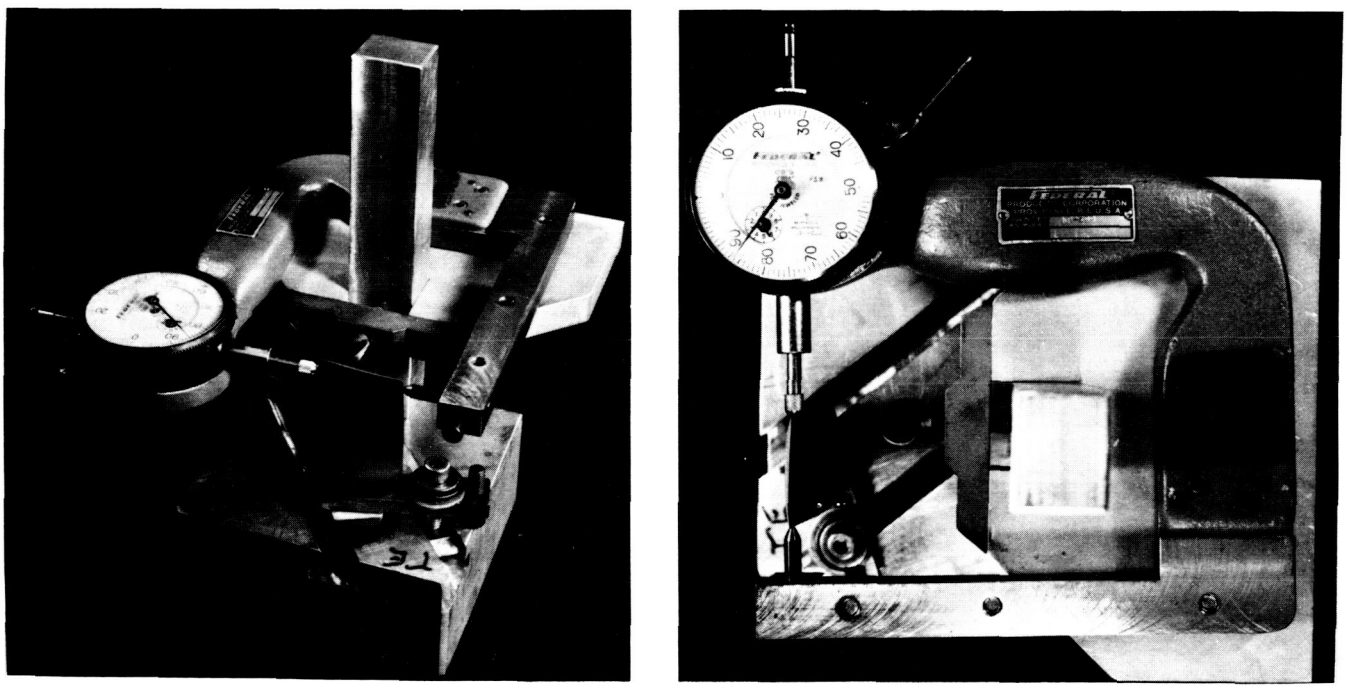

Figure 50 Photographs of Airfoil Chord Measurement Unit

Erosion data obtained on plasma coated JT8D 8th stage and JT9D 7th stage airfoils are presented in Figures 51 through 54. There was considerable scatter observed in the JT8D chord loss measurement after the fourth hour of the erosion test, as shown in Figure 51. This scatter is due to the allowable blueprint tolerance for trailing edge thickness. Blades with thin trailing edges eroded faster than those with thicker trailing edges.

Figure 51 Volume Loss Data of JT8D 8th Stage Airfoils

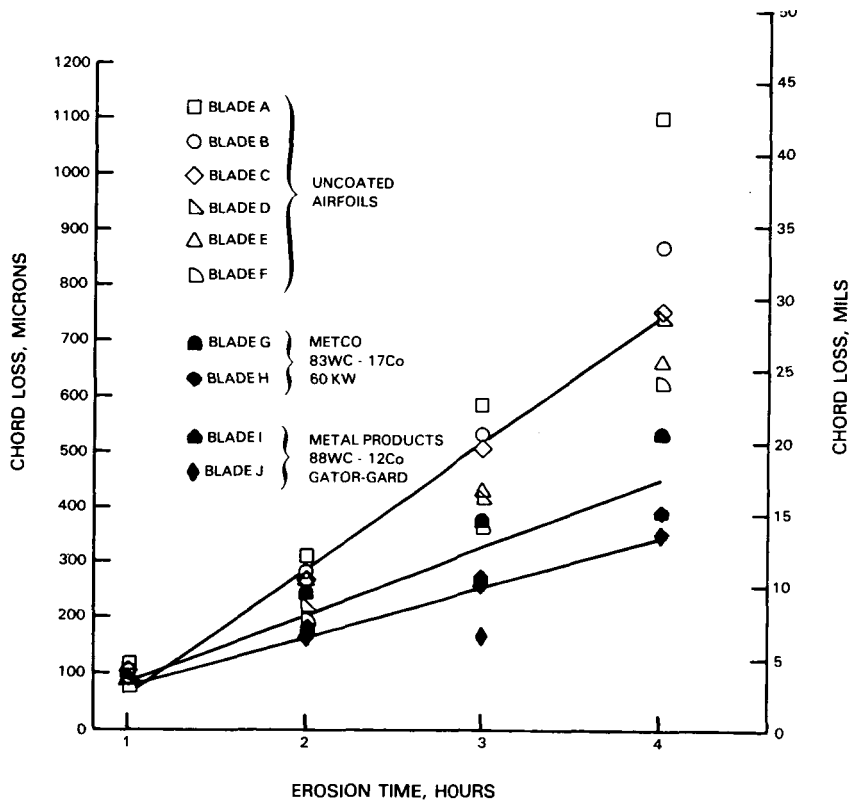

Figure 52 Chord Loss Data of JT8D 8th Stage Airfoils

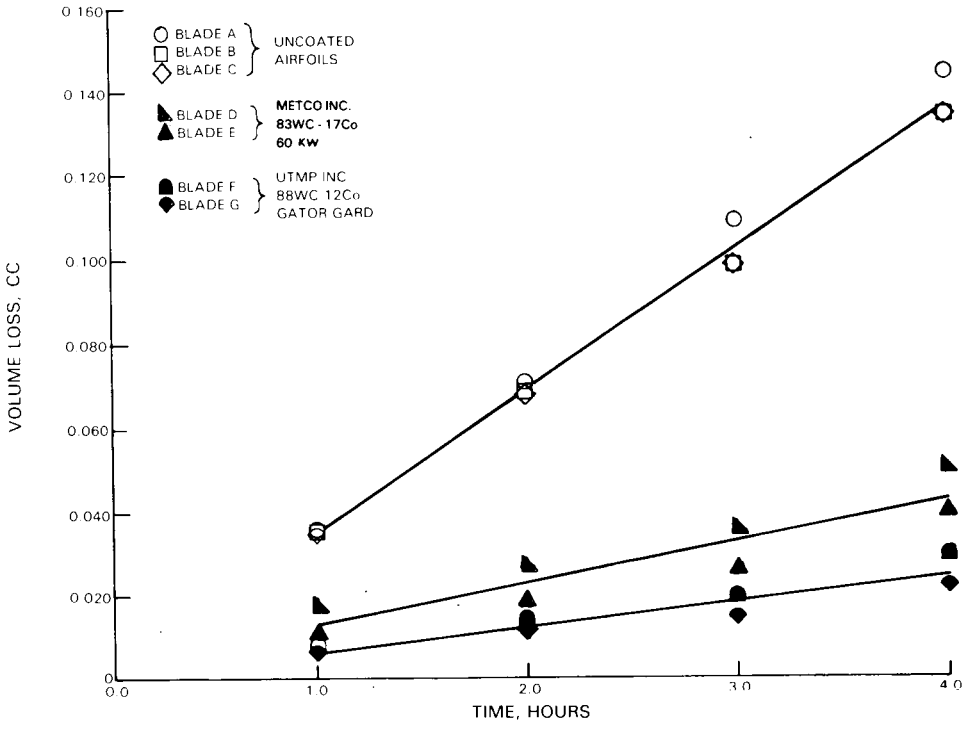

Figure 53 Volume Loss Data of JT9D 7th Stage Airfoils

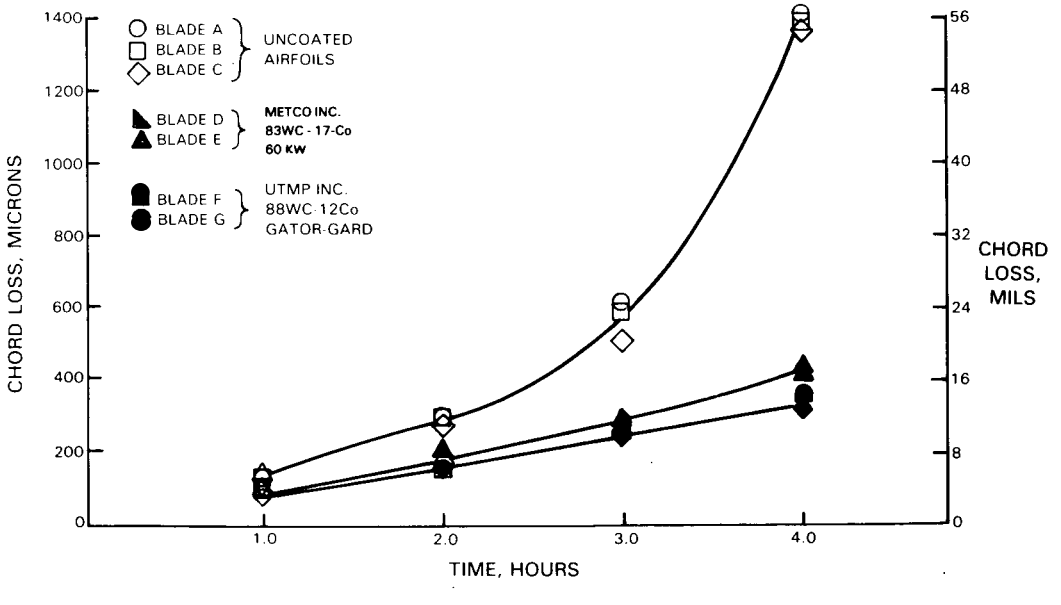

Figure 54 Chord Loss Data of JT9D 7th Stage Airfoils

After the four hour test, a comparison of uncoated and coated airfoil data indicated the following improvements in erosion resistance:

	Plasma Coatings	
	83WC-17Co, 60 KW	88WC-12Co, Gator-Gard
Volume loss basis		
JT9D 7th stage	3.1X	5.4X
JT8D 8th stage airfoil	5.5	8.6
Chord loss basis		
JT9D 7th stage	3.3	4.3
JT8D 8th stage	1.7	2.1

The observed differences in erosion behavior between the uncoated JT8D 8th and JT9D 7th stage airfoils were attributed to (1) differences in airfoil geometry (camber and thickness) and (2) differences in the air angle (Figure 55). Although the latter quantity differed by only 2° (β = 32° for the JT9D 7th stage airfoil and 34° for the JT8D 8th stage airfoil) the airfoil geometries resulted in substantially different abrasive impingement angles, along the concave trailing edge surfaces, the region in which the majority of the erosion occurred (Figure 55); the JT9D 7th stage airfoil abrasive impingement angles were nearly twice those of the JT8D 8th stage airfoil.

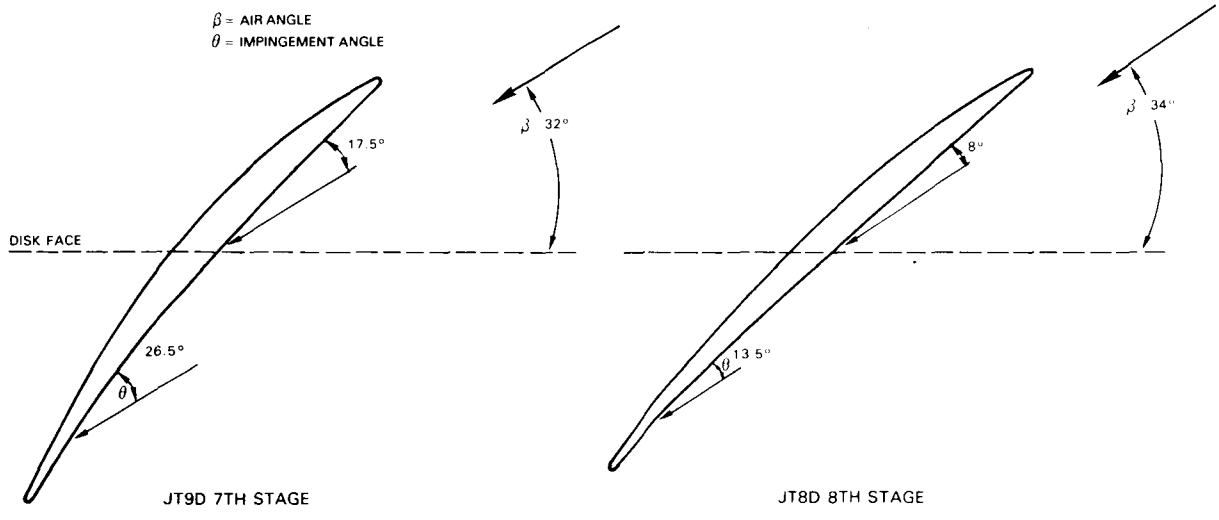

Figure 55 Airfoil Erosion Rate is Reduced at Low Impingement Angles

A well known relation[1] has been developed between erosion rate and abrasive impingement angle (Figure 56). Maximum erosion for materials which respond in a ductile manner occur at a 20-30° impingement angle. Brittle type erosion is characterized by a rate which increases with higher impingement

(1) I. Finnie, "An Experimental Study of Erosion", S.E.S.A. Proceedings, Vol. XVII, No. 2, presented at the Spring Meeting of the Society for Experimental Stress Analysis, Washington, D.C., May 1959.

angle. Compressor airfoil materials exhibit ductile type behavior. As can be observed, ductile materials, i.e., AMS 4928, were highly sensitive to small changes in abrasive impingement angle. Since the abrasive impingement angles for the JT9D 7th and JT8D 8th stage airfoils were less than θ critical, which was approximately 30°, smaller increases in the impingement angles, up to θ critical, result in greater erosion rates. This relation was confirmed by the uncoated four hour test data which showed that chord loss for the 7th stage airfoil was 1420 microns (56 mils), while the corresponding chord loss on the 8th stage airfoil was 760 microns (30 mils). Thus the difference in erosion resistance on the two airfoil stages was attributed to differences in airfoil camber.

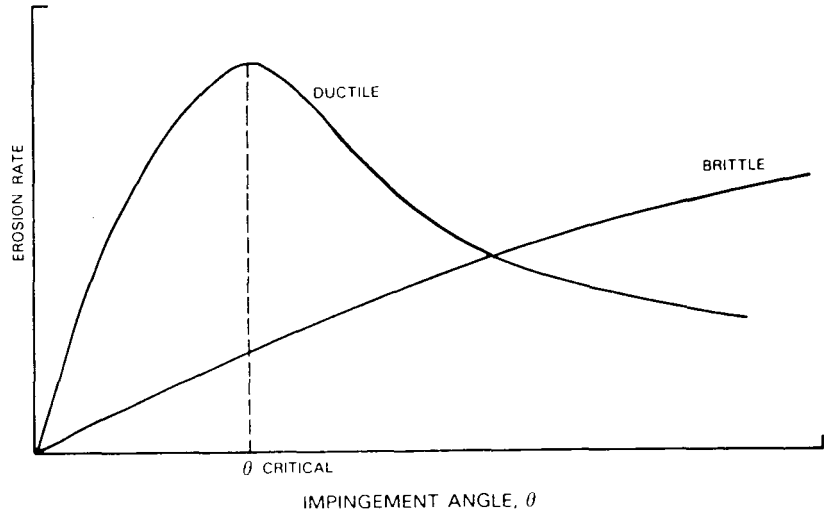

Figure 56 Typical Erosion Behavior of Materials

The erosion test parameters used to evaluate the JT8D 10th and 12th stage airfoils were as follows:

Parameter	Test Conditions	
	JT8D 10th	JT8D 12th
Gas Velocity	270 m/sec (885 ft/sec)	260 m/sec (860 ft/sec)
Gas Temperatures	490°C (920°F)	480°C (900°F)
Nozzle to Specimen Distance	20 cm (8 in.)	20 cm (8 in.)
Abrasive Powder Feed	6.2 g/min (0.01 lb/min)	6.2 g/min (0.01 lb/min)
Air Angle	35°	38°

After 4 hours of erosion testing, measurements of coated and uncoated JT8D 10th stage airfoils indicated that the Metco 60 KW plasma coating provided 2.8X and 1.3X improvements in erosion resistance based on volume loss and chord loss, respectively. For Cr+B coated JT8D 10th stage airfoils, significant degradation of the leading and trailing edge surfaces was found after the four hour erosion test. The Cr+B coating provided an improvement in erosion resistance of 2.2X on a volume basis. However, on a chord loss basis, the Cr+B coating did not show an improvement in erosion resistance compared to the uncoated condition (Figures 57 and 58).

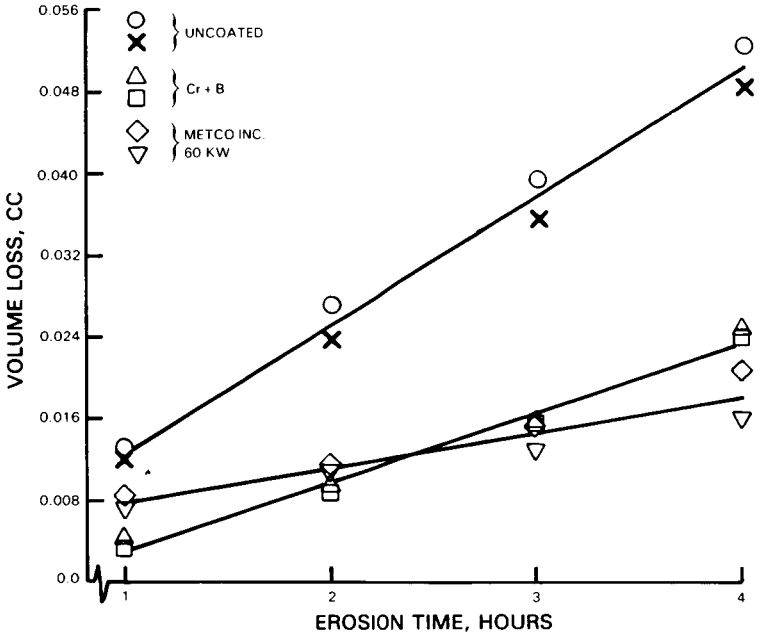

Figure 57 Volume Loss Data of JT8D 10th Stage Airfoils

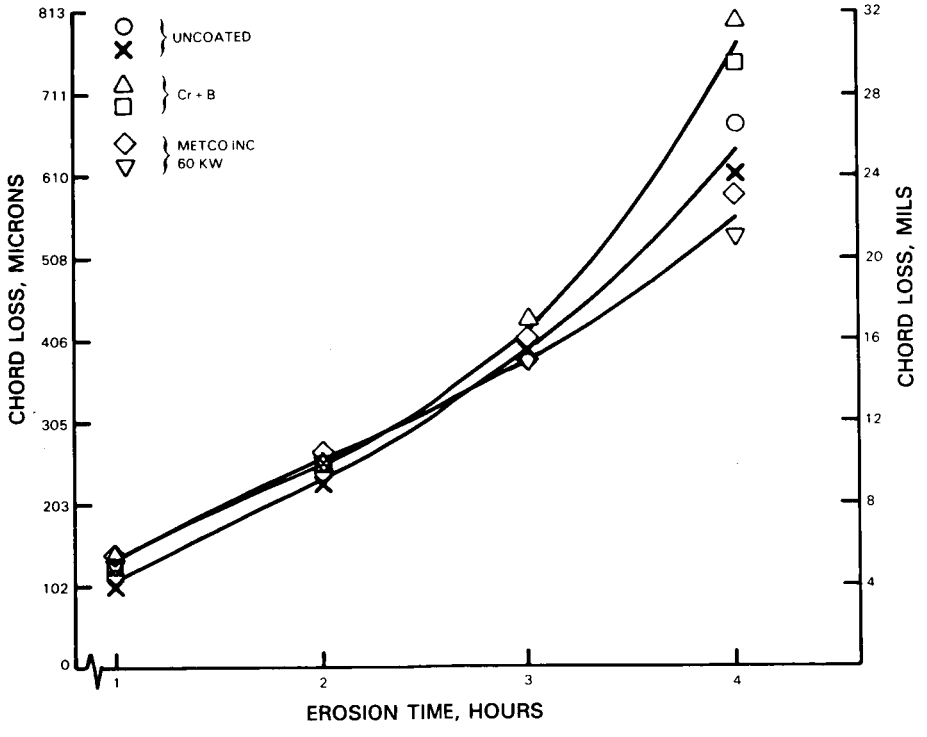

Figure 58 Chord Loss Data of JT8D 10th Stage Airfoils

Test results on JT8D 12th stage airfoils indicated that the uncoated airfoil reached the Overhaul Manual chord limit in approximately 3.2 hours. For this short test duration, on a volume loss basis, the plasma and diffusion applied coatings provided erosion improvements of 2.3 and 1.9X, respectively. On a chord loss basis, the plasma and diffusion applied coatings provided improvements of 1.70X and 1.25X, respectively (Figures 59 and 60).

Since JT8D analytical evaluations indicated that the limiting conditions for use of high pressure compressor airfoils are trailing edge loss and the associated engine stall condition, coated 10th and 12th stage airfoils were tested for periods longer than required for the uncoated blade to reach the Overhaul Manual minimum chord limit. Testing of the 10th stage was conducted for a total of six hours; at this point, the coated airfoil had met the OHM minimum chord limit. The calculated erosion improvement factors, compared to the uncoated condition, for the 60 KW plasma coating were 3.0X and 2.3X on volume and chord loss bases, respectively (Figures 61 and 62). Testing also indicated that the uncoated blade suffered accelerated trailing edge loss while use of the plasma coating precluded this occurrence (Figure 63). Testing of JT8D 12th stage blades, although terminated after four hours of testing revealed the same trend, i.e., retention of the blade trailing edge on coated blades while uncoated blades experienced accelerated trailing edge loss (Figure 64). Calculated coating improvement factors, relative to the uncoated condition, for the 12th stage airfoils after the four hour test are tabulated below.

COATING IMPROVEMENT IN EROSION RESISTANCE

Coating System	Erosion Resistance Improvement Factor	
	Volume Loss Basis	Chord Loss Basis
60 KW 83WC-17Co	1.6	2.6
Cr+B	1.9	2.3

The testing of JT8D and JT9D AMS 4928 airfoils indicated the significant effect of geometry on uncoated airfoil erosion behavior. Airfoil geometry dictates the impingement angle at which the Al_2O_3 particulate strikes the airfoil. The relationship between particulate impingement angle and chord loss for uncoated AMS 5616 airfoils is similar to that observed for uncoated AMS 4928 airfoils, i.e., higher impingement angles resulted in greater airfoil chord loss. Coated airfoils showed less sensitivity to impingement angle changes compared to uncoated airfoils (Table VII). No comparison between the data for AMS 4928 and AMS 5616 airfoils was made due to different test parameters.

TABLE VII
EROSION TEST DATA SHOWING EFFECT OF IMPINGEMENT ANGLE ON AIRFOIL CHORD LOSS

Substrate	Engine/ Rotor Stage	Abrasive Impingement Angle			Chord Loss After 4 Hr Test microns (mils)		
		50% Chord	75% Chord	90% Chord	Uncoated	88WC-12Co Gator-Gard	83WC-17Co 60 KW
AMS 4928	JT8D/8	8°	10.5°	13.5°	815(30)	355(15)	455(20)
AMS 4928	JT9D/7	17.5°	23.5°	26.5°	1420(55)	355(15)	430(15)
AMS 5616	JT8D/10	10.5°	14°	17°	635(25)	--	560(20)
AMS 5616	JT8D/12	14.5°	23.5°	26.5°	1120(45)	--	430(15)

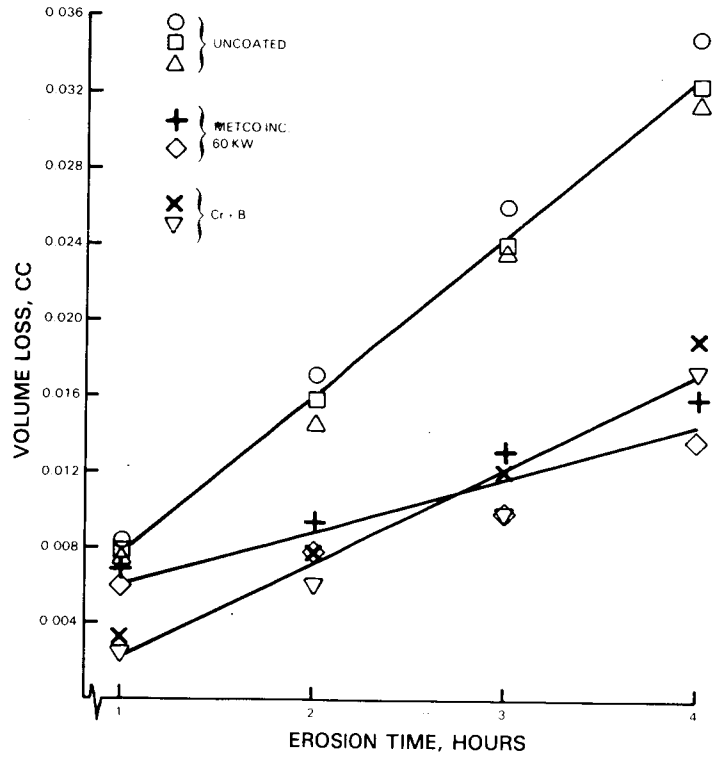

Figure 59 Volume Loss Data of JT8D 12th Stage Airfoils

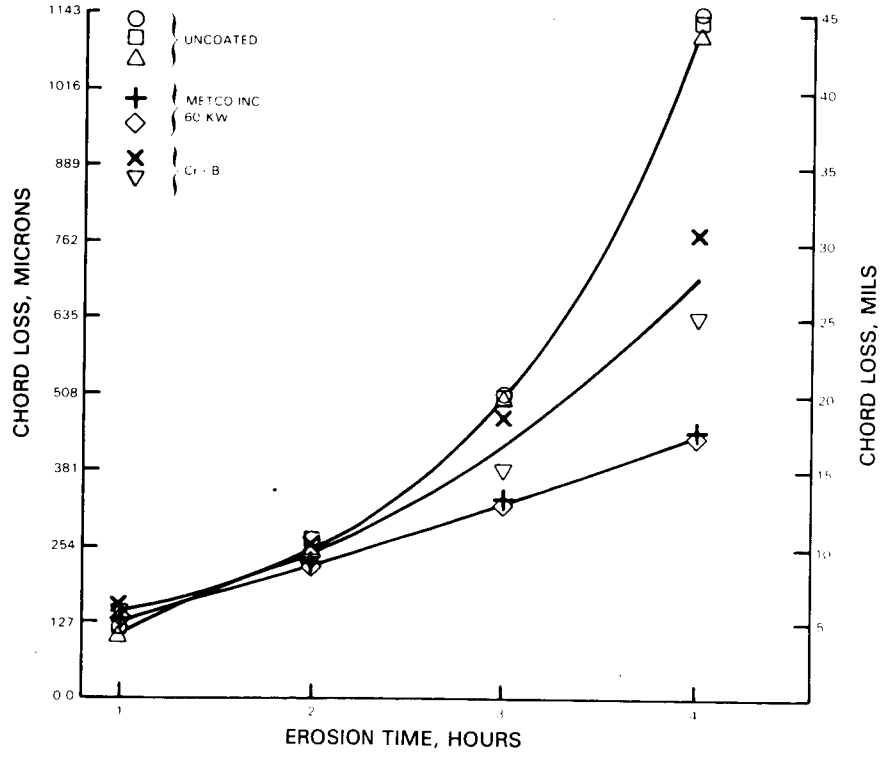

Figure 60 Chord Loss Data of JT8D 12th Stage Airfoils

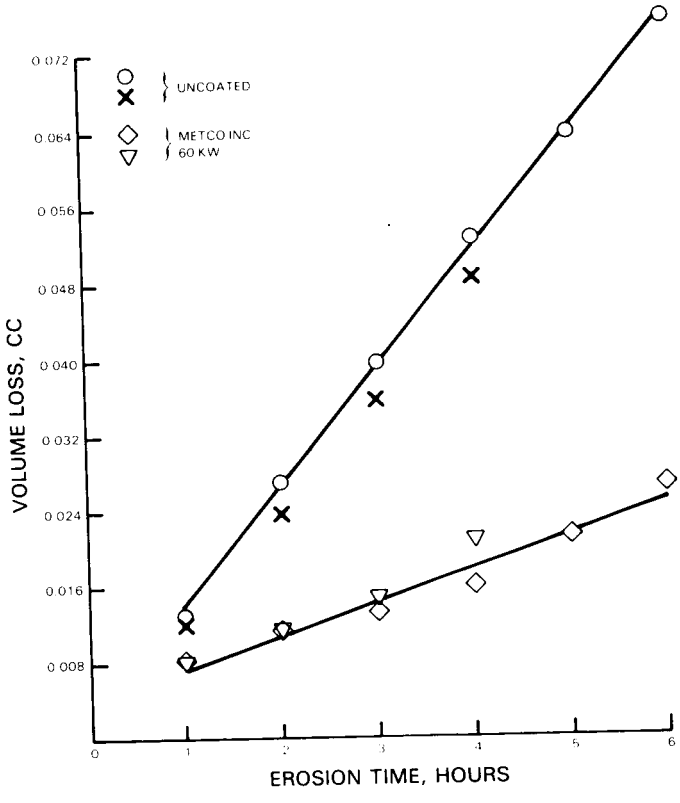

Figure 61 Volume Loss Data of JT8D 10th Stage Airfoils

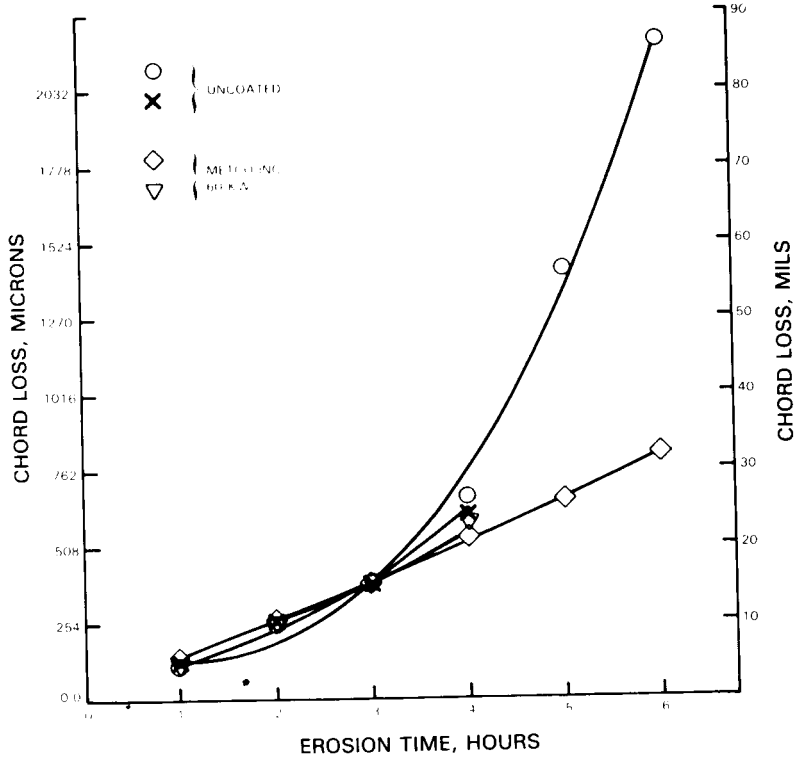

Figure 62 Chord Loss Data of JT8D 10th Stage Airfoils

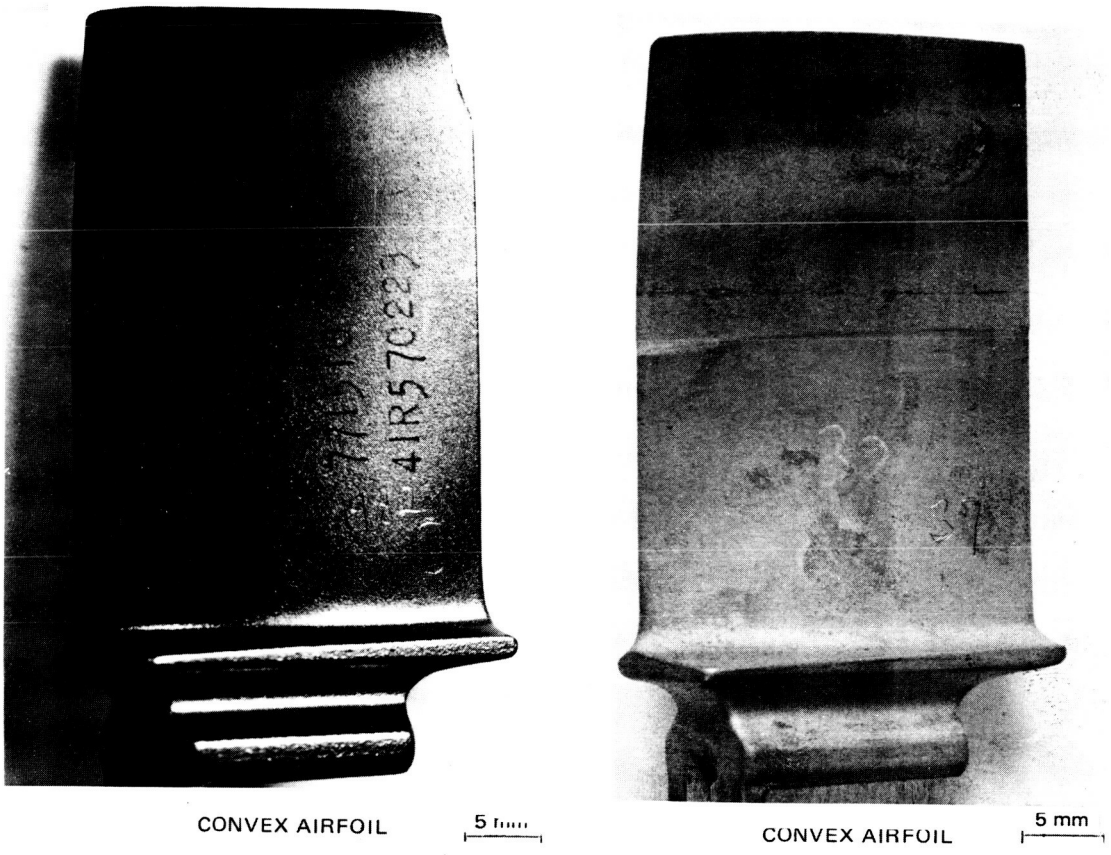

Figure 63 JT8D 10th Stage Airfoils Uncoated (left) and Metco 60 KW Plasma Coated 83WC-17Co (right) After 6 Hours of Erosion Testing

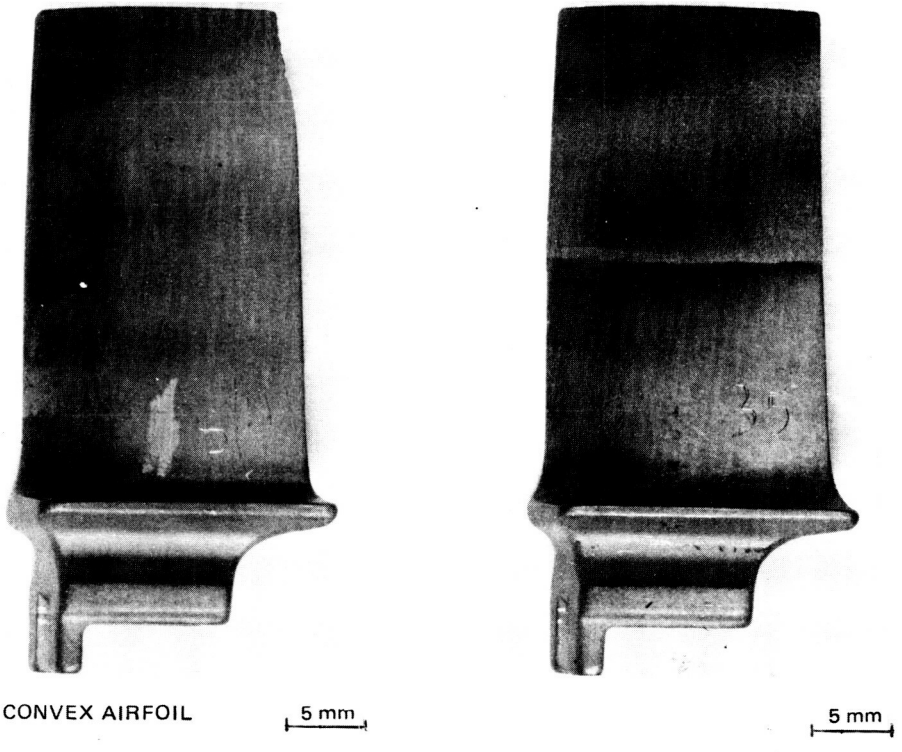

Figure 64 JT8D 12th Stage Airfoils Uncoated (left) and Metco 60 KW Coated 83WC-17Co Plasma Coated (right) After 4 Hours of Erosion Testing

Six coating systems were evaluated on JT9D 14th and 15th Incoloy 901 airfoils.The Cr+B pack diffusion coating was applied to the entire airfoil and root surfaces; the Task III HCF data indicated no fatigue strength debit for Incoloy 901 coated with Cr+B. The erosion test parameters used to evaluate the JT9D 14th and 15th stage airfoils were as follows:

Parameter	Test Conditions	
	JT9D 14th	JT9D 15th
Gas Velocity	285 m/sec (935 ft/sec)	305 m/sec (990 ft/sec)
Gas Temperature	575°C (1065°F)	590°C (1095°F)
Nozzle to Specimen Distance	19.5 cm (7.5 in.)	20 cm (7.5 in.)
Abrasive Powder Feed Rate	5.2 gm/min (0.01 lb/min)	5.2 gm/min (0.01 lb/min)
Air Angle	32°	30°

Volume and chord loss measurements of erosion tested JT9D 14th and 15th stage coated and uncoated airfoils are presented in Figures 65-68. These data revealed the following improvements in erosion resistance compared to the baseline uncoated condition:

Coating System	Erosion Resistance Improvement Factor			
	Volume Loss Basis		Chord Loss Basis	
	JT9D 14th	JT9D 15th	JT9D 14th	JT9D 15th
D-Gun 90WC-10Co	1.7X	1.8X	1.8X	1.5X
LPCS 88WC-12Co	5.6	3.3	1.8	1.6
Gator-Gard 88WC-12Co	3.3	2.9	2.3	1.6
60 KW 83WC-17Co	2.7	2.3	2.0	1.6
Cr+B	8.7	4.3	2.5	2.2

The pack diffusion Cr+B coating applied to Incoloy 901 airfoils provided the greatest degree of erosion resistance for both volume and chord loss. These results are in agreement with test data generated in Task III. Although the magnitude of improvement for the Cr+B coating is not equivalent to that observed in Task III evaluations, significant differences exist between the two test procedures which account for the difference.

(B) Frequency Behavior

Tests were also conducted on JT9D 7th stage airfoils to determine the effect of plasma applied coatings on airfoil resonant frequency behavior. The blades were plasma coated with 88WC-12Co powder on the outer 50% of the airfoil surface to the target thickness. Two coating configurations were tested, (1) coating applied to the concave and convex airfoil surfaces and (2) coating applied only to the concave airfoil surface. Since erosion testing indicated that erosion degradation was confined to the airfoil leading edge and concave trailing edge surfaces, it was believed that configuration (2) could provide the required airfoil erosion protection. Frequency measurements revealed that there was an approximate 9% reduction in first mode vibratory frequency with coating configuration (1) and an approximate 5% reduction with configuration (2).

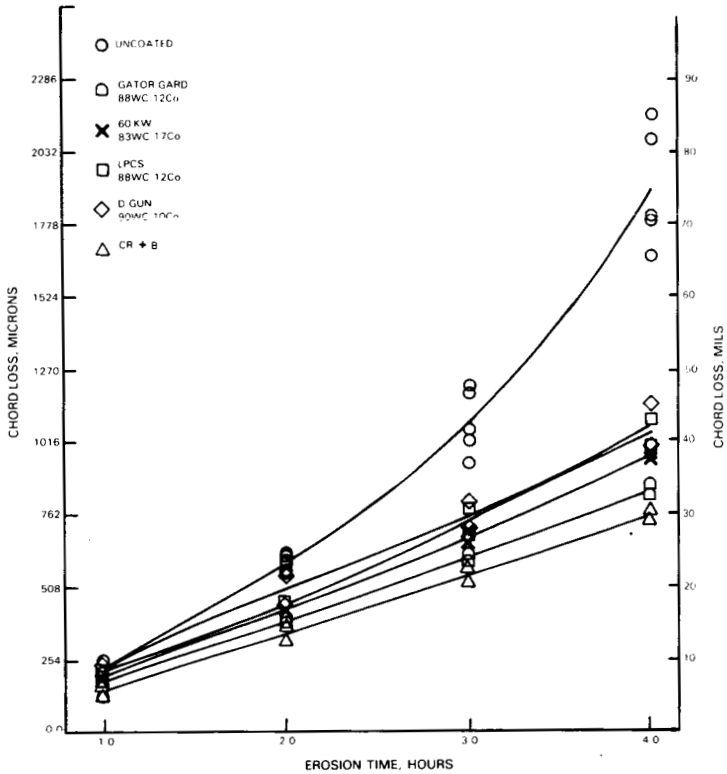

Figure 65 Chord Loss of Eroded JT9D 14th Stage Airfoils

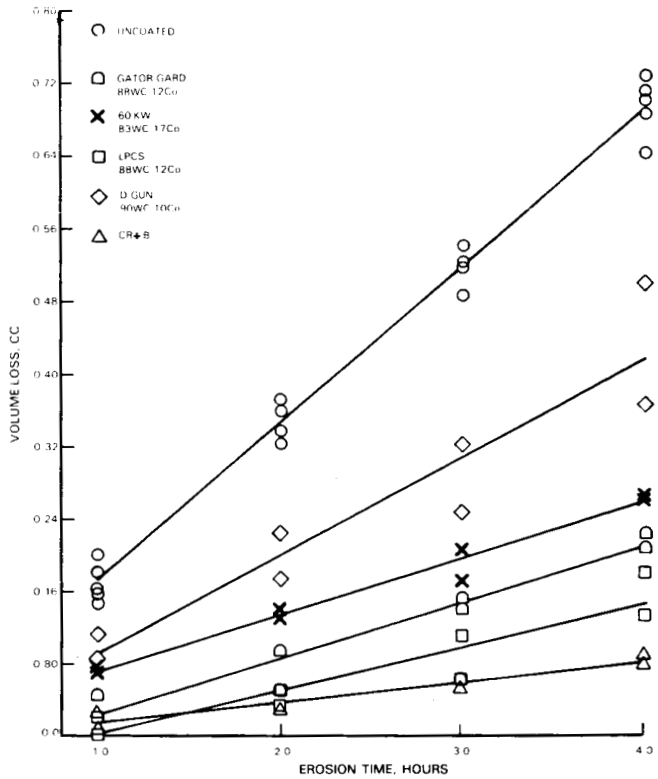

Figure 66 Volume Loss of Eroded JT9D 14th Stage Airfoils

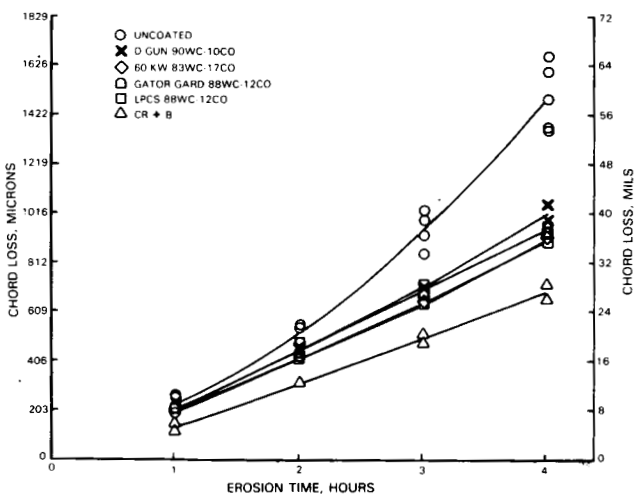

Figure 67 Chord Loss of Eroded JT9D 15th Stage Airfoils

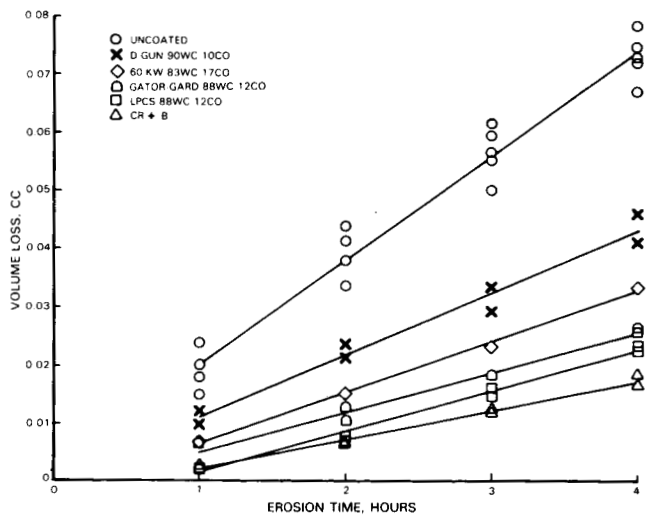

Figure 68 Volume Loss of Eroded JT9D 15th Stage Airfoils

The 9% frequency debit is comparable to the reduction observed on JT9D 7th stage blades coated with Gator-Gard applied 88WC-12Co (11%) and 60 KW applied 83WC-17Co (9%). While these results were obtained on blades in the as-coated condition, there was little or no difference in the frequency behavior of coated blades which were surface treated to 20-30 AA.

(C) High Cycle Fatigue Testing

High cycle fatigue (HCF) testing was performed to determine the fatigue strength of the coated airfoil relative to the baseline uncoated condition. All plasma spray coatings were applied to the outer 50% of the convex and concave airfoil surfaces to the target thickness. The airfoils were tested in the as-coated condition.

The HCF tests were performed at room temperature. Each airfoil was mounted in a fixture attached to an electro-dynamic exciter. The airfoils were excited at their first bending resonant frequencies with strain gauges applied to determine the maximum stress location. Once the first bend maximum stress point was determined, all airfoils were excited at their first bending resonant frequencies and deflection amplitude was monitored and controlled to maintain a constant stress during the test. Airfoils were tested to 10^7 cycles or failure, whichever was applicable.

The fatigue test results are presented in Figure 69. JT9D 14th and 15th stage Incoloy 901 airfoils experienced no observable fatigue debit. This was, as expected, in agreement with the Task III results.

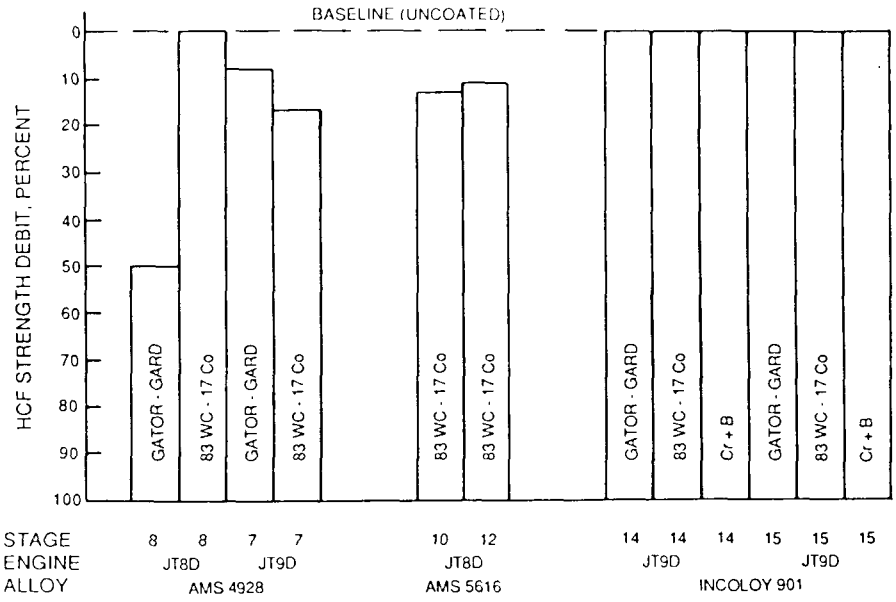

Figure 69 High Cycle Fatigue Test Results of Coated Airfoils

With respect to JT8D 10th and 12th stage AMS 5616 airfoils, the HCF results were similar for the plasma sprayed 83WC-17Co coated blades, showing 13 and 11% debits, respectively. Specimen HCF test results generated in Task III for the Gator-Gard plasma sprayed coating indicated a similar debit of 14%.

Coating performance on AMS 4928 depended on which airfoil was tested. The 83WC-17Co coated JT8D airfoil resulted in no fatigue debit. However, JT9D airfoils with the same coating provided a 17% debit. The Gator-Gard coating had a higher fatigue life debit on JT8D airfoils than on JT9D airfoils.

An analytical evaluation of all of the data revealed that coated blades had adequate fatigue strength for engine test purposes although significant debits in HCF strength existed for plasma sprayed coatings on AMS 4928 blades.

The results of the engine tests of coated blades are presented in Volume II.

CONCLUSIONS

Plasma and diffusion coatings and associated application processes were identified for the improvement of compressor airfoil erosion resistance.

- The goal of a 2X improvement in erosion resistance was met by plasma sprayed Gator-Gard and Metco 60 KW coatings on AMS 4928, AMS 5616 and Incoloy 901 substrates and by the diffusion Cr+B coating on AMS 5616 and Incoloy 901 substrates.

- Plasma spray coatings such as Gator-Gard applied 88WC-12Co and Metco applied 83WC-17Co, which exhibited high concentrations of discrete carbide particles, were more erosion resistant than plasma coatings with low concentrations of discrete carbide particles.

- Pack diffusion Cr+B coatings which were developed for AMS 5616 and Incoloy 901 alloy subsrates provided superior erosion resistance to plasma spray coatings.

- Erosion testing of coated airfoils indicated that Cr+B coating was the most erosion resistant pack coating while Gator-Gard applied 88WC-12Co was the most erosion resistant plasma spray coating.

- High cycle fatigue specimen testing revealed strength reductions for all plasma spray coated AMS 4928 and AMS 5616 substrates.

- High cycle fatigue specimen testing of Cr+B coated Incoloy 901 resulted in a strength improvement on Incoloy 901 and a strength reduction on AMS 5616.

- High cycle fatigue testing of coated AMS 4928 airfoils resulted in a fatigue life debit which was dependent on airfoil configuration. On AMS 5616, plasma spray coatings resulted in a strength debit; on Incoloy 901, all coatings tested did not affect fatigue strength.

- Analytical studies showed that erosion prone areas could be coated without affecting airfoil fatigue strength requirements.

- A polishing technique was developed which produced a surface finish of 20-30 AA on coated airfoils which did not affect leading and trailing edge coating thickness.

- The following alloy-coating systems were selected for engine testing.

Alloy	Coating
AMS 4928	Gator-Gard plasma spray 88WC-12Co
AMS 5616	60 KW plasma spray 83WC-17Co
Incoloy 901	Gator-Gard plasma spray 88WC-12Co
Incoloy 901	Pack diffusion Cr+B

APPPENDIX A

TABLE A-I
SIEVE ANALYSIS AND PARTICLE SIZE DISTRIBUTION
OF COARSE AMS 7879 (88WC-12Co) PLASMA SPRAY POWDER

Sieve Analysis

Sieve Designation	Micron Size	Weight % of Powder Retained	Weight % of Powder Passed
Number 140	105	0.0	100.0
Number 170	88	0.08	99.92
Number 200	74	3.00	96.92
Number 230	63	28.82	68.10
Number 270	53	62.95	5.15
Number 325	44	5.08	0.07
Pan	-44	0.68	-

Sub-Sieve Particle Distribution

Particle Size (microns)	Weight (%)
40-44	1.4
20-40	2.8
10-20	1.2
5-10	0.0
0-5	0.0

TABLE A-2
SIEVE ANALYSIS AND PARTICLE SIZE DISTRIBUTION
OF FINE AMS 7879 (88WC-12Co) PLASMA SPRAY POWDER

Sieve Analysis

Sieve Designation	Micron Size	Weight % of Powder Retained	Weight % of Powder Passed
Number 140	105	0.0	100.0
Number 170	88	0.0	100.00
Number 200	74	0.0	100.00
Number 230	63	0.0	100.00
Number 270	53	0.0	100.00
Number 325	44	0.05	99.95
Pan	-44	99.60	-

Sub-Sieve Particle Distribution

Particle Size (microns)	Weight (%)
40-44	2.7
20-40	39.0
10-20	38.5
5-10	15.3
0-5	4.2

TABLE A-3
SIEVE ANALYSIS AND PARTICLE SIZE DISTRIBUTION
OF METCO 73F-NS-1 (83WC-17Co) PLASMA SPRAY POWDER

Sieve Analysis

Sieve Designation	Micron Size	Weight % of Powder Retained	Weight % of Powder Passed
Number 140	105	0.0	100.0
Number 170	88	0.17	99.83
Number 200	74	0.41	99.42
Number 230	63	0.43	98.99
Number 270	53	5.55	93.44
Number 325	44	7.40	86.0
Pan	-44	86.09	-

Sub-Sieve Particle Distribution

Particle Size (microns)	Weight (%)
40-44	16.1
20-40	38.5
10-20	8.5
5-10	0.0
0-5	4.2

TABLE A-4
SIEVE ANALYSIS AND PARTICLE SIZE DISTRIBUTION
OF UCAR 205 (83Ni-17W,Ti)C) PLASMA SPRAY POWDER

Sieve Analysis

Sieve Designation	Micron Size	Weight % of Powder Retained	Weight % of Powder Passed
Number 140	105	0.0	100.0
Number 170	88	0.0	100.0
Number 200	74	0.02	99.98
Number 230	63	0.74	99.24
Number 270	53	0.10	99.14
Number 325	44	0.50	98.64
PAN	-44	98.10	-

Sub-Sieve Particle Distribution

Particle Size (microns)	Weight (%)
40-44	10.6
20-40	56.0
10-20	19.0
5-10	2.5
0-5	0.5

UNITED STATES GOVERNMENT PRINTING OFFICE 1987/748-120/40422

1. Report No.	2. Government Accession No.	3. Recipient's Catalog No.
NASA CR-179622		

4. Title and Subtitle	5. Report Date
Materials for Advanced Turbine Engines (MATE). Project 4 - Erosion Resistant Compressor Airfoil Coating	May 1987
	6. Performing Organization Code

7. Author(s)	8. Performing Organization Report No.
J.M. Rashid, M. Freling, and L.A. Friedrich	PWA 5574-206
	10. Work Unit No. 505-63-01

9. Performing Organization Name and Address	11. Contract or Grant No.
United Technologies Corporation Pratt & Whitney Engineering Division East Hartford, Connecticut 06108	NAS3-20072
	13. Type of Report and Period Covered Contractor Report
12. Sponsoring Agency Name and Address National Aeronautics and Space Administration Lewis Research Center Cleveland, Ohio 44135	14. Sponsoring Agency Code

15. Supplementary Notes

Project Manager, Susan M. Benford, Materials Division, NASA, Lewis Research Center Cleveland, Ohio 44135.

16. Abstract

The objective of the program was to identify and demonstrate the ability of coatings to provide at least a 2X improvement in particulate erosion resistance for steel (AMS 5616), nickel (Incoloy 901) and titanium (AMS 4928) compressor airfoils. Coating materials evaluated in this program included plasma sprayed cobalt tungsten carbide, nickel (tungsten, titanium) carbide and diffusion applied chromium plus boron. Several processing parameters for plasma spray processing and diffusion coatings were evaluated to identify coating systems having the most potential for providing airfoil erosion resistance. Based on laboratory results and analytical evaluations, selected coating systems were applied to gas turbine blades and evaluated for surface finish, burner rig erosion resistance and effect on high cycle fatigue strength. Based on these tests, the following coatings were recommended for engine testing: Gator-Gard plasma spray 88WC-12Co on titanium alloy airfoils, plasma spray 83WC-17Co on steel and nickel alloy airfoils, and Cr+B on nickel alloy airfoils.

17. Key Words (Suggested by Author(s))	18. Distribution Statement
Erosion; Coatings; Compressor blades; Plasma spray; Diffusion; Steel alloys; Titanium alloys; Nickel alloys; High cycle fatigue	Unclassified - unlimited STAR Category 26

19. Security Classif. (of this report)	20. Security Classif. (of this page)	21. No. of pages	22. Price*
Unclassified	Unclassified	81	A05

*For sale by the National Technical Information Service, Springfield, Virginia 22161